

GEOLOGICA ULTRAIECTINA

Mededelingen van het
Instituut voor Aardwetenschappen der
Rijksuniversiteit te Utrecht

No. 32

METAMORPHISM OF SILICEOUS
DOLOMITES IN THE HIGH-GRADE
PRECAMBRIAN OF ROGALAND,
SW NORWAY

**METAMORPHISM OF SILICEOUS
DOLOMITES IN THE HIGH-GRADE
PRECAMBRIAN OF ROGALAND,
SW NORWAY**

PROEFSCHRIFT

TER VERKRIJGING VAN DE GRAAD VAN DOCTOR IN
DE WISKUNDE EN NATUURWETENSCHAPPEN AAN
DE RIJKSUNIVERSITEIT TE UTRECHT, OP GEZAG VAN
DE RECTOR MAGNIFICUS PROF. DR. O. J. DE JONG,
VOLGENS BESLUIT VAN HET COLLEGE VAN DECANEN
IN HET OPENBAAR TE VERDEDIGEN OP MAANDAG
9 MEI 1983 DES NAMIDDAGS TE 4.15 UUR

DOOR

PAULUS CLEMENS CORNELIS SAUTER

GEBOREN OP 31 OKTOBER 1952 TE EINDHOVEN

1983
OFFSETDRUKKERIJ KANTERS B.V., ALBLASSERDAM

Promotor: Prof. Dr. A. C. Tobi

Dit proefschrift kwam tot stand mede
onder leiding van: Dr. J. B. H. Jansen.

aan Flens
Floor en Daan



Forsterite marbles of the Faurefjell formation, underlain by quartz-diopside gneisses and intruded by pegmatite. Location B, height exposure about 3 m. By courtesy of Rob Blok.

VOORWOORD

Bij het tot stand komen van dit proefschrift wil ik in het bijzonder bedanken:

Mijn promotor, Prof. Dr. A.C. Tobi, voor zijn suggesties tijdens het onderzoek en zijn kritische kanttekeningen bij de tekst;

Dr. Ben Jansen. Een middagje bij jou Ben, hielp vaak meer dan een hele week zelf ploeteren;

Ir. G.A.E.M. Hermans en Dr. C. Maijer, mijn oud-kamergenoten Frans Rietmeijer en Hugo Swanenberg, Rob Blok en alle andere studenten petrologie, die direct of indirect hun bijdrage aan dit proefschrift hebben geleverd. Dankzij hen bewaar ik erg goede herinneringen aan de barak, de Uithof en vooral Rogaland;

Al diegenen die mij behulpzaam zijn geweest bij het verzamelen van de benodigde analyses:

Dr. C. Kieft en W.J. Lustenhouwer, voor hun hulp bij de microprobe analyses op het Instituut voor Aardwetenschappen van de Vrije Universiteit te Amsterdam;

Dr. Renee Poorter en Drs. Manfred van Bergen voor de microprobe analyses in Utrecht;

Dr. Rob Kreulen voor de koolstof en zuurstof isotopen bepalingen en voor zijn discussies over het desbetreffende hoofdstuk;

K.M. Stephan en F.J.G.M. Anten voor de whole-rock analyses;

Charles Laman voor het maken van röntgenopnamen van soms wel zeer minuscule korreltjes;

In hen bedank ik alle technici en analisten achter de schermen.

Dr. Jim Boland en Dra. Daphne Scholten ben ik erkentelijk voor hun discussies over de calcië-dolomiet omtrentingen;

Ook bedank ik hierbij alle medewerkers van de bibliotheek, slijpkamer en foto- en tekenkamer van het IVAU voor hun bijdrage in de voorbereiding en vormgeving van dit proefschrift;

Detty Huisman-Erkens wil ik erg hartelijk bedanken voor het vele typewerk;

Ton Vermeulen typete de laatste stukjes tekst en was bovendien onmisbaar bij het knip- en plakwerk;

Richard Lisle, Tony Senior en Mike Barton dank ik voor hun correcties op de Engelse tekst;

Jeg vil også gjerne takke Yngvar, Gudrun og barna Johansson fra Lauvås, Sandnes. De har med sitt vennskap og sin gjestfrihet gjort mitt feltarbeid om sommeren i Norge til et spesielt godt minne.

Tot slot bedank ik mijn ouders, die bij mij al vroeg belangstelling voor de natuur hebben gewekt.

Dit proefschrift kwam tot stand met financiële steun van de Nederlandse Organisatie voor Zuiver-Wetenschappelijk Onderzoek (Z.W.O.), door middel van A.W.O.N. subsidie 18.21.06. Microprobe analyse faciliteiten in Amsterdam en Utrecht werden verzorgd door W.A.C.O.M., gesubsidiëerd door Z.W.O.

En voor Plons zijn geen woorden.

INDEX

Voorwoord	7
Index	9
Abstract	11
Samenvatting	12
Introduction	14
Chapter 1. Mineral relations in siliceous dolomites and related rocks in the high-grade metamorphic Precambrian of Rogaland, SW Norway	17
Introduction	17
Petrography	21
Mineral relations	24
Mineral chemistry	27
Discussion and conclusions	30
Chapter 2. Zoning in diopside from granulite facies marbles from Rogaland, SW Norway	33
Introduction	33
Petrography	35
Morphology of the zoning	39
Chemical characteristics of the zoning	40
Chemistry of the clinopyroxenes	43
Discussion	50
Chapter 3. Exsolution, major element and isotope chemistry of Rogaland carbonates	57
Introduction	57
Calcite-dolomite microstructures	60
Description	60
Distribution of the microstructures	65
Origin of the microstructures	66
Chemistry of the carbonates	68
Samples and results	70
Geothermometry	72

Carbon and oxygen isotopes	73
Samples	73
Results	79
Discussion	81
Chapter 4. Mineralogy and petrogenesis of the marbles	91
Introduction	91
Main minerals	92
Forsterite	92
Phlogopite	95
Spinel	100
Minor and secondary minerals	103
Enstatite	103
Magnesio-hornblende	105
Hornblende-group minerals	106
Tremolite	110
Chlorite	112
Serpentine	114
Hydrotalcite	114
Accessory minerals	116
Wollastonite	116
Element distribution and geothermometry	117
General petrogenesis	122
Chapter 5. Whole-rock chemistry	129
Introduction	129
Results and discussion	130
Discussion of origin	134
Appendix	137

ABSTRACT

In the Precambrian granulite facies terrain of Rogaland, SW Norway, some small occurrences of marbles are present. They are mainly exposed at three locations A, B and C, at increasing distance from the anorthositic and monzonitic intrusions. The Precambrian basement in Rogaland has undergone several high-grade metamorphic events: M1 around 1200 Ma, the granulite facies M2 around 1050 Ma and M3 around 950 Ma. Late retrogressive events M4a and M4b have a Caledonian age.

The marbles belong to the Faurefjell formation, which furthermore consists mainly of quartzites, quartz-diopside gneisses, diopside rocks, alkali-feldspar-rich rocks and norites (Chapter 1). The marbles are mainly forsterite marbles with the mineral association Fo-Cc-Phl-Di-Di+Sp. The mineral associations in the forsterite marbles indicate metamorphic temperatures of about 700°C for location C to higher temperatures for location A. Some diopside marbles occur, showing the mineral association Di-Phl-Cc. These rocks and the diopside rocks (Di, Di-Phl) typically show high-variance assemblages, indicative of a metasomatic origin. The minerals in the marbles show a high-Mg chemistry. X_{Mg} is higher than 0.85 for all minerals. With increasing X_{Mg} the order of minerals is: Sp>Cc>Fo>Phl-Di-No.

Diopside (Chapter 2) can be strongly zoned, showing an Al-, Ti- and Fe³⁺-rich core and Mg- and Si-rich rims. The maximum range observed in one crystal (containing the highest Al content) is 2.5 to 8.5 wt% Al₂O₃. The highest Al contents in diopside are found in spinel-bearing marbles. A late, low-Al stage of diopside formation has taken place as a result of metasomatic reactions, presumably during M3.

The calcites in the marbles show a considerable amount of dolomite exsolution (Chapter 3). Dolomite exsolution in the form of tablets, rhombohedra and symplectites is the most common. The tablet exsolution type formed during the post-metamorphic cooling stage, the rhombohedral and symplectitic types presumably during Caledonian M4a and M4b retrogressive events. The exsolution of dolomite has resulted in a decrease of the Mg content of calcite. Recalculated Mg contents reveal temperatures of about 700°C for locations B and C. Because of the absence of dolomite, the higher temperature marbles of location A show lower Mg contents in calcite.

The carbon and oxygen isotope ratios of calcite show a trend from $\delta^{13}C = -4$ (PDB) and $\delta^{18}O = +21$ (SMOW) for location A, values close to those of unmetamorphosed Precambrian carbonate rocks, to $\delta^{13}C = -7.5$ and $\delta^{18}O = +14$ for location C. Isotopic compositions of veins and Caledonian marbles close to or just above the Caledonian boundary, indicate that the isotopic depletion in the Precambrian marbles mainly is the result of interaction with Caledonian retrogressive fluids.

The chemistry of forsterite, phlogopite and spinel is fairly constant within a sample (Chapter 4). They show the Mg-rich chemistry

common in siliceous dolomites. Forsterite shows comparatively high Mn contents (up to 0.8 wt% MnO). Phlogopite shows high Ba contents, up to 4.8 wt% BaO in a normal phlogopite, and about 20% BaO and 12 wt% TiO₂ in a single occurrence of Ba-phlogopite. Spinel contains Zn, up to 2.4 wt% ZnO.

Mg-Fe distribution between forsterite and diopside is mainly dependent on the Al content of diopside. A single occurrence of diopside-enstatite in location A suggests high (900°C) equilibration temperatures. Forsterite and spinel show extensive re-equilibration chemistry. Geothermometry for these Cr-free spinel-olivine pairs is not reliable.

Textural and chemical data for the minerals indicate a polymetamorphic, partly metasomatic history of the Rogaland marbles. Several main minerals were formed pre-M1, and during M1, M2 and M3. The formation of retrograde minerals, like clinohumite, tremolite and chlorite, took place from late-M3 to M4b stages.

The whole rock chemistry of the Faurefjell rocks (Chapter 5) shows a trend from Ca-Mg rich, Si-poor compositions in the forsterite marbles, towards compositions higher in Si, Al and alkalies in diopside-phlogopite rocks, diopside-alkalifeldspar rocks, quartz-diopside gneisses and quartz-alkalifeldspar rocks. Chemical characteristics of the marbles, especially the Ca/Mg and the Sr/Ca ratios, indicate sedimentary affinities for these rocks, while anomalous high contents of, in particular, Ba and Si indicate possibly early hydrothermal activity as well as higher-grade metasomatism.

SAMENVATTING

In het Precambrische granuliet faciesgebied van Rogaland, zuidwest Noorwegen, zijn enkele kleine voorkomens van marmers aanwezig. Zij zijn voornamelijk ontsloten in drie lokaties A, B en C, op een toenemende afstand van de anorthositische en monzonitische intrusiva. Het Precambrische basement in Rogaland heeft verschillende hoog-gradige metamorfe fasen ondergaan: M1 rond 1200 miljoen jaar, de granuliet facies M2 rond 1050 miljoen jaar en M3 rond 950 miljoen jaar. Laat retrograde stadia M4a en M4b hebben een Caledonische ouderdom.

De marmers behoren tot de Faurefjell formatie, die verder voornamelijk bestaat uit kwartsieren, kwarts-diopsied gneizen, diopsied rotsen, alkaliveldspaat-rijke gesteenten en norieten (Hoofdstuk 1). De marmers bestaan voornamelijk uit forsteriet-marmers met de mineraal-associatie Fo-Cc-Phl±Do±Di±Sp. De mineraalassociaties in de forsteriet marmers wijzen op metamorfe temperaturen van ongeveer 700°C voor lokatie C tot hogere temperaturen voor lokatie A. Enkele diopsied marmers komen voor, met de mineraalassociatie Di-Phl-Cc. Deze gesteenten en de diopsied rotsen (Di, Di-Phl) hebben karakteristieke hoog-variante assemblages, kenmerkend voor een metasomatische oorsprong. De mineralen in de marmers vertonen een hoog-Mg chemie.

X_{Mg} is groter dan 0.85 in alle mineralen. Het toenemende X_{Mg} is de volgorde van de mineralen: Sp>Cc>Fo>Phl-Di-Do.

Diopsied (Hoofdstuk 2) kan sterk gezoneerd zijn. Het vertoont een

Al-, Ti- en Fe³⁺-rijke kern en Mg- en Si-rijke randen. Het maximale bereik gevonden in één kristal (met tevens het hoogste Al-gehalte) is 2.5 tot 8.5 gewichtsprocent Al₂O₃. De hoogste Al-gehalten in diopsied worden gevonden in spinel-houdende marmers. Een laat, laag-Al stadium van diopsiedvorming heeft plaatsgevonden als gevolg van metasomatische reacties, waarschijnlijk gedurende M3.

De calcieten in de marmers vertonen een aanzienlijke hoeveelheid dolomiet-ontmenging (Hoofdstuk 3). Dolomiet-ontmenging in de vorm van tabletten, rhomboëders en symplektieten is het meest algemeen. De tablet-ontmengingsvorm werd gevormd gedurende de post-metamorfe koeling, de rhomboëdrische en symplektietische types waarschijnlijk gedurende de Caledonische M4a en M4b retrograde fasen. De ontmenging van calciet heeft een verlaging van het Mg-gehalte tot gevolg gehad. Teruggereken- de Mg-gehalten wijzen op temperaturen van 700°C voor lokaties B en C. Vanwege de afwezigheid van dolomiet, vertonen de hoger-temperatuur-marmers van lokatie A lagere Mg-gehalten in calciet.

De koolstof en zuurstof isotopenverhoudingen van calciet vertonen een trend van δ¹³C=-4 (PDB) en δ¹⁸O=+21 (SMOW) voor lokatie A, waarden dicht bij die van niet-gemetamorfiseerde Precambrische karbonaat-gesteenten, tot δ¹³C=-7.5 en δ¹⁸O=+14 voor lokatie C. Isotopensamen- stellingen van anders en Caledonische marmers dichtbij of juist boven de grens met de Caledoniden wijzen erop dat de isotopendepletie in de Precambrische marmers voornamelijk het gevolg is van uitwisseling met Caledonische retrograde fluids.

De chemie van forsteriet, phlogopiet en spinel is redelijk konstant binnen een monster (Hoofdstuk 4). Deze mineralen vertonen Mg-rijke samenstellingen die gewoonlijk in siliceuze dolomieten gevonden worden. Forsteriet heeft vergelijkendewijs hoge Mn-gehalten (tot 0.8 gew.% MnO). Phlogopiet vertoont hoge Ba-gehalten, tot 4.8 gew.% BaO in een normale phlogopiet en ongeveer 20% BaO en 12 gew.% TiO₂ in een enkel voorkomen van Ba-phlogopiet. Spinel bevat Zn, tot 2.4 gew.% ZnO.

De Mg-Fe verdeling tussen forsteriet en diopsied is voornamelijk afhankelijk van het Al-gehalte in diopsied. Een enkel voorkomen van diopsied-enstatiet in lokatie A suggereert hoge (900°C) equilibratie-temperaturen. Forsteriet en spinel vertonen een sterke reëquilibratie-chemie. Geothermometrie aan deze Cr-vrije spinel-olivijn paren is onbetrouwbaar.

Texturele en chemische gegevens voor de mineralen wijzen op een polymetamorfe, deels metasomatische geschiedenis van de Rogaland-marmers. Verschillende hoofdmineralen werden pre-M1 en gedurende M1, M2 en M3 gevormd. De vorming van retrograde mineralen zoals clinohumiet, tremoliet en chloriet vond plaats vanaf de laat-M3 tot in het M4b stadium.

De whole-rock chemie van de Faurefjell gesteenten (Hoofdstuk 5) vertoont een trend vanaf Ca-Mg-rijke, Si-arme samenstellingen in de forsteriet marmers, tot samenstellingen rijker aan Si, Al en de alkalies in diopsied-phlogopiet rotsen, diopsied-alkaliveldspaat rotsen, kwarts-diopsied gneizen en kwarts-alkaliveldspaat rotsen. Chemische karakteristieken van de marmers, speciaal de Ca/Mg en de Sr/Ca verhoudingen, wijzen op sedimentaire verwantschappen van deze gesteenten, terwijl de afwijkend hoge gehalten aan vooral Ba en Si zowel wijzen op een mogelijk vroeg hydrothermale activiteit als wel op metasomatische tijdens hoog-gradiger omstandigheden.

INTRODUCTION

The siliceous dolomite system is comparatively well studied, in the field as well as by experiments (see for a review Winkler (1979), and more recent data of Käse and Metz (1980), Eggart and Kerrick (1981), Widmark (1980, 1981)). The successive reactions in $T-X_{CO_2}$ space define well-mappable isogrades in several regional- to contact-metamorphic areas (e.g. the Alps, Trommsdorff (1966), aureoles in Montana, USA (Rice 1977a, b), on Naxos, Greece (Jansen et al., 1978)). In closed systems the fluid composition is buffered by the mineral assemblage. However, the reactivity of the dolomites makes them very susceptible for metasomatism. Then open system behaviour is often observed (e.g. Glassley 1975, Bucher-Nurminen 1977, 1982).

In the high-grade metamorphic Precambrian of Rogaland, SW Norway, marbles, occurring in the Faurefjell formation, were reported by Hermans et al. (1975). The marbles are observed in the granulite facies terrain (Fig. 1, Chapter 1). They cover only a very small part of the total mapped area, approximately 0.01%. Other members of the formation, notably the quartz-diopside gneisses, cover larger areas (Location D, Fig. 1, Chapter 1).

Several internal reports of the Department of Petrology of the Rijksuniversiteit Utrecht, the Netherlands, deal with aspects of the Faurefjell formation (Hakstege, Hilversum, Teske, Wegelin, Venhuis, Blok, Meertens). Also a part of the thesis of Legrand (1976) was devoted to these rocks.

The main subject of the present thesis is the chemical evolution of the marbles, projected in the regional metamorphic history of the Precambrian of Rogaland. Fieldwork was carried out in the summers of 1979 to 1981. Detailed descriptions of field occurrences of the marbles are given in internal reports.

In Chapter 1 a general view of the Faurefjell formation is given.

Field relations, petrography, assemblages and an introduction in the mineral chemistry are treated. This chapter was published under the same title in *Norsk Geologisk Tidsskrift*, Vol. 61, 1981. After completion of this chapter Schreurs (internal report 1982) reported some small occurrences of marbles south of location A. They probably form a southward extension of the marble layers at A. The observed assemblages are the same as in that location. An occurrence of wollastonite in quartz-diopside gneisses recently was reported by Venhuis (internal report 1982). It is shortly described in Chapter 4.

The simple concept of equilibrium outlined in Chapter 1 was tested with the help of additional microprobe analyses and, as usual, a far more complex story evolved.

Particularly the strong Al-zoning in diopside attracted the attention and a detailed microprobe study of this phenomenon was made; the results are shown in Chapter 2.

Optically better visible, particularly after staining, were inhomogeneities in calcite, due to exsolution of dolomite. In Chapter 3 the time relationship between the beautifully developed microstructures is settled, with an attempt to correlate them to the regional metamorphic history. Of course, the dolomite exsolution caused a significant chemical change in calcite, but recalculation of original Mg contents gives some indications of metamorphic temperatures. Carbon and oxygen isotopic compositions were determined and again, the polymetamorphic history of the Rogaland area was established: the isotopic depletion trend indicates the importance of Caledonian retrogressive processes.

With the help of textural and chemical data of the minerals in the marbles, in Chapter 4 a general petrogenesis is given. The rather complex history of the marbles is depicted, certainly still too simple, in Fig. 22 of this chapter.

The high amount of silicates in the marbles, the high concentration of some elements, such as Ba and Zn, analysed in some minerals and the occurrence of some peculiar rock types in the Faurefjell formation raised questions on the origin of the rocks. With the help of whole-

rock analyses the origin is discussed in Chapter 5. Again the findings confirm the complex history of this polymetamorphic Precambrian terrain.

REFERENCES

- Bucher-Nurminen, K. 1977: Die Beziehung zwischen Deformation, Metamorphose und Magmatismus im Gebiet der Bergeller Alpen. Schweiz. mineral. petrogr. Mitt. 57, 413-434.
- Bucher-Nurminen, K. 1982: Mechanism of mineral reactions inferred from textures of impure dolomitic marbles from East Greenland. J. Petro. 23, 325-343.
- Eggert, R.G. and Kerrick, D.M. 1981: Metamorphic equilibria in the siliceous dolomite system: 6 kbar experimental data and geological implications. Geochim. Cosmochim. Acta 45, 1039-1049.
- Glassley, W.E. 1975: High grade regional metamorphism of some carbonate bodies: significance for the orthopyroxene isograd. Am. J. Sci. 275, 1133-1163.
- Hermans, G.A.E.M., Tobl, A.C., Poorter, R.P.E. and Maijer, C. 1975: The high-grade metamorphic Precambrian of the Sirdal/Ørsdal area, Rogaland/Vest-Agder, South-West Norway. Nor. Geol. Unders. 318, 51-74.
- Jansen, J.B.H., Kraats, A.H. van de, Rijst, H. van der, and Schilling, R.D. 1978: Metamorphism of siliceous dolomites of Naxos, Greece. Contrib. Mineral. Petrol. 67, 279-288.
- Käse, H.R. and Metz, F. 1980: Experimental investigation of the metamorphism of siliceous dolomites. II Equilibrium data for the reaction: 1 diopside + 3 dolomite = 2 forsterite + 1 calcite + 2CO₂. Contrib. Mineral. Petrol. 73, 151-159.
- Legrand, J.-M. 1976: Etude pétrologique des séries gneissiques et anatectiques catazonales du Dôme de Sandnes-Håla. Les équilibres minéralogiques. Thèse Bruxelles, 219 pp.
- Rice, J.M. 1977a: Contact Metamorphism of Impure Dolomitic Limestone in the Boulder Aureole, Montana. Contrib. Mineral. Petrol. 59, 237-259.
- Rice, J.M. 1977b: Progressive metamorphism of impure dolomitic limestone in the Marysville Aureole, Montana. Am. J. Sci. 277, 1-24.
- Trommsdorff, V. 1966: Progressive Metamorphose kieseliger Karbonatgesteine in den Zentralalpen zwischen Bernina und Simplon. Schweiz. mineral. petrogr. Mitt. 46, 431-460.
- Widmark, E.T. 1980: The reaction Chlorite + Dolomite = Spinel + Forsterite + Calcite + Carbon Dioxide + Water. Contrib. Mineral. Petrol. 72, 175-179.
- Widmark, T. 1981: Hydrothermal experiments: the reaction chlorite + dolomite = forsterite + calcite + spinel + fluid and ideas about a new buffer technique. Geol. Fören. Stockholm Förh. 103, 128-130.
- Winkler, H.G.F. 1979: Petrogenesis of metamorphic rocks. 5th ed., Springer-Verlag, Berlin-Heidelberg-New York, 348 pp.

CHAPTER 1

MINERAL RELATIONS IN SILICEOUS DOLOMITES AND RELATED ROCKS IN THE HIGH-GRADE METAMORPHIC PRECAMBRIAN OF ROGALAND, SW NORWAY

P.C.C. SAUTER

Norsk Geologisk Tidsskrift, 61 (1981), 35-45.

ABSTRACT

Forsterite- and diopside-bearing marbles, calc-silicate rocks, and quartz-rich rocks occur in the Precambrian granulite facies terrain of SW Norway. Most minerals in these rocks have a Mg-rich composition. Calcite-dolomite geothermometry, phase relations, and element distribution suggest a temperature gradient from about 700°C in the northern part of the area to higher temperatures near the intrusive complexes in the south. The formation of high-variance mineral assemblages, for instance at contacts between carbonate-rich and silica-rich rocks, is attributed to metasomatic activity.

INTRODUCTION

The Precambrian basement of SW Norway consists of anorthositic masses, the lopolith of Bjerkreim-Sokndal and surrounding high-grade metamorphic migmatites. The migmatites contain intercalations of garnetiferous migmatites, augengneisses and rocks of the Faurefjell formation (Hermans et al. 1975). The mineral relations in rocks of this formation, which is mainly composed of marbles and calc-silicate rocks, are the subject of this paper.



Fig. 1. Geological sketch-map of SW Norway. Outcrops of the Faurefjell formation, at locations A, B, C and D, are indicated in black.

In the eastern part of the area (Fig. 1) metamorphism has reached amphibolite facies conditions. Towards the west the grade of metamorphism gradually changes into a granulite facies. The increasing grade is marked by the hypersthene-in isograd (Hermans et al. 1975), the omphacite-in isograd (Majner et al. 1981) and a change in amphibole properties (Dekker 1978). Two-pyroxene and Fe-Ti oxide geothermometry on metabasites revealed temperatures of about 800°C near Oltedal in the north increasing to 1000°C near the lopolith (Jacques de Dixmude 1978). Pyroxene crystallization temperatures of the upper quartz-monzonitic phase of the Bjerkreim-Sokndal lopolith are calculated at 900°-1050°C (Rietmeijer 1979).

Isotopic age determinations indicate ages of 1500, 1200 and around 1000 Ma for the main metamorphic and/or magmatic events (Wielens et al. 1980). The M2 granulite facies metamorphism (Majner et al. 1981) is dated at about 1050 Ma, the intrusion of the quartz-monzonitic phase of the lopolith at about 950 Ma (Wielens et al. 1980). Retrogressive metamorphism down to the prehnite-pumpellyite facies is locally observed throughout the area. This metamorphism (M4) presumably has a Caledonian age as reflected by K-Ar and Rb-Sr ages of green biotite (400-450 Ma, Verschure et al. 1979) and lower-intercept ages of zircon U-Pb discordia plots (300-400 Ma, Wielens et al. 1980).

The rock types in the Faurefjell formation are shown in schematic sections in Table 1. Outcrops are found at locations A, B, C and D, at various distances from the intrusive complexes (Fig. 1). In most places the rocks of the formation form relatively thin layers or lenses within the migmatites. The rocks are well-banded and locally intensely folded. Generally the contacts with the migmatites are concordant, but discordant contacts are present at location C. The thickness of the formation varies from 10 to 50 metres, except at location D, where the quartz-diopside gneisses may reach a thickness of 200 metres. This may be caused by intense folding or migration of quartz into fold hinges (Wegelin 1979b).

Forsterite marbles are the most characteristic part of the formation. The dark, weathered surfaces are very conspicuous. Diopside marbles are present in minor amounts at B and C. Diopside rocks in the marbles occur as concordant layers, as discordant veins and, at A, as rounded blocks of various sizes. Diopside rocks also occur at contacts between marbles and silica-rich rocks. Thin alkali-feldspar-phlogopite rocks (only several centimetres thick) are interlayered in diopside rocks at A. Quartzites are associated with the marbles at locations A and B. They form thick, concordant layers or, as at B, discordant bodies. Diopside-alkali-feldspar rocks are found concordantly within the marbles. The quartz-alkali-feldspar rocks may contain bluish veins of pure alkali-feldspar, particularly at A. The quartz-diopside gneisses are finely laminated with thin quartz bands (several millimetres to centimetres thick). At D these gneisses form the main part of the formation. Thin layers of andradite-hedenbergite quartzite may be intercalated in the quartz-diopside gneisses, whereas pure andradite-hedenbergite rocks are found at the contact between marble and a norite at location B.

Table 1. Schematic sections of the Faurefjell formation at locations A, B, C and D.

Location A thickness 30 m ¹⁾	Location B ²⁾ 30-50 m	Location C 10 m	Location D 40-200 m
country rock	country rock	country rock	country rock
Q-Di gneiss ³⁾			
Quartzite	Q-Di gneiss		
Di rock		Di rock and Di-Kfsp rock	
Fo marble	Di rock		
Q-Kfsp/Di-Kfsp and Di rock	Fo marble and Di rock	Di marble and Di rock	
Q-Kfsp rock	Di rock	Fo marble	Q-Di gneiss with small intercalations of Di rock, quartzite, And-Med quartzite and (in the east) Fo marble
Di rock	Di rock	Di marble	
Fo marble and Di rock	Fo marble, Di marble and Di rock	Di-Kfsp rock	
Di rock	Di rock	Di marble and Fo marble	
marble	marble and And-Med rock	Di rock and Q-Kfsp rock	
quartzite	quartzite		
country rock	country rock	country rock	country rock

Rock nomenclature mainly after Hermans et al. (1975). 1) Westward the formation becomes thicker and grades into the Q-Di gneisses of location D. 2) Compilation of several exposures at location B. 3) Abbreviations used in this table and elsewhere: Fo=forsterite, Di=diopside, Ph=phlogopite, Sp=spinel, C=calcite, Do=dolomite, Tr=tremolite, Q=quartz, Kfsp=alkalifeldspar, An=anorthite, And=andradite, Hed=hedenbergite, Scap=scapolite.

PETROGRAPHY

Nature and relative amounts of minerals in the main rock types of the Faurefjell formation are presented in Table 2. A petrographic description is given below. Terminology of textures is according to Moore (1970).

Forsterite marbles have a grain size of 1 to 3 mm and a granoblastic inequigranular texture. Forsterite (2V=90°) has curved boundaries. Locally serpentinization has occurred. Calcite is the predominant carbonate phase. Some dolomite is present in most samples at locations B and C, both as primary dolomite and as an exsolution product from calcite. This exsolved dolomite occurs as orientated, tablet-like crystals and as symplectitic intergrowth (cf. Legrand 1976). Colourless to light-brown phlogopite is generally present in the forsterite marbles. Most crystals are slightly bent and occasionally kinked. Colourless diopside (+2V=60°) is observed in most samples, but only in minor amounts. Most diopside crystals are subhedral but in some samples diopside rims around forsterite are found. These rims may be connected with each other to form one large poikiloblastic crystal. Subhedral spinel, restricted to some samples at A and B, has a very pale-green to green colour. Clinohumite, apparently replacing forsterite, has yellow pleochroic colours and it often shows twin lamellae.

Diopside marbles have a grain size of about 1 mm and a granoblastic equigranular texture. Poikiloblastic diopside crystals occur up to several centimetres. Diopside marbles contain less calcite than the forsterite marbles. Exsolved dolomite is omnipresent, primary dolomite is very rare. In many samples the parallel arrangement of abundant phlogopite defines a good foliation.

Diopside rocks have a grain size of 1 to 2 mm, although larger crystals occur. The texture is equigranular and tends to be polygonal. Phlogopite can be abundant, it generally has a more brownish colour than in the marbles. Spinel and forsterite are some of the additional constituents.

Alkalifeldspar-phlogopite rocks have a grain size of 1 to 2 mm. Orthoclase is the main alkalifeldspar, sanidine may occur. The brown phlogopite flakes define a good foliation. Green spinel forms small euhedral crystals.

SAMPLE

within each rock type samples are listed alphabetically. Mineral assemblage does not always mean existence of mineral assemblage. Minerals are: 1) major; 2) minor; 3) accessory; 4) retrogressive (based on textural grounds); 5) abundantly retrogressive; 6) totally or for the greater part decomposed; 7) exsolved dolomite (also) present; 8) either amphibole (when tremolite) or edenbergite; 9) montmorillonite; 10) intercaline; 11) orthoclaire; 12) scapolite; 13) An; 14) plagioclase; 15) albite only at rim around forsterite.

Diopside-alkalifeldspar rocks have a grain size of 0.5 to 1 mm. Diopside and alkalifeldspar, forming an equigranular polygonal texture, are present in approximately equal amounts. Locally diopside forms large poikiloblastic crystals. Generally orthoclase (~2V-60°) and sanidine (~2V-20°) occur at location A and orthoclase and microcline (~2V-80°) at B and C. Spene, forming anhedral crystals, is a minor but characteristic constituent.

Quartzites are usually coarse grained (grain size larger than 5 mm). The grain boundaries are irregular, most grains show undulatory extinction. Diopside and calcite may occur in minor amounts.

Quartz-alkalifeldspar rocks have an equigranular interlobate texture. The grain size is less than 1 mm. Alkalifeldspar variation is the same as in the diopside-alkalifeldspar rocks. Diopside may occur. Small needles of magnesioriebeckite are observed at A.

Quartz-diopside/hedenbergite gneisses have a grain size of 2 to 5 mm. Quartz is mainly concentrated in small seams (several millimetres to centimetres thick) and it is commonly associated with colourless to green clinopyroxene, plagioclase (up to 83% An) and alkali feldspar (orthoclase and microcline). Calcite and brownish phlogopite may be present in minor amounts. Retrogressive metamorphism is widespread.

Andradite-hedenbergite quartzites and rocks have a grain size of 2 to 5 mm. Green hedenbergite forms subhedral crystals whereas the brown andradite grains are anhedral and poikiloblastic. In the quartzites almost pure anorthite, partly replaced by scapolite, may be present. Especially in the andradite-hedenbergite rocks sphene may be abundant.

Evidence of some slight retrogressive metamorphism can be found in all these rock types. The occurrence of the minerals serpentine (formed from forsterite and occasionally from diopside), clinohumite (from forsterite?) and scapolite (from plagioclase) has already been mentioned. Furthermore tremolite and chlorite may partly or wholly replace diopside and phlogopite respectively. Epidote, zoisite and colourless mica are frequently observed as alteration products of plagioclase. Pumpellyite is present in some quartz-diopside gneisses. Extensive retrogressive metamorphism has been especially observed in some exposures at location B. Strong alteration has resulted in the occurrence of serpentine-, tremolite- and talc-rich rocks. The exposures are situated next to a small fault and a large discordant

quartzite body. The quartzite contains only H₂O-rich fluid inclusions, in contrast to most other quartzite bands and veins in the Faurefjell formation, where mainly CO₂-rich inclusions are found (Swanenberg 1980).

Table 3. Mineral assemblage..

A: system CaO-MgO-SiO ₂ -CO ₂ -H ₂ O			
Assemblage	Rock type	Loc.	Abundance
For-Di-Cc-Do	marble	B,C	common
For-Cc-Do	marble	B,C	scarce
For-Di-Cc	marble	A	common
Di-Cc-Do	marble	C	rare
Di-Q-Cc	Q-Di gneiss	D	scarce
Di-Cc	marble	A,B,C	common
Di-Q	Q-Di gneiss	A,B,D	common
Di	Di rock	A,B,C,D	common

B: system CaO-MgO-K ₂ O-Al ₂ O ₃ -SiO ₂ -CO ₂ -H ₂ O ¹⁾			
low-silica/low-potassium			
Assemblage	Rock type	Loc.	Abundance
For-Di-Phl-Sp-Cc	marble	A	common
For-Di-Phl-Cc-Do	marble	B,C	common
For-Di-Sp-Cc-Do	marble	B	rare
For-Di-Phl-Cc	marble	A	common
For-Sp-Cc-Do	marble	B	rare

high-silica/high-potassium			
Assemblage	Rock type	Loc.	Abundance
Di-Phl-Q-Kfsp-An	Q-Di gneiss	D	rare
Di-Q-Kfsp-An-Cc	Q-Di gneiss	D	scarce
Di-Q-Kfsp-An	Q-Di gneiss	A,B,D	common
Di-Q-Kfsp	Q-Di gneiss	A,B,C,D	common
Di-Q-Kfsp	Q-Di gneiss	A,B,C,D	common
Di-Kfsp-Cc	Di-Kfsp rock	A,C	scarce
Phl-Sp-Kfsp	Kfsp-Phl rock	A	scarce
Q-Kfsp	Q-Kfsp rock	A,B,C	common
Di-Kfsp	Di-Kfsp rock	A,B,C	common

1) Only main assemblages in this system are mentioned.

MINERAL RELATIONS

Most primary Mg-Fe minerals in rocks of the Faurefjell formation have a Mg-rich composition, which is reflected in their optical properties and demonstrated by microprobe analyses (Table 4). Therefore the mineral relations can be described in the system CaO-MgO-K₂O-Al₂O₃-SiO₂-CO₂-H₂O, if the Na content of the feldspars is also neglected. In most thin sections of the rocks, equilibrium between the mineral phases can be assumed on textural grounds. The occurrence

of diopside rims around forsterite and of replacement textures of minerals such as tremolite or clinohumite point to non-equilibrium conditions.

As a first approximation the subsystem CaO-MgO-SiO₂-CO₂-H₂O will be discussed. The assemblages in the subsystem are listed in Table 3A and the phase relations are illustrated by Fig. 2. The four-mineral assemblage For-Di-Cc-Do represents the isobaric univariant assemblage of reaction (14): 1Di+3Do=2Fo+4Cc+2CO₂. The presence of this assemblage and of the assemblage For-Cc-Do point to T-XCO₂ conditions on respectively above reaction (14) for the locations B and C (see Fig. 3). At A the presence of the assemblage For-Di-Cc, coupled with the absence of dolomite and of primary tremolite, indicates metamorphic conditions only on the high-temperature side of the reactions (14) and (13): 3Tr+5Cc=11Di+2Fo+5CO₂+3H₂O. The assemblage Di-Cc-Do, only found at C, could represent conditions of the low-temperature side of reaction (14). Both forsterite and dolomite are found to be incompatible with quartz in all the rocks of the Faurefjell formation. The assemblage Di-Q-Cc is not indicative for the P-T-XCO₂ range involved. Some rocks only consist of the assemblages Di-Cc or Di-Q or even only of Di. Regarding the widespread occurrence it is rather unlikely that these rocks have been isochemically formed from very special bulk compositions. Therefore the assemblages suggest an origin by metasomatic processes (Thompson 1959). Indeed, such nearly-monomineralic rocks are frequently observed in reaction zone sequences between carbonate-bearing and quartz-bearing rocks (e.g. Vidale 1969, Glassley 1975). In samples where diopside forms rims

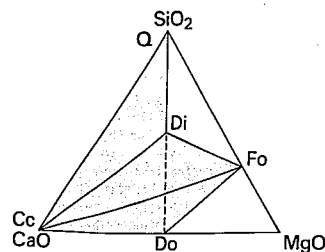


Fig. 2. Phase relations in the subsystem CaO-MgO-SiO₂-CO₂-H₂O. Shaded areas indicate stable mineral assemblages.

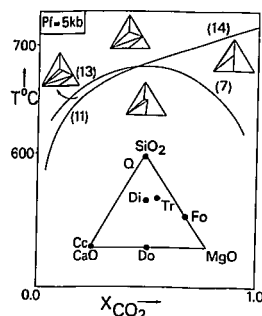


Fig. 3. Isobaric T - X_{CO_2} diagram for the system CaO - MgO - SiO_2 - CO_2 - H_2O at $P=5$ kb. Small triangles indicate possible stable mineral assemblages. Reactions (13) and (14) are given in the text. (13): $1 Tr + 3 Ca = 1 Do + 4 Di + 1 CO_2 + 1 H_2O$. (14): $1 Tr + 11 Do = 8 Fo + 13 Ca + 9 CO_2 + 1 H_2O$. (After Winkler 1979)

around forsterite, the minerals forsterite, diopside and calcite do not reflect an equilibrium assemblage. Here diopside formation might be explained by the reversed reaction (14): $2Fo + 4Ca + 2CO_2 = 1Di + 3Do$. Dolomite production, however, is not observed near the diopside rims. Another explanation is that forsterite and calcite reacted with a later influx of SiO_2 to form diopside, according to the reaction: $1Fo + 2Cc + 3SiO_2 = 2Di + 2CO_2$ (Weeks 1956). The observed textures, such as the connected diopside rims, seem to favour the possibility of a metasomatic activity.

The assemblages with phlogopite, spinel, alkali-feldspar and anorthite are described in the system CaO - MgO - K_2O - Al_2O_3 - SiO_2 - CO_2 - H_2O (Fig. 4). The main assemblages are listed in Table 3B. The low silica, low potassium assemblages of marbles and diopside rocks all plot in the projected triangle diopside-dolomite-spinel. The five-mineral assemblage Fo - Di - Phl - Sp - Cc is a low-variance assemblage possibly related to the reaction $6Phl + 7Cc = 7Di + 4Fo + 3Sp + 7CO_2 + 3H_2O + 3K_2O$. This reaction has been proposed by Glassley (1975), taking K_2O as a mobile component in the vapor phase. Other low-variance assemblages can be derived from assemblages in the subsystem CaO - MgO - SiO_2 - CO_2 - H_2O by adding phlogopite or spinel. Formation of high-variance assemblages, such as Di - Phl , Di - Phl - Cc and Di - Phl - Sp could have resulted from metasomatism.

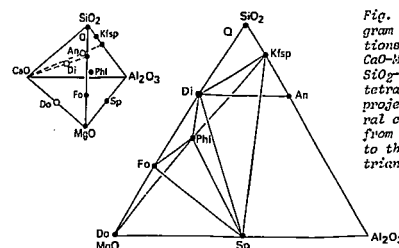


Fig. 4. Schematic diagram of phase relations in the system CaO - MgO - K_2O - Al_2O_3 - SiO_2 - CO_2 - H_2O . Small tetrahedron shows projection of mineral compositions from the CaO apex onto the SiO_2 - MgO - Al_2O_3 triangle.

In the high-silica, high-potassium part of the rock system, assemblages with quartz, alkali-feldspar and anorthite occur. One of the main assemblages is Di - Q - Kfs - An , with some additional phlogopite or calcite in a few samples. Common assemblages are Di - Q - Kfs , Di - Kfs (occasionally with some calcite) and Q - Kfs . Although interpretation of these assemblages, in terms of reactions or P - T estimates, is more difficult than in the "marble" system, metasomatism might have been an important process in the formation of, at least, the high-variance assemblages. The individual minerals quartz, alkali-feldspar and anorthite are found to be mutually incompatible with forsterite, spinel and dolomite. The only exception is the pair spinel-alkali-feldspar in the scarcely occurring assemblage Phl - Sp - Kfs .

MINERAL CHEMISTRY

As an illustration of the mineral chemistry some electron microprobe analyses of the minerals forsterite, clinopyroxene, phlogopite, spinel, garnet, scapolite, calcite and dolomite are given in Table 4.

Forsterite. - It has a X_{Mg} -ratio of 0.92 to 0.95 ($X_{Mg} = Mg(\text{atoms}) / (Mg + Fe + Mn)(\text{atoms})$). The MnO and CaO contents of forsterite are relatively high, up to 0.7 and 1.4 wt% respectively. Preliminary data show low Ca contents in forsterite cores and high (twice as much) in rims.

Table 3. Microprobe analyses.

min. 1	Fe	Fe	Fe	Al	Al	Al	Sp	min. 2	Fe	Fe	Fe	Al	Al	Al	Sp
sample	Q133	Q133	Q133	Q133	Q133	Q133	Q133	sample	Q133	Q133	Q133	Q133	Q133	Q133	Q133
loc. 1	A	B	C	D	E	F	G	loc. 2	A	B	C	D	E	F	G
wt%								wt%							
SiO ₂	54.3	51.0	52.5	51.6	51.6	50.7	0.26	SiO ₂	54.9	51.1	51.5	52.1	50.2	52.1	
TiO ₂	n.d.	n.d.	n.d.	0.18	0.84	0.50	n.d.	TiO ₂	0.79	0.51	0.53	0.18	0.36	n.d.	
Al ₂ O ₃	n.d.	0.3	0.6	3.21	0.21	5.19	0.7	Al ₂ O ₃	18.0	14.2	16.5	3.59	7.38	27.3	
FeO	0.95	0.55	7.80	0.21	0.18	0.27	0.31	FeO	1.52	1.22	3.28	19.8	12.17	n.d.	
MnO	0.41	0.42	0.43	0.21	0.18	0.27	0.31	MnO	0.96	0.81	0.88	0.42	0.24	n.d.	
MgO	57.7	52.8	50.5	49.5	49.5	49.5	23.2	MgO	26.1	26.3	25.2	5.78	0.35	n.d.	
CaO	0.75	0.17	0.08	21.8	15.7	35.5	0.84	CaO	n.d.	0.53	0.4	23.3	37.3	20.6	
Total	99.51	99.22	100.29	100.84	99.79	99.82	99.49	Total	99.51	99.22	100.29	100.84	99.79	99.82	99.49
X _{Mg}	0.957	0.949	0.921	0.961	0.924	0.905	0.908	X _{Mg}	0.967	0.974	0.971	0.935			

Clinopyroxene. - In the marbles X_{Mg} of diopside varies from 0.94 to 0.98. $Wt\% Al_2O_3$ is 0.2 to 3.2. The highest Al contents occur in spinel-bearing marbles. Preliminary data seem to point to Al-rich cores and Al-poor rims of the subhedral diopside crystals. Diopside rims (around forsterite) generally have a low Al content. In the diopside rocks X_{Mg} is 0.88 to 0.91. $Wt\% Al_2O_3$ varies between 1.8 and 5.2. Fe-rich clinopyroxenes occur in quartz-diopside gneisses and in andradite-hedenbergite bearing rocks. In reality "hedenbergite" has a composition of salite to ferrosalite. The X_{Mg} can be as low as 0.30. (Pure hedenbergite has been observed in an isolated occurrence of andradite-hedenbergite rock north of Tonstad (Wegelin 1979a)). In the clinopyroxenes TiO_2 may be present to a maximum of 0.50 wt% (in a diopside rock). Generally Ti shows a positive correlation with Al (Al:Ti is about 15:1). MnO is present up to 0.70 wt% (in an andradite-hedenbergite rock).

Phlogopite. - X_{Mg} varies from 0.94 to 0.97 in the marbles and from 0.91 to 0.93 in the diopside rocks. Phlogopite inclusions in diopside grains tend to have lower X_{Mg} values than other phlogopites. Phlogopite, mainly in barite-bearing marbles, may contain several percent of BaO. The F content varies from 0.2 to 3.3 wt%.

Spinel. - This is relatively rich in Fe compared with other minerals in the marbles. A nearly colourless spinel in marble has a X_{Mg} of 0.90.

Garnet. - This is a solid solution mainly between andradite and grossular. Molar ratios of andradite/grossular vary between about 55/34 and 75/21. Pyrope and spessartine components may amount to 1 or 2 mol% each, almandine may be present up to 7 mol%.

Scapolite. - This is a very melonite-rich variety. MeX is 85 to 87 which is about the maximum amount possible.

Calcite. - The $MgCO_3$ content in calcite varies from 2.5 to a maximum of approximately 11 wt% (microprobe and XRD analyses (Teste 1977)). X_{Mg} is about 0.80 in the lowest Mg-calcites and 0.95 in the highest. The $MnCO_3$ content is generally higher than the $FeCO_3$ content. Maxima are 0.8 and 0.5 wt% respectively.

Dolomite. - The $CaCO_3$ content in dolomite varies from 55 to 59 wt%. Exsolved dolomite with a high Ca content occurs in high Mg-calcites, dolomite with a lower Ca content in low Mg-calcites. Primary dolomite seems to have incorporated less Ca than exsolved dolomite. X_{Mg} in both types of dolomite is approximately 0.97. $Wt\% FeCO_3$ and $MnCO_3$ have maxima of 1.6 and 0.7 respectively.

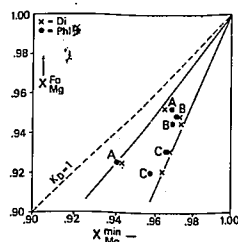


Fig. 5. X_{Mg} -plot for the minerals forsterite, diopside and phlogopite from locations A, B and C. Averages of X_{Mg} values are used for each mineral. Solid lines indicate maximum (near $Kp=1$) and minimum Kp values. $Kp = X_{Fo}(1-X_{Mg}^{min})/X_{Mg}^{min}(1-X_{Fo})$.

DISCUSSION AND CONCLUSIONS

The sequence of the minerals with a decreasing X_{Mg} , Do-Di-Pl>Fo>Cc-Sp, is similar to that found by Glassley (1975) and Rice (1977a, 1977b). In Fig. 5 the X_{Mg} of forsterite is plotted against the X_{Mg} of diopside and phlogopite. Values of each location fall approximately on one K_p -line. This suggests a local attainment of equilibrium for the Mg, Fe and Mn distribution between the three phases. K_p -values for location A are higher than for the other locations. This could be the result of higher metamorphic temperatures in the southern part of the area near the intrusive complexes. Application of calcite-dolomite geothermometry has revealed temperatures of about 670°C for location C, 740°C for B and 600°C for A. These results, especially the temperature for A, are not in close agreement with other independently determined temperature estimates (e.g. Jacques de Dixmude 1978, Maijer et al. 1981). This is due to 1) the absence of dolomite at location A, resulting in a Mg content in the calcite not being determined by the calcite-dolomite solvus, and 2) the dolomite exsolution in calcite at B and C, causing the formation of a lower Mg-calcite than the original unexsolved Mg-calcite. Therefore the temperatures must be considered as minimum values. The highest minimum temperature at a given location can be derived from the highest Mg content found in calcite. Calculation has been done with the formula given by Rice (1977a), based on the experimental data of Graf and Goldsmith (1955) and Goldsmith and Newton (1969): $\log X_{Mg}^{CaCO_3} = -1690/T^{\circ}K + 0.795$. Both the $FeCO_3$ and $MnCO_3$ content are low in the analysed calcites and they will not have large effects on the calculated temperatures (Bickle and Powell 1977).

Total pressures in the region near the leplolith are estimated at 3-6 kb (Hermans et al. 1976). At a pressure of 5 kb phase relations in the marbles indicate temperatures of about 670°C and higher (especially at A) at moderate to high X_{CO_2} ratios (Fig. 3), assuming that (14) is the most determining reaction for the mineral assemblages in the marbles. Indeed relatively high X_{CO_2} ratios are found in fluid inclusions in quartz pods and veins enclosed in the marbles (Swanenberg 1980).

All these factors, element distribution, calcite-dolomite geothermometry (only regarding B and C) and phase relations suggest a temperature gradient from low temperatures at location C to high temperatures at A, possibly reflecting the M2 phase of metamorphism (Maijer et al. 1981). From phase relations it is also concluded that metasomatism has played a certain role in establishing the mineral assemblages. This is supported by field observations such as the occurrence of diopside rocks between marbles and silica-rich rocks.

Acknowledgements. The author wishes to thank Dr. J. Ben H. Jansen, who suggested this study and whose stimulating discussions were indispensable. Drs. A.C. Tobl, C. Maijer, G.A.E.M. Hermans, F.J.M. Rietmeijer, H.E.C. Swanenberg and A. Senior are kindly thanked for their support and critical reading of the manuscript. A. Wegelin is thanked for his permission to use some of his microprobe analyses.

This work forms part of a study on the siliceous dolomites in Rogaland, made possible by financial support from the Netherlands organization for the advancement of pure research (Z.W.O.) (grant 18.21.06). Minerals were analysed using a TPD electron microprobe which was financially supported by Z.W.O.

REFERENCES

- Bickle, M.J. and Powell, R. 1977: Calcite-dolomite thermometry of iron-bearing carbonates. The Glockner area of the Tauern window, Austria. *Contrib. Mineral. Petrol.* 59, 281-292.
- Dekker, A.G.C. 1978: Amphiboles and their host rocks in the high-grade metamorphic Precambrian of Rogaland, S.W. Norway. *Geol. Ultrafascina* 17, 277 pp.
- Glassley, W.E. 1975: High grade regional metamorphism of some carbonate bodies: significance for the orthopyroxene isograd. *Am. J. Sci.* 275, 1133-1163.
- Goldsmith, J.R. and Newton, R.C. 1969: p-T-X relations in the system $CaCO_3$ - $MgCO_3$ at high temperatures and pressures. *Am. J. Sci.* 267-A (Schairer vol.), 160-190.
- Graf, D.L. and Goldsmith, J.R. 1955: Dolomite-magnesian calcite relations at elevated temperatures and CO_2 pressures. *Geochim. Cosmochim. Acta* 7, 109-128.
- Hermans, G.A.E.M., Hakstge, A.L., Jansen, J.B.H. and Poorter, R.P.E. 1976: Sapphirine occurrence near Vikeså in Rogaland, southwestern Norway. *Nor. Geol. Tidsskr.* 56, 397-412.
- Hermans, G.A.E.M., Tobl, A.C., Poorter, R.P.E. and Maijer, C. 1975: The high-grade metamorphic Precambrian of the Sirdal-Bredal area, Rogaland/Vest-Agder, South-west Norway. *Nor. Geol. Unders.* 318, 51-74.
- Jacques de Dixmude, S. 1978: Géothermométrie comparée de roches du faciès granulite du Rogaland (Norvège méridionale). *Bull. Minéral.* 101, 57-65.
- Legrand, J.-M. 1976: Etude pétrologique des séries gneissiques et anatectiques catazonales du dôme de Sandnes-Håle. Les équilibres minéralogiques. Thèse Bruxelles, 219 pp.
- Maijer, C., Jansen, J.B.H., Hebeda, E.H., Verschure, R.H. and Andriessen, P.A.M. 1981: Osumilite, an approximately 970 Ma old high-temperature index mineral of the granulite facies metamorphism in Rogaland, SW Norway. *Geol. Mjnb.* 60, 267-272.

- Moore, A.C. 1970: Descriptive terminology for the textures of rocks in granulite facies terrains. *Lithos* 3, 123-127.
- Rice, J.M. 1977a: Contact metamorphism of impure dolomitic limestone in the Boulder aureole, Montana. *Contrib. Mineral. Petrol.* 59, 237-259.
- Rice, J.M. 1977b: Progressive metamorphism of impure dolomitic limestone in the Marysville aureole, Montana. *Am.J.Sci.* 277, 1-24.
- Rietmeijer, F.J.M. 1979: Pyroxenes from iron-rich igneous rocks in Rogaland, SW Norway. *Geol. Ultrafascina* 21, 341 pp.
- Swanenberg, H.E.C. 1980: Fluid inclusions in high-grade metamorphic rocks from S.W. Norway. *Geol. Ultrafascina* 25, 147 pp.
- Teske, H. 1977: Geologisch en petrologisch onderzoek aan de marmeren in Rogaland. Internal report, Dept. of Petrology, Rijksuniversiteit Utrecht. 42 pp.
- Thompson, J.B. 1959: Local equilibrium in metasomatic processes, 437-457. In Abelson, P.H. (ed.), *Researches in geochemistry*. John Wiley and Sons, Inc., New York.
- Verschure, R.H., Andriessen, P.A.M., Boelrijk, N.A.I.M., Hebeda, E.H., Maijer, C., Friem, H.N.A. and Verdurmen, E.A.Th. 1979: Coexisting primary biotite of sveconorwegian age and secondary biotite of caledonian age in sveconorwegian basement rocks close to the caledonian front in SW Norway. *Abstr. of papers EOCG VI. Lillehammer*.
- Vidale, R. 1969: Metasomatism in a chemical gradient and the formation of calc-silicate bands. *Am.J.Sci.* 267, 857-874.
- Weeks, W.F. 1956: A thermochemical study of equilibrium relations during metamorphism of siliceous carbonate rocks. *J.Geol.* 64, 245-270.
- Wegelin, A. 1979a: Enkele aspecten van de associatie andradiet-hedenbergiet-scapoliet in Rogaland/Vest-Agder, zuidwest Noorwegen. Internal report, Dept. of Petrology, Rijksuniversiteit Utrecht. 79 pp.
- Wegelin, A. 1979b: Veldwerk in het gebied Riggård-Gjesdal-Nedrabø. Internal report, Dept. of Petrology, Rijksuniversiteit Utrecht. 98 pp.
- Wielons, J.B.W., Andriessen, P.A.M., Boelrijk, N.A.I.M., Hebeda, E.H., Friem, H.N.A., Verdurmen, E.A.Th. and Verschure, R.H. 1980: Isotope geochronology in the high-grade metamorphic Precambrian of southwestern Norway: new data and reinterpretations. *Nor. Geol. Unders.* 359, 1-30.
- Winkler, H.G.F. 1979: *Petrogenesis of Metamorphic Rocks*. 5th ed., Springer-Verlag, Berlin-Heidelberg-New York, 348 pp.

CHAPTER 2

ZONING IN DIOPSIDE FROM GRANULITE FACIES MARBLES FROM ROGALAND, SW NORWAY

ABSTRACT

Mg-rich clinopyroxenes from marbles and diopside rocks from the granulite facies terrain of Rogaland, SW Norway, can be strongly zoned. The zoning, in general optically not visible, is characterized by an Al-rich core, in some cases enriched in Ti and Fe³⁺, and a rim, rich in Mg and Si. The zoning is observed to be strongest in spinel-bearing marbles and in phlogopite-bearing diopside rocks. The most determining factors in its formation are changes in the activity-ratio of Al and Si, while coupled substitutions play an important role in the chemistry of the pyroxene during growth. Presumably the zoning in the clinopyroxenes was formed in a prograde metamorphic as well as in a late, metasomatic stage.

INTRODUCTION

Several exposures of marbles and calc-silicate rocks, known as the Faurefjell formation, occur within the migmatites of the high-grade metamorphic Precambrian of Rogaland, SW Norway (Sauter 1981) (Fig. 1). These migmatites surround intrusive complexes of anorthosites and of the leuconoritic to quartz monzonitic lopolith of Bjerkreim-Sokndal (Hermans et al. 1975). Several stages of metamorphism, M1 to M4, have been recognized in garnetiferous intercalations within the migmatites (Kars et al. 1980, Maijer et al. 1981). The upper amphibolite facies metamorphism of the M1 stage is followed by the M2 stage, characterized

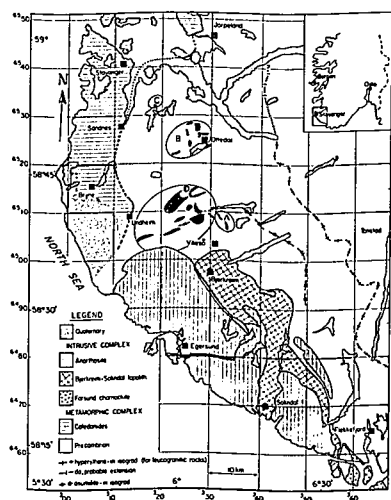


Fig. 1. Geological sketch-map of SW Norway. Outcrops of the Faurefjell formation, at locations A, B, C and D, are indicated in black.

by a granulite facies metamorphism. The age of this stage is estimated at about 1050 Ma (Wielens et al. 1981). The temperature of this metamorphic event shows a gradual increase from about 800°C at some 25 to 30 km north of the intrusive masses to 1000°C near the intrusives (Jacques de Dixmude 1978, Hermans et al. 1976, Meijer et al. 1981). The M3 stage is a low granulite to upper amphibolite facies metamorphism. M4 represents a retrogressive stage and has presumably a Caledonian age.

In marbles and diopside rocks of the Faurefjell Formation compositional zoning in diopside has been recognized by means of electron microprobe analysis. In metamorphic rocks compositional zoning in clinopyroxene is rare, or at least rarely described. In

garnet-bearing rocks however, zoned clinopyroxenes have been observed together with zoned garnet (e.g. Loomis 1977, Coolen 1980). In volcanic rocks zoning may be very common, due to fractionation processes between phenocrysts and the melt and a rapid cooling. In metasomatic rocks like skarns zoning may be present as result of fluctuating fluid compositions during growth (e.g. Kwak and Tan 1981).

PETROGRAPHY

In the marbles of the Faurefjell formation the main rock types are forsterite marble and diopside marbles, characterized by the following main mineral associations: Fo-Phl-Cc+Di+Do+Sp and Di-Phl-Cc respectively (Sauter, 1981). Diopside rocks, intercalated in the marbles or at contacts between marbles and silica-rich rocks, mainly consist of diopside with varying amounts of phlogopite and calcite. Very seldomly forsterite or enstatite are present. The mineral content of the samples used in this paper is given in Table 1.

Table 1: List of mineral contents.

Sample	loc	Fo	Di	En	Phl	Sp	Cc	Do ¹⁾
X A164 Fo marble	A	x	o		x			
● B624 Fo marble	A	x	o		o	o	x	
+ C163 Di-Phl rock	C		x		x		s	
■ C235 Di marble	C		x		x		x	
■ C336 Fo marble	A	x	o ²⁾		o	o ³⁾	x	
▲ C347 Di-Fo-En rock	A	x	x	o	s		s	
□ C372 Fo marble	B	x	a		a	o	x	x
○ C480 Fo marble	A	x	a		a	o	x	
△ Q75 Fo marble	B	x	o ⁴⁾		x		x	
□ Q138 Fo marble	B	x	o		o	o	x	o
○ H5208 Fo marble	B	x	o		o		x	o

Only main minerals are mentioned. x=major, o=minor, a=accessory. 1) Exsolved dolomite not included. 2) Mainly in clusters, partly surrounded by forsterite rims. 3) Only a single grain, as inclusion in forsterite. 4) Only as rims around forsterite. Fo=forsterite, Di=diopside, En=enstatite, Phl=phlogopite, Sp=spinel, Cc=calcite, Do=dolomite.

In all the rocks studied here, except in sample C480, diopside is completely colourless. It may contain inclusions of calcite and, especially in the diopside-phlogopite rock, inclusions of phlogopite. Twin lamellae parallel to (100) and occasionally clinopyroxene exsolution lamellae parallel to (001) may be present.

In many forsterite marble samples diopside is only a minor constituent, representing only a few percent of the total rock volume. Diopside often contacts forsterite, and its crystals may partly enclose the rounded forsterite grains (Fig. 2). Small rims of diopside around forsterite also occur (Fig. 3), while in a few samples rims around several forsterite grains are connected to each other along calcite grain boundaries (Fig. 4). In this case an optically homogeneous, poikiloblastic diopside crystal has been formed. This diopside may also partly enclose phlogopite. In some forsterite marbles, e.g. C336, clusters of diopside grains occur, which are surrounded by a rim of forsterite or its retrogressive product serpentine. The forsterite may have a poikiloblastic appearance (Fig. 8). In the same thin section normal, rounded forsterite grains occur, occasionally with partly surrounding diopside grains and rims. Forsterite rims are also frequently observed at contacts between diopside rocks and forsterite marbles.



Fig. 2. Diopside, partly surrounding rounded forsterite. Diopside, as well as forsterite are locally serpentinized. Photomicrograph, sample C372. Plane polarized light. See Fig. 6 for drawing. Abbreviations: Dt = diopside, Fo = forsterite, Co = calcite, Do = dolomite, Phl = phlogopite, Clh = clinohumite.

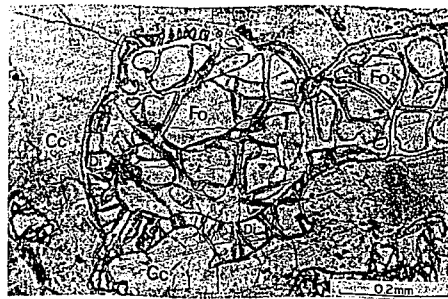


Fig. 3. Rim of diopside around forsterite. Photomicrograph, A164. Plane polarized light. Abbr.: see Fig. 2.



Fig. 4. Diopside rims around forsterite. The rims are connected with each other along calcite grain boundaries. Diopside forms one large poikiloblastic crystal. Photomicrograph, 375. Plane polarized light. Abbr.: see Fig. 2.

In spinel-bearing forsterite marbles spinel can be incorporated in forsterite or it may occur as individual grains. No spinel inclusions have been observed in diopside. Phlogopite in these marbles is mainly present as inclusions in forsterite.

In diopside marbles diopside is a major constituent, forming a more or less equigranular polygonal texture with phlogopite and calcite.

In the diopside-phlogopite rocks, e.g. C165, the same texture is mainly formed out of diopside and phlogopite. The texture is in some cases obliterated by the occurrence of large diopside poikiloblasts, with inclusions of small phlogopite grains.

In the enstatite-bearing diopside rock, C347, layers of pure diopside alternate with forsterite in irregular zones parallel to the diopside rock - marble contact. Textures indicate that the fine-grained enstatite has formed at the expense of diopside and forsterite.

Summarizing, it can be concluded on textural grounds that phlogopite and spinel are early phases, formed prior to forsterite. At least a part of diopside, i.e. those grains or parts of grains which surround forsterite, and the discrete diopside rims around forsterite, have been

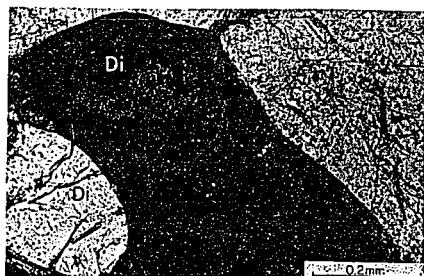


Fig. 5. Zoning in diopside, visible as region of different optical orientation. Photomicrograph, C480. Crossed polarizers. See Fig. 7 for drawing. Abbr.: see Fig. 2.

formed late in the metamorphic/metamorphic history of the marbles. A more detailed account of the succession of formation of the minerals is given in Chapter 4.

MORPHOLOGY OF THE ZONING

The pattern of the Al distribution is optically only visible, as it will appear later, in the Al- and Ti-rich clinopyroxenes of the forsterite-spinel-diopside marble C480. In plane-polarized light, parts of some crystals show a very faint brownish pleochroism. With crossed polarizers these parts are more clearly defined by means of a zonal extinction (Fig. 5). Although the boundaries between the zones are somewhat diffuse, clearly an inner and outer zone can be distinguished. The zonal extinction, although most evident at the zonal boundaries, is gradual through the whole crystal. In another clinopyroxene section in the same sample, the limits of the zones are accentuated by thin growth layers. Using the universal stage, the orientation of these growth layers could be determined as approximately (112) and (203). The boundaries of the zones in the clinopyroxene of Fig. 5 seem to have the same orientation.

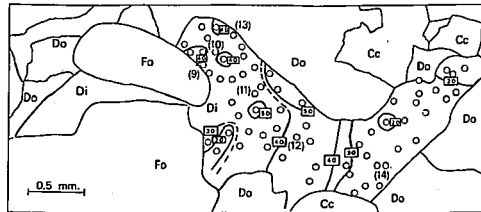


Fig. 6. Zoning of Al in diopside. Heavy lines represent Al contours. Numbers in rectangles indicate wt% Al_2O_3 . Small circles are microprobe spots, numbers in parenthesis correspond with the complete analyses given in the Appendix. Other analyses are partial. Observed range is 1.2 to 5.7 wt% Al_2O_3 . Drawing after photomicrograph (see Fig. 2), C372. Abbr.: see Fig. 2.

ANALYTICAL PROCEDURE

Electron microprobe analyses have been obtained using the Cambridge Scientific Instruments Geoscan and Microscan M-9 at the Vrije Universiteit in Amsterdam. Operating conditions were 20KV accelerating potential and 25nA beam current. Various synthetic and natural oxides and silicates were used as standards. Raw data were corrected with the M-9 computer program.

CHEMICAL CHARACTERISTICS OF THE ZONING

Electron microprobe analyses of the clinopyroxenes, as listed in the Appendix, show a considerable spread in composition. This variation, especially reflected in the Al content, can be observed between samples, within a sample and even within one grain. As the chemical variation is generally not expressed in optical properties, except for

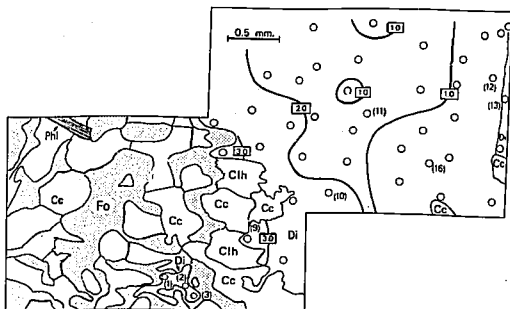


Fig. 8. Zoning of Al in diopside. Explanation in text of Fig. 6. Observed range in the large diopside grain 0.3 to 3.4 wt% Al_2O_3 , in the small grain enclosed by forsterite (bottom left) 2.7 to 3.9 wt% Al_2O_3 . The large diopside grain is part of a cluster of diopside grains, surrounded by an irregular, poikiloblastic rim of forsterite. Drawing after photomicrograph, C336. Abbr.: see Fig. 2.

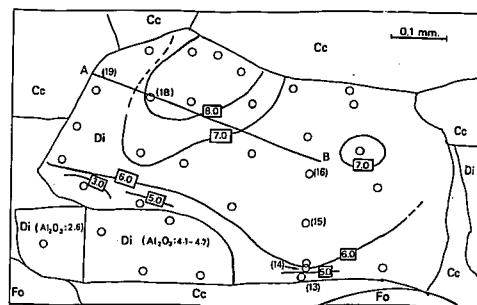


Fig. 7. Zoning of Al in diopside. Explanation: see Fig. 6. Observed range 2.5 to 8.6 wt% Al_2O_3 (small grains at bottom left not included). Drawing after photomicrograph (see also Fig. 5), C480. A-B: microprobe stepscan of Fig. 8. Abbr.: see Fig. 2.

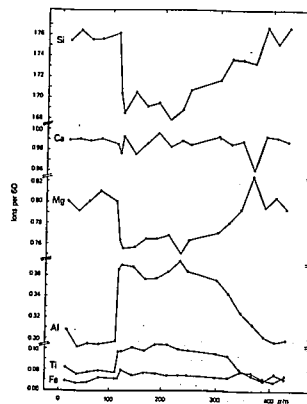


Fig. 9. Microprobe stepscan across profile A (left) - B (right) in diopside of C480 (see Fig. 7). Semi-quantitative microprobe analyses.

clinopyroxenes from sample C480, the chemical morphology of the zoning has been made visible by means of several microprobe analyses of Al within one crystal (Figs. 6, 7 and 8). As it is clear from these figures, the Al distribution shows a zonal, somewhat irregular pattern. The compositional gradients may be sharp at some places, gradual at others. There is no evidence of a relation between the zoning pattern and the composition of the adjacent crystals. Compositional differences within a crystal may be very large, e.g. from 2.5 to 8.6 wt% Al_2O_3 in sample C480 (Fig. 7).

A microprobe scan has been made over the high-Al region of the clinopyroxene of this sample to show the variation in Al, Si, Ca, Mg, Fe and Ti (Fig. 9). The central part of the pyroxene profile indicates an enrichment in Al, Ti and slightly in Fe, while the outer regions are enriched in Si and Mg. Ca shows no definite preference for either of the zones. Striking is the sharp jump in the amount of Al in the left-hand side of the figure, from about 6.8 to 8.3 wt% Al_2O_3 . At the right-hand side the drop in Al is more gradual. The high-Al part of the crystal, depicted in Figs 7 and 9, coincides very well with the zone of different optical orientation as shown in Fig. 5.

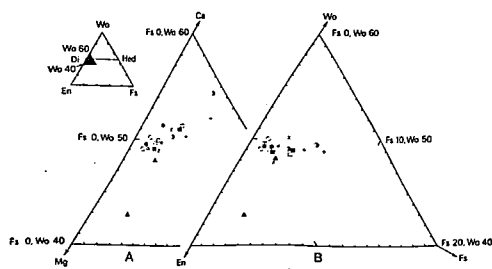


Fig. 10. Compositions of the analysed clinopyroxenes in the pyroxene quadrilateral. Inset (left) shows position of compositional triangles. From samples with strongly varying compositions only the two extremes are plotted. A: Compositions plotted as functions of Ca, Mg, Fe+Mn ions. B: End-members calculated according to Cawthorn and Collerson (1974). Symbols: see Table 1.

CHEMISTRY OF THE CLINOPYROXENES

Although the chemical variations are large, the compositions of the pyroxenes only occupy a small part of the pyroxene quadrilateral (Fig. 10). The pyroxenes have a Mg-rich composition, as is usual for minerals from metamorphosed siliceous dolomites (e.g. Glassley 1975, Rice 1977a, 1977b). The ferrosilite component does not exceed 7%. Fe-richer clinopyroxenes occur in the more siliceous parts of the Faurefjell formation, e.g. the quartz-diopside gneisses (Sauter, 1981), but these are not included in this study.

Several analyses in the quadrilateral, plotted as functions of Ca, Mg and Fe+Mn (Fig. 10A), show a trend into wollastonite contents higher than 50%. These are not due to a higher amount of Ca, but to a lower Mg content and relatively low Mg+Fe+Mn totals in Al-rich clinopyroxenes. This distorting effect can be compensated for by assigning Al mainly to the Ca-Tschermak's molecule ($\text{CaAl}_2\text{SiO}_6$), by calculating the pyroxene end members using the scheme of Cawthorn and Collerson (1974) (Fig. 10B). Anomalously low wollastonite contents are found for clinopyroxenes from a diopside-forsterite-enstatite rock

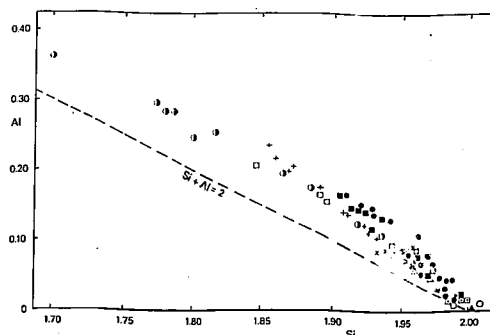


Fig. 11. Si versus Al plot (ions per 6 O) for the analysed clinopyroxenes. Symbols: see Table 1.

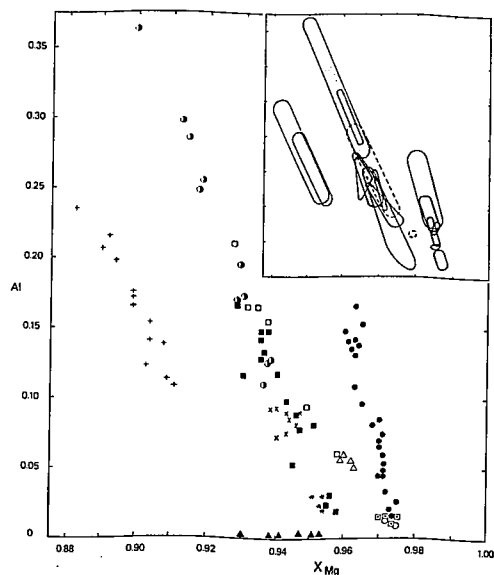


Fig. 12. Variation of X_{Mg} with Al for the analysed clinopyroxenes. $X_{Mg} = Mg/(Mg+Fe+Mn)$, where all Fe has been calculated as Fe^{2+} . Highest Al content found, in C480, corresponds to 8.3 wt% Al_2O_3 . Inset shows the X_{Mg} -Al range within each analysed grain in the samples C165, C480, C372, C336 and BE24. Left: C165, two grains. Middle: Stippled: C480, three grains. Middle: Interrupted lines: C372, two grains. Middle: solid lines: C336, four grains. Right: BE24, six grains. Lowest range from diopside rim around forsterite. Symbols: see Table 1.

(sample C347). The compositional range encountered here is not the result of a variation in Al, but it is due to real variations in Ca and Mg.

In the analysed clinopyroxenes the amount of Al is more than sufficient to compensate for silica deficiency on the pyroxene tetrahedral sites (Fig. 11). Excess Al, indicated as the amount of Al larger than $Si+Al=2$, thus enters the octahedral M1 site. The variation of octahedral Al with total Al is different for the various samples. With increasing total Al, in the analyses of samples C480 and C372 octahedral Al remains nearly constant, while for the samples C165 and BE24 an increase of octahedral Al can be observed.

The variation in total Al in the clinopyroxenes is well correlated with a change in X_{Mg} , calculated as $Mg/(Mg+Fe+Mn)$ (Fig. 12). Generally excellent negative correlations exist between analyses within one grain, between grains from the same sample, and also between several samples. High Al contents are especially found in pyroxenes in the spinel-bearing samples (BE24, C372 and C480) and in the diopside-phlogopite rock (C165). Different grains from the same sample

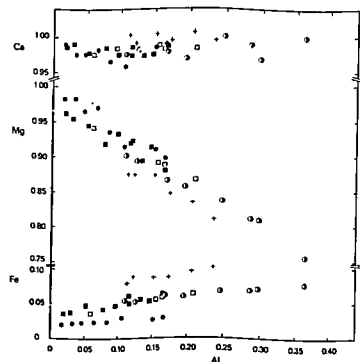


Fig. 13. Variation of Ca, Mg and total Fe (as Fe^{2+}) with Al content (ions per 6 O) for the clinopyroxenes from the samples BE24, C165, C336, C372 and C480. Symbols: see Table 1.

generally all show the same negative correlation between Al and X_{Mg} , although range, and maximum and minimum Al content vary (See inset of Fig. 12). Diopside rimming forsterite, in sample BE24, shows the lowest amount of Al in this particular sample. Here there seems to be a complete transition from high Al contents in a large diopside crystal, via intermediate contents in small crystals to the low amount of Al in the diopside rims. In the spinel-lacking marble Al64 the composition of diopside rims along forsterite is almost equal to that of the larger diopside crystals. In sample C336 a small diopside rim reveals a relatively high Al content, while the composition of large diopside crystals in a cluster grades into low Al values. A more or less homogeneous composition and a low Al content in the clinopyroxenes is encountered in the spinel lacking marbles.

The variation in X_{Mg} with Al, as shown in Fig. 12, is the reflection of both a decrease of Mg as an increase of total Fe with increasing Al in the pyroxene composition (Fig. 13). The amount of Ca, and of Mn (not shown) does not seem to be influenced by a variation in Al.

As has been stated at the discussion of Fig. 11, the amount of octahedral Al in pyroxenes from the samples C480 and C372 remains constant, irrespective of the total and tetrahedral Al content. Therefore, charge balance and replacement of Mg at the octahedral sites (see fig. 13) must be accomplished by some other ion species. In these

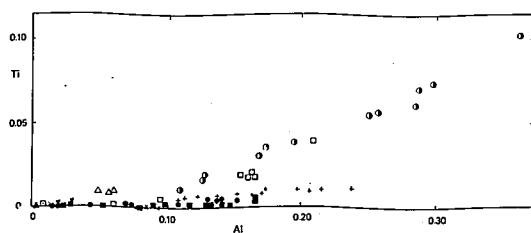


Fig. 14. Variation of Ti with Al (ions per 6 O) for the clinopyroxenes. Note the different slopes for different samples. Symbols: see Table 1.

particular samples, the high Ti contents, up to 3.6 wt% TiO_2 , and the good positive correlations between Al and Ti (Fig. 14), indicate that Ti plays a major role. Samples with low amounts of Ti, such as BE24 and C165, also show positive Al-Ti correlations. In the low-Al pyroxenes, only sample Q75 (diopside rims around forsterite) contains relatively high amounts of Ti.

The presence of Ti however, is not in all analyses sufficient for a total charge balance. Therefore it is assumed that a part of total Fe is present as Fe^{3+} , a fact which is also supported by high cation sums

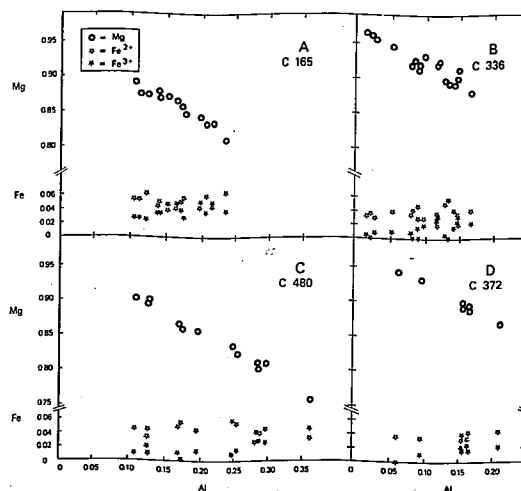


Fig. 15. Variation of Mg, Fe^{2+} and Fe^{3+} with Al content (ions per 6 O) for analysed clinopyroxenes in samples C165 (A), C336 (B), C480 (C) and C372 (D).

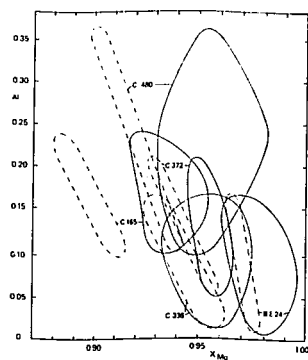


Fig. 16. Shift of X_{Mg} in the pyroxene X_{Mg} -Al plot as a result of the correction for Fe^{3+} . Interrupted lines: X_{Mg} -Al variation for C224, C165, C336, C372 and C480, X_{Mg} calculated with total Fe as Fe^{2+} (as in Fig. 12). Solid lines: X_{Mg} , corrected for Fe^{3+} , is calculated as $Mg/(Mg+Fe^{2+}+Mn)$.

displayed in several analyses. The presence of Fe^{3+} has also been demonstrated in two samples (C165 and C235) by wet chemical analyses of diopside concentrates (see Appendix). In the microprobe analyses Fe^{3+} has been calculated using the charge balance equation $Al^{VI}+Fe^{3+}+2Ti=Al^{IV}+Na$, according to Papke et al. (1974). Unfortunately, calculation of Fe^{3+} is inaccurate, due to errors in Si and Al measurements, which may contribute to relatively high errors in Al^{IV} and Al^{VI} determinations. Wet chemically determined Fe^{3+}/Fe^{2+} ratios in the samples mentioned are considerably lower than those calculated from microprobe analyses. Nevertheless, some trends in the behaviour of Fe^{3+} can be recognized, which may give more understanding of the role of ferric iron in the formation of the pyroxenes.

In Fig. 15, where for four samples total Fe has been divided in Fe^{2+} and Fe^{3+} , an increasing Al content seems to be coupled with an increasing amount of Fe^{3+} present. On the other hand Fe^{2+} seems to remain constant with variations in Al and Mg. Therefore, the positive correlation of total Fe with Al (Fig. 13) and the negative correlation of X_{Mg} with Al (Fig. 12), presumably are for the largest part due to a presence of Fe^{3+} in the Al-rich clinopyroxenes.

Recalculation of X_{Mg} , corrected for Fe^{3+} , and replotting the X_{Mg} values in the X_{Mg} -Al plot (Fig. 16), reduces the total range of X_{Mg} observed, from approximately 0.88-0.98 to 0.92-0.99, and shifts and obscures the earlier trends. The new trends in X_{Mg} -Al, although much more ill-defined, presumably by the errors in Fe^{3+} calculation mentioned above, show an almost constant X_{Mg} value, or a small decrease in X_{Mg} with increasing Al.

It is noteworthy that clinopyroxenes from several other studied areas, in more or less comparable rock types, show the same chemical behaviour with respect to the (uncorrected) X_{Mg} -Al relation as the Faurefjell clinopyroxenes do (Glassley 1975, Rice 1977a, 1977b, Kretz 1980). However, this holds only true for relations between samples, as chemical variation within a sample or within one crystal has not been reported from these studies. In Fig. 17 clinopyroxene data from several studies have been plotted. The trend within a sample of the Rogaland rocks is indicated by a solid line. Although for the y-axis in this figure another parameter has been used (wt% Al_2O_3 instead of cations

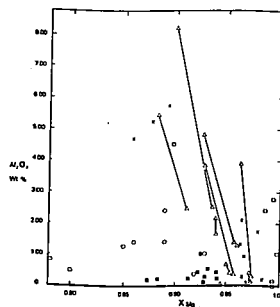


Fig. 17. X_{Mg} - Al_2O_3 plot for clinopyroxenes from several areas. Note: symbols have different meaning than in other figures. Open circles: Kretz (1980). Clinopyroxenes from high-grade Precambrian carbonate rocks, Grenville Province. Open squares: Rice (1977a). Contact metamorphic marbles, occasionally spinel bearing, Boulder aureole, Montana. Solid squares: Rice (1977b). Contact metamorphic marbles, Marysville aureole, Montana. Crosses: Glassley (1975). High grade metamorphic marbles and diopside rocks, Lofoten, Norway. Triangles: This work. For pyroxenes with large variations in Al content, only the extreme compositions are plotted, connected with a solid line. For all references, except Kretz: $X_{Mg}=Mg/(Mg+Fe^{2+}+Mn)$. For Kretz: $X_{Mg}=Mg/(Mg+Fe^{2+})$.

Al), these trends can easily be traced back to those in Fig. 12. Al-rich clinopyroxenes, occurring in spinel-bearing marbles (Rice 1977a, this work) or in diopside rocks (three points with highest Al content from Glassley 1975, this work) generally have lower X_{Mg} values with respect to the Al-poor pyroxenes from the same areas. The spinel-free marbles from the Montana aureole (Rice 1977b) also show low Al contents. Pyroxenes from Grenville marbles (Kretz 1980) do not show a definite trend.

DISCUSSION

Formation of the clinopyroxenes, reaction sequences in T - X_{CO_2} space.

Pyroxene growth in the forsterite marbles is possible at various stages in the metamorphic history. If the prograde metamorphism of the marbles has taken place under isochemical conditions, involving an internally buffered fluid composition, diopside will be formed prior to forsterite in the relatively Si- and Mg-rich calcareous rocks which are under interest here. The same is the case in externally buffered systems, where however the formation of diopside is dependent on the initial X_{CO_2} ratio.

In all these prograde reaction sequences forsterite will be formed from diopside- and tremolite-consuming reactions. No textural indications for the formation of forsterite have been found in the Rogaland marbles.

A later, post-forsterite, formation of diopside, as is apparently the case for at least a part of the marble pyroxenes, is possible in two ways, retrogressively and metasomatically. The retrogressive reaction $2Fo + 4Cc + 2CO_2 = Di + 3Do$, possible at high and low X_{CO_2} values (e.g. Eggert and Kerrick 1981) is one way to create diopside later than forsterite. Several authors (Martignole 1975, Legrand 1976, Lasnier 1977, Zingg 1980) report thin diopside rims around forsterite and some of them (Martignole and Zingg) indeed favour this retrogressive formation. In the Rogaland case however, no new formation of dolomite has been observed along these rims, neither an incorporation of Mg in the calcite is expected with decreasing temperature. The diopside rims around forsterite are therefore better explained by metasomatic reactions. Textures like the interconnected diopside rims (Fig. 4) also strongly suggest a metasomatic origin. These reactions could be

initiated by silica-rich fluids and they may be of the type $1Fo + 2Cc + 3SiO_2 = 2Di + 2CO_2$ and $1Do + 2SiO_2 = 1Di + 2CO_2$. Not only the thin rims around forsterite but also crystals and parts of crystals which partly enclose forsterite grains (see for example Fig. 2) may have originated as a result of these reactions.

Development of the zoning.

Some of the zoning patterns of the clinopyroxene, see for example Fig. 6 and 7, and the steep transition between high- and low-Al zones in Fig. 9, are reminiscent of sector zoning. This type of zoning, in which during growth chemical inequalities are produced in different crystallographic directions, has especially been observed in pyroxenes, notably titanaugites, in volcanic rocks (e.g. Hollister and Hargraves 1970, Wass 1973, Leung 1974) but also in staurolites in contact-metamorphic rocks (Hollister 1970) and in biotites in skarns (Kwak 1981). Apparently a relatively rapid crystal growth is one of the requirements for the origin of sector zoning.

In the Rogaland case an accurate determination of the zoning pattern in terms of crystal sectors is not possible, due to the scarce and faint optical expressions of the chemical zoning. In the crystal in Fig. 7 however, the chemistry of the high-Al zone, which perhaps could be designated as a basal sector, is in contradiction with the chemistry observed in basal sectors of titanaugites, which are low in Al (e.g. Leung 1974). Therefore it is assumed that the compositional zoning observed in the clinopyroxenes is not a sector zoning, but a more normal growth-zoning which originated during growth of the clinopyroxene, from a core rich in Al, and locally rich in Ti and Fe^{3+} , to rims rich in Si and Mg. Diopside in a cluster in C336 (Fig. 8) shows an Al-rich zone at the rim of the large crystal. This too indicates a growth zoning: this metasomatically grown diopside started to form at the contact of a quartz pod or vein with the marble, and grew inwards towards lower Al compositions.

As the largest Al contents and the largest spread in Al has been observed in clinopyroxenes in spinel-bearing marbles and in the diopside-phlogopite rock, so in Al-rich bulk compositions, it is inferred that the activity of Al, coupled with that of Si, is the most determining factor in the origin of the zoning. These activities may change as the result of a fractionation-depletion process, initially

described by Hollister (1966). Hereby the activity of, in this case, Al in the system is reduced by a continuous removal of Al by incorporation into the growing clinopyroxene. Concomitant crystallization of other Al-rich phases, like phlogopite or spinel, will enlarge the concentration gradient between core and rim of the clinopyroxene. During growth, coupled substitutions control the incorporation of other ions in the pyroxene structure. This is perfectly demonstrated by the well-defined trends in the several Al plots shown.

Timing of clinopyroxene growth and zoning.

Regarding the fact that the initial pyroxene composition apparently is dependent on the local bulk composition, e.g. Al-rich pyroxenes in spinel-bearing marbles, Ti-rich in C480, Fe-rich in C165, Fe-poor in BE24, one way of thought would be to assume that the Al-rich parts of the clinopyroxenes crystallized during the normal prograde metamorphism, before forsterite, in equilibrium with the other Al-bearing phases. The later, Al-poorer parts and rims around forsterite could be formed metasomatically after the forsterite formation.

The other alternative is a completely metasomatic origin for the whole clinopyroxene crystal, after the forsterite growth. In this case the link between pyroxene and bulk chemistry has to be explained, particularly the clinopyroxene Al-richness in spinel-bearing marbles. Spinel itself is a relatively early phase, in view of its inclusions in forsterite, and thus there is no way to assume a simultaneous, metasomatic growth of spinel and clinopyroxene from a Si- and Al-rich fluid. Furthermore no evidence has been found for spinel-consuming reactions which form Al-rich clinopyroxene. On the contrary, spinel has a fairly euhedral appearance and shows no relation with clinopyroxene.

Therefore, to explain the compositional relationship between clinopyroxene and bulk in a metasomatic origin it has to be assumed that an intruding Si-rich fluid has mixed with an intergranular Al-rich fluid phase. Zoning in the clinopyroxene may then develop by the fractionation-depletion process and by a dilution of the intergranular fluid by its metasomatic intruder.

It is difficult to decide which mode of origin is the most likely for the formation of the zoned clinopyroxenes in the marbles. Only for the diopside-phlogopite rock it seems clear, from field observations and phase relations (Sauter 1981), that the clinopyroxene formed under metasomatic conditions from a locally Si-, Al- and K-rich fluid. For the diopsides in the marbles a formation mainly in two stages, a high-Al prograde stage and a lower-Al metasomatic stage, seems to be the most likely. Zoning may have formed during both stages.

Striking features of the observations made here are the fact that this zoning is present in such high-grade rocks and that the zoning locally displays such sharp boundaries between high- and low-Al zones (see Fig. 9). For garnets it is demonstrated that original zoning patterns are often obliterated during high-grade metamorphism (Anderson and Olimpio 1977, Woodsworth 1977). Little is known however about Al diffusion in clinopyroxene. On crystal chemical grounds generally low diffusion rates for Al in silicates are expected (Dowry 1980). At about 1200°C and 1 bar, Al-diffusion in diopside (Seitz 1973) has approximately the same magnitude as Mn-Fe diffusion in garnet (Freer 1979), but extrapolation of high-temperature data to lower temperatures is dangerous because of the possible abrupt change in slope of the D/T curve (Dowry 1980).

REFERENCES

- Anderson, D.E. and Olimpio, J.C. 1977: Progressive homogenization of metamorphic garnets, south Morar, Scotland: evidence for volume diffusion. *Can. Mineral.* 15, 205-216.
- Cawthorn, R.G. and Collerson, K.D. 1974: The recalculation of pyroxene end-member parameters and the estimation of ferrous and ferric iron content from electron microprobe analyses. *Am. Mineral.* 59, 1203-1208.
- Coolen, J.J.M.M.M. 1980: Chemical petrology of the Furus granulite complex, southern Tanzania. *GUA papers of Geol. series 1*, no. 13, 258 pp.
- Dowry, E. 1980: Crystal-chemical factors affecting the mobility of ions in minerals. *Am. Mineral.* 65, 174-182.
- Eggert, R.G. and Kerrick, D.M. 1981: Metamorphic equilibria in the siliceous dolomite system: 6 kbar experimental data and geologic implications. *Geochim. Cosmochim. Acta* 45, 1039-1049.
- Freer, R. 1979: An experimental measurement of cation diffusion in almandine garnet. *Nature* 280, 220-222.

- Glassley, W.E. 1975: High grade regional metamorphism of some carbonate bodies: significance for the orthopyroxene isograd. *Am. Journ. Sci.* 275, 1133-1163.
- Hermans, G.A.E.M., Hakstge, A.L., Jansen, J.B.H. and Poorter, R.P.E. 1976: Sapphirine occurrence near Vikesø in Rogaland, southwestern Norway. *Nor. Geol. Tidsskr.* 56, 397-412.
- Hermans, G.A.E.M., Tobi, A.C., Poorter, R.P.E. and Maijer, C. 1975: The high-grade metamorphic Precambrian of the Sirdal-Ørsdal area, Rogaland/Vest-Agder, South-west Norway. *Nor. Geol. Unders.* 318, 51-74.
- Hollister, L.S. 1966: Garnet zoning: An interpretation based on the Raleigh fractionation model. *Science* 154, 1647-1651.
- Hollister, L.S. 1970: Origin, mechanism and consequences of compositional sector-zoning in staurolite. *Am. Mineral.* 55, 742-766.
- Hollister, L.S. and Hargraves, R.B. 1970: Compositional zoning and its significance in pyroxenes from two coarse grained Apollo 11 samples. *Proc. Apollo 11 Lun. Sci. Conf.* 1, 541-550.
- Jacques de Dixmude, S. 1978: Géothermométrie comparée de roches de faciès granulite du Rogaland (Norvège méridionale). *Bull. Minéral.* 101, 57-65.
- Karr, H., Jansen, J.B.H., Tobi, A.C. and Poorter, R.P.E. 1980: The metapelitic rocks of the polymetamorphic Precambrian of Rogaland, SW Norway - Part II. Mineral relations between cordierite, hercynite and magnetite within the omulite-in isograd. *Contrib. Mineral. Petrol.* 74, 235-244.
- Kretz, R. 1980: Occurrence, mineral chemistry and metamorphism of Precambrian carbonate rocks in a portion of the Grenville province. *Journ. Petrol.* 21, 573-620.
- Kvak, T.A.P. 1981: Sector-zoned annite, phlogopite, micas from the Mt. Lindsay Sn-W(-Be) deposit, Tasmania, Australia. *Can. Mineral.* 19, 643-650.
- Kvak, T.A.P. and Tan, T.H. 1981: The geochemistry of zoning in skarn minerals at the King Island (Dolphin) mine. *Ec. Geol.* 76, 468-497.
- Lasnier, B. 1977: Persistance d'une série granulitique au cœur du Massif Central Français. Haut-Allier. Les termes basiques, ultrabasiques et carbonatés. Thèse Université de Nantes, 351 pp.
- Legrand, J.-M. 1976: Etude pétrologique des séries gneissiques et anatectiques catazonales du dôme de Sandnes-Håle. Les équilibres minéralogiques. Thèse Bruxelles, 219 pp.
- Leung, I.S. 1974: Sector-zoned titanite: morphology, crystal chemistry and growth. *Am. Mineral.* 59, 127-138.
- Loomis, T.P. 1977: Kinetics of a garnet granulite reaction. *Contrib. Mineral. Petrol.* 62, 1-22.
- Martignole, J. 1975: Le Précambrien dans le sud de la province tectonique de Grenville (Bouclier Canadien). Etude des formations catazonales et des complexes anorthositiques. Thèse Toulouse. Université de Montréal, 405 pp.
- Maijer, C., Jansen, J.B.H., Hebeda, E.H., Verschure, R.H. and Andriessen, P.A.M. 1981: Omulite, an approximately 970 Ma old high-temperature index mineral of the granulite facies metamorphism in Rogaland, SW Norway. *Geol. Mijnb.* 50, 267-272.
- Papike, J.J., Cameron, K.L. and Baldwin, K. 1974: Amphiboles and pyroxenes: characterization of other than quadrilateral components and estimates of ferric iron from microprobe data. *Abstr. with Progr.* 1974, 1053-1054.
- Rice, J.H. 1977a: Contact metamorphism of impure dolomitic limestone in the Boulder aureole, Montana. *Contrib. Mineral. Petrol.* 59, 237-259.
- Rice, J.H. 1977b: Progressive metamorphism of impure dolomitic limestone in the Marysville aureole, Montana. *Am. Jour. Sci.* 277, 1-24.
- Sauter, P.C.G. 1981: Mineral relations in siliceous dolomites and related rocks in the high-grade metamorphic Precambrian of Rogaland, SW Norway. *Nor. Geol. Tidsskr.* 61, 35-45.
- Seitz, M.G. 1973: Uranium and Thorium diffusion in diopside and fluorapatite. *Carnegie Inst. Wash. Yearb.* 72, 586-588.
- Wase, S.Y. 1973: The origin and petrogenetic significance of hour-glass zoning in titaniferous clinopyroxenes. *Min. Mag.* 39, 133-144.
- Wielens, J.B.W., Andriessen, P.A.M., Boelrijk, N.A.I.M., Hebeda, E.H., Fries, H.N.A., Verdurmen, E.A.Th. and Verschure, R.H. 1981: Isotope geochronology in the high-grade metamorphic Precambrian of southwestern Norway: New data and reinterpretations. *Nor. Geol. Unders.* 359, 1-30.
- Woodsorth, G.J. 1977: Homogenization of zoned garnets from pelitic schists. *Can. Mineral.* 15, 230-242.
- Zingg, A. 1980: Regional metamorphism in the Ivrea Zone (Southern Alps, N-Italy): Field and microscopic investigations. *Schweiz. Mineral. Petrogr. Mitt.* 60, 153-179.

CHAPTER 3

EXSOLUTION, MAJOR ELEMENT AND ISOTOPE CHEMISTRY OF ROGALAND CARBONATES

ABSTRACT

The Mg-calcites in the Rogaland marbles show a large amount of dolomite exsolution. Several exsolution types can be recognized, of which tablet-like, rhombohedral and symplectitic types are the most important. The rhombohedral and a fine-grained symplectitic type may be correlated to retrograde metamorphic events.

The exsolution of dolomite has caused a decrease of the Mg-content of calcite. Original, pre-exsolution Mg-contents may have amounted up to 12 mole% MgCO_3 , corresponding to a temperature of about 700°C for locations B and C. The Mg-content of calcite in the dolomite-free marbles of location A is lower.

The carbon and oxygen isotope ratios of calcite show a trend from about $\delta^{13}\text{C} = -4$ (FDB) and $\delta^{18}\text{O} = +21$ (SHOW) for location A, to $\delta^{13}\text{C} = -7.5$ and $\delta^{18}\text{O} = +14$ for location C, close to the Caledonian front. Isotope ratios of calcites from veins and Caledonian marbles close to or just above the Caledonian boundary do not fit in the main trend. They show a $\delta^{13}\text{C}$ of -1 to -7 and a $\delta^{18}\text{O}$ of about +11. The decrease of the isotope ratios of calcites in the Precambrian marbles is mainly attributed to the activity of Caledonian retrogressive fluids.

INTRODUCTION

Marbles in the granulite facies Precambrian of Rogaland, SW Norway, occur in the Faurefjell formation, which rocks are intercalated in mainly charnockitic migmatites (Sauter 1981). These migmatites envelop

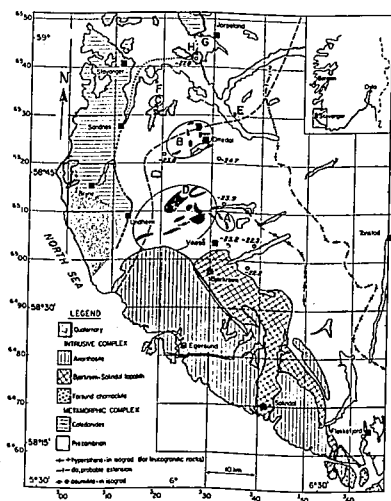


Fig. 1. Schematized geological map of Rogaland, SW Norway. In black (A to D): outcrops of the Faurefjell formation. E to H: locations of other carbonate samples used for isotope analysis. Numbers (-22.2 etc.): $\delta^{13}C$ of graphite in garnet-bearing rocks and breccia. Broken line: Green biotite in isograd.

the intrusive complexes consisting of anorthosites and the lopolith of Bjerkreim-Sokndal (Hermans et al. 1975) (Fig. 1). The marbles mainly consist of forsterite marbles, containing the mineral association Fo-Phl-Cc+Do+Di+Sp, while diopside marbles show the main association Di-Phl-Cc. Other rock types in the Faurefjell formation include diopside rocks, alkali-feldspar-rich rocks, quartzites and quartz-diopside gneisses. During the M2 granulite facies metamorphism temperatures in the migmatites reached values up to 1000°C close to the lopolith, grading towards lower temperatures around 800°C more to the north and the east (Jacques de Dixmude 1978). The hypersthene-in isograd marks the transition from amphibolite to granulite facies metamorphism. The peak of metamorphism M2 is dated at approximately 1050 Ma, earlier phases M0 and M1 at 1500 and 1200 Ma respectively

(Wielens et al. 1981). At 950 Ma a M3 stage is recognized. A late-Precambrian peneplanization is followed by a Cambro-Silurian sedimentation and subsequent burial metamorphism (M4a). A part of the very low-grade metamorphic effects in the Precambrian basement is ascribed to this event (Sauter et al. 1983). Caledonian thrusting and metamorphism follows, the resulting retrograde greenschist facies metamorphism (M4b) is effective in the basement in a zone close to the Caledonian boundary (Verschure et al. 1980).

As part of a study of the metamorphic evolution of the Rogaland marbles investigations were carried out into the calcite-dolomite microstructures, the major element chemistry of the carbonates and into the carbon and oxygen isotopic composition of the carbonate minerals. Mainly samples from three marble locations were studied, locations A, B and C (Fig. 1) (Sauter 1981). These three locations all had different temperature histories. Location A, close to the intrusives, suffered very high temperatures during the granulite facies metamorphism, but was not affected by the retrograde greenschist facies. Location C, further north and close to the Caledonian front, underwent high-grade temperatures around 700-750°C only, but it suffered a severe Caledonian impact, amounting to at least 400°C (Verschure et al. 1980). Location B lies just at the edge of the retrograde greenschist zone and had an intermediate position with regard to temperature.

Generally the marbles, including related rocks such as diopside rocks and alkali-feldspar-rich rocks, occur as lenses within the migmatites (Sauter 1981). Location A is one of the largest occurrences of marbles. Here the Faurefjell formation as a whole is exposed over at least 600 m and it is at least 20 m thick. The marbles occur in several levels with layer thicknesses up to 10 m. Numerous small lenses and blocks of diopside rocks are included. The bottom of the formation consists of a 7 m thick, coarse-grained quartzite. To the south the formation thins out; to the northwest it evolves into the thick quartz-diopside gneisses of location D. Here sporadically marbles are found, indicating the relation with the marbles of location A. Location B consists of several large and small lenses of the Faurefjell formation, most of which seem to belong to a certain level within the migmatites. Many diopside rocks are intercalated in the marbles. Some exposures, close to a fault and a large quartzite body, are heavily retrograded, showing tremolite, talc and chlorite. Location C is a small road cut in a Faurefjell lens, approximately 30 m long and

several meters high, within the migmatites. The marbles generally are less than 1 m thick. Diopside rocks and diopside-alkalifeldspar rocks form a large part of the exposure.

CALCITE-DOLomite MICROSTRUCTURES

DESCRIPTION

In almost every sample from the Rogaland marbles at least one type of dolomite intergrowth in calcite can be recognized with normal light-microscopic methods. Besides these generally fine-grained dolomite intergrowths coarser-grained dolomite may also occur, often as elongated grains at calcite and silicate grain boundaries. In the text all not-intergrown dolomite will be referred to as "primary", to distinguish from the exsolved dolomite types 1 to 6, although a part of this primary dolomite presumably will be secondary.

Earlier, calcite-dolomite intergrowths in the Rogaland marbles were described by Legrand (1976).

The distinction between calcite and dolomite in thin section was greatly enhanced by etching. For this purpose the uncovered thin section was firstly etched in a 1.5% acetic acid solution for 10 seconds and then immersed in a soiled Alizarin Red S solution for 2 minutes (the method described by Hutchison 1974).

The grain size of the carbonates in the marbles varies greatly. Generally the carbonates in the forsterite marbles are coarse grained (up to 5 mm). In several samples the grain size is reduced by recrystallization (occasionally down to 0.25 mm). The carbonate grain size in the diopside marbles is small (0.5 mm). Twin lamellae in calcite and dolomite are widespread. The grain boundaries may be straight to highly irregular. At some calcite-silicate boundaries thin rims of recrystallized calcite occur, with or without fine-grained dolomite intergrowths.

Six different types of dolomite intergrowths in calcite have been recognized in the Rogaland marbles, in approximate order of origin, type 1 to 6. Three of these types, 1, 4 and 5, are common in the Rogaland marbles, the other three are subordinate.

Type 1. This type of dolomite intergrowth has the form of small tablets (Fig. 2A, 2B). The diameter of the tablets may range from about 15 to 70 μm , the thickness from 5 to 25 μm . The tablets have a strict crystallographic relationship with the host calcite. The c-axes are parallel to each other, the flat sides of the tablets lie in the (0001) plane of calcite. Deviations from this structural pattern are caused by later processes (see type 5). The tablets may be homogeneously distributed in the host calcite, but in some cases they are concentrated in certain parts of the crystal. Borders of calcite grains are free of dolomite tablets. In some cases the tablets seem to have coarsened and to have lost their typical habit, so giving rise to type 2 and possibly to type 3.

To my knowledge, this tablet-like dolomite intergrowth in calcite has never been described from elsewhere.

Type 2. This type, only rarely found, is characterized by lamellar type of inclusions. The dolomite lamellae may be broad and irregular (Fig. 2C) or thin and elongated (Fig. 2D). The thickness of the broad lamellae may reach about 100 μm , their length to 3 mm. The thickness of the thin lamellae is 5 to 10 μm , their length may amount to 4 mm. The largest dimension of the lamellae lies in the (0001) plane of calcite, the crystallographic orientation is the same as of the calcite hosts and also of the dolomite tablets (type 1), which may be present in the same calcite grain. In fact, in some cases dolomite tablets may be observed at one of the ends of a lamella. In sample C510 a few lamellae lie in other calcite planes and may have a slightly different crystallographic orientation (Fig. 2D).

Lamellar or rod-like dolomite intergrowths in calcite have been described, for instance, by Coomaraswamy (1902) in Ceylon marbles, by Van der Veen (1965) in several carbonatites and a marble, by Puustinen (1974) in a carbonatite complex in Finland, and by Kretz (1980) in Grenville metamorphic marbles.

Type 3. This type is a coarse-grained symplectitic type of dolomite intergrowth (Fig. 2E), to be distinguished from the fine-grained symplectite of type 5. Its occurrence is not very common. The size of the elongated dolomite blebs is generally about 25 μm , exceptionally 50 μm . Again, the intergrown dolomite has the same crystallographic orientation as the calcite host. Dolomite, showing only a vaguely symplectitic habit, is situated in large calcite

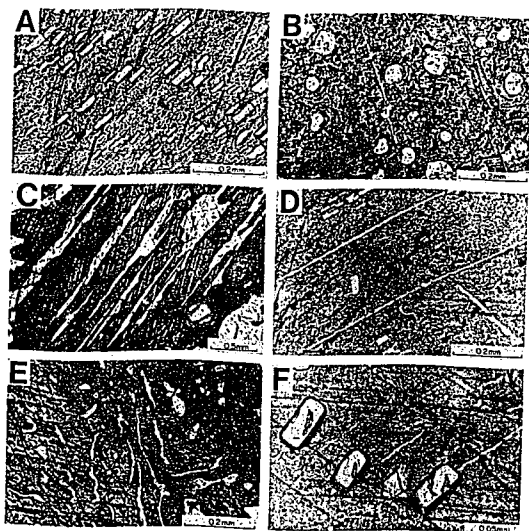


Fig. 2. Photomicrographs of calcite-dolomite exsolutions. A: Type 1. Dolomite tablets, section // c-axis (C509). B: Type 1. Dolomite tablets, section \perp c-axis (C511). C: Type 2. Coarse dolomite lamellae (C372). D: Type 2. Thin dolomite lamellae (SW to NE), lamellae with different orientation (SE to NW), dolomite tablets (upper left) and dolomite rhombohedra (between thin lamellae) (C510). E: Type 3. Coarse-grained symplectite (C515). F: Type 3. Dolomite tablets (inner parts, approx. N-S), overgrown by dolomite (SW-NE) in coarse-symplectite bearing calcite (C510). All photographs: plane polarized light. Calcite (stained by Alizarine) dark, dolomite light.

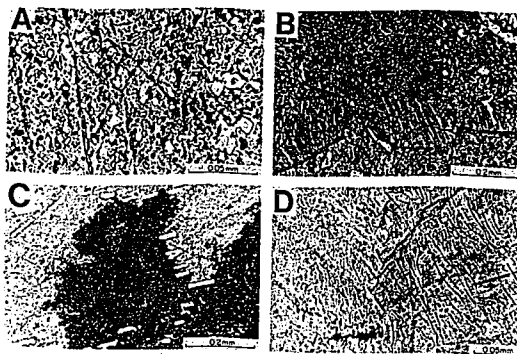


Fig. 3. Photomicrographs of calcite-dolomite exsolutions. A: Type 4. Dolomite rhombohedra (C405). B: Type 5. Fine-grained symplectite (C236). C: Type 5. Fine-grained symplectite (dark), growing into tablet-bearing calcite (light) (C511). D: Type 6. Fine-grained symplectite. Right: calcite and dolomite in same crystallographic orientation, showing little contrast. Left: different orientation, showing large contrast. Note the same direction of the dolomite vermicula on both sides of the calcite grain boundary (Q138). A, B: plane polarized light, calcite (stained by Alizarine) dark, dolomite light. C: crossed polarizers. D: plane polarized light, very thin section.

grains. In the same sample equal-sized calcite grains may contain dolomite tablets. Sporadically tablets are also present in symplectite-bearing calcite grains, with the same orientation. Other tablets however, as well as symplectitic blebs, may show different optical orientations and overgrowing textures (Fig. 2F).

Type 4. This type is represented by very small rhombohedron-like particles of dolomite (Fig. 3A). Their size may vary from less than 1 μ m to, exceptionally, 50 μ m, but generally they do not exceed 5 to 10 μ m. The planes of the dolomite rhombohedra are parallel to the

calcite cleavage planes and both calcite and dolomite have the same crystallographic orientation. This type of dolomite intergrowth is very common. The particles are concentrated in trails, or they are evenly distributed in the calcite together with other small impurities, giving it a cloudy appearance. Often a precipitation-free zone can be observed around the larger dolomite intergrowths of types 1, 2 and 3.

Small rhombohedral dolomite inclusions in cloudy calcites have been described before by e.g. Goldsmith (1960) and Hörmann and Morteau (1972).

Type 5. In all types of calcite-dolomite intergrowths described above, a second, fine-grained, type of symplectite may be observed (Fig. 3B, 3C). Again, the dolomite particles have the same crystallographic orientation as the calcite host. The symplectites typically occur at calcite grain boundaries, where they grow into adjacent calcite grains, involving grain boundary migration. Calcite in the symplectite has the same orientation as the grain from which it grows, different from the orientation of the calcite into which it is growing. Swapped boundaries, where grain boundary migration and formation of symplectites develop at two sides of the calcite grain boundary, are occasionally observed. During their growth, the symplectites may enclose preexisting dolomite tablets. Because the optical orientation of these tablets remains fixed, the resulting configuration is a calcite with a fine-grained symplectite, including dolomite tablets with a different optical orientation (Fig. 3C). Dolomite rhombohedra (type 4) however are consumed, so that the new calcite in the symplectite is cleaner than the often cloudy calcite into which it is growing.

Type 5 symplectite is much more widespread than the coarse-grained symplectite type 3. The fine-grained type 5 symplectite may even be present within a type 3 symplectite. The main differences between the two types are: 1) Type 5 is finer-grained, with respect to both the dolomite particles (1-10 μ m, occasionally amounting to 30 μ m), and the calcite host (generally not exceeding 1 or 2 μ m). 2) Type 5 does not contain the dolomite rhombohedra of type 4. In some cases however, the distinction can not be easily made.

Calcite-dolomite symplectites have often been described in literature, for instance by Coomaraswamy (1902) in Ceylon marbles, by Joplin (1935) in a contact-zone in New South Wales, by Goldsmith

et al. (1955) in granulite facies marbles from West Greenland, by Puustinen (1974) in a carbonatite from Finland, by Legrand (1976) in Rogaland marbles, by Kretz (1980) in Grenville marbles and by Valley and O'Neil (1981) in Adirondack marbles.

Type 6. This type of microstructure is represented by a calcite-dolomite symplectite, in which calcite and dolomite have different optical orientations (Fig. 3D). It occurs only within grains with symplectite of type 5. In parts of type 5 symplectite calcite has changed its orientation whereas the morphology of the calcite-dolomite intergrowth and the orientation of dolomite have remained the same.

DISTRIBUTION OF THE MICROSTRUCTURES

The distribution of dolomite and its exsolution types over the various locations is given in Table 1. One of the striking features is the virtual absence of dolomite at location A, only exsolution types 4 and 5 are rarely found. Locations B and C show the same intergrowths, except for types 2 and 3, which are restricted to forsterite marbles from location B. The dolomite tablets (type 1) tend to be somewhat larger in location B. Exsolution in the diopside marbles has only been observed in types 1, 4 and 5, and it is not as abundant as in the

Table 1: Distribution of dolomite exsolution types over the locations.

	Dolomite type						
	0	1	2	3	4	5	6
Location A					x	x	
Location B	x	x	o	o	x	x	o
Location C	x	x			x	x	x

o=primary dolomite, see text for explanation of other dolomite types. x=abundant, o=minor, =rare.

forsterite marbles.

There exist some relations between the occurrence or abundance of some microstructural types and the primary or retrogressive assemblage in the marbles. The absence of dolomite tablets in primary-dolomite-free marbles (at least in location A) has already been mentioned. Furthermore, in all locations the amount and grain size of the rhombohedron-type dolomite (type 4) is larger in samples with strongly serpentinized forsterite. No clear relations with primary or retrogressive assemblages have been found for the other types. Serpentinization of the olivines is not necessarily related to calcite grain boundary migration and the occurrence of fine-grained symplectites. This symplectite shows some tendency to occur in samples containing clinohumite and retrogressively altered diopside, phlogopite or spinel, but this is certainly not a general rule. Type 2 and perhaps also type 3 seem to grow from the tablets of type 1 but there is no indication of any relation with the assemblage. Types 1 to 3 can be found together in the same thin section, even within one grain. Type 6, the last symplectite type, occurs only in samples with a large amount of type 5 symplectite. The occurrence of microstructural types could also not be related to special field relations within a locality, such as distance to the country rock, diopside rocks or pegmatites.

ORIGIN OF THE MICROSTRUCTURES

It is difficult to establish the nature of the coarse dolomite grains at calcite and silicate grain boundaries. A part of this dolomite will be primary, especially those large grains concentrated near the silicate phases, but the smaller, elongated grains at calcite grain boundaries might well be the product of exsolution. The fact that the border zones of calcite grains are free of dolomite tablets, is indeed an indication that dolomite has exsolved from these regions and has concentrated at the grain boundaries. The textures of types 1 and 4, the tablets and the rhombohedra, are thought to have originated by a "normal" exsolution process. During the post-metamorphic cooling the Mg-calcite becomes supersaturated in Mg and a dolomite phase starts to exsolve, firstly as tablets. The later exsolution of the rhombohedral type of dolomite, in the relatively high-Mg zones between the tablets, seems to be enhanced by the presence of a fluid: the fine dolomite particles often lie in trails, crossing calcite grain boundaries. Moreover this type of exsolution especially occurs in serpentinized

samples. The textures of type 2, the dolomite lamellae, can best be interpreted as a product of coarsening of the dolomite tablets. The coarse-grained symplectite, type 3, partly appears to have the same origin. The tablets seem to coarsen in irregular forms and to produce a symplectitic habit. In some samples however the coarse symplectites do not show their initial crystallographic relationship with the host calcite. Locally they also seem to have overgrown preexisting tablets. This suggests a separate, perhaps later coarsening, type of symplectitic exsolution. Type 5 symplectites are found in all foregoing types 1 to 4, and they are interpreted to represent the youngest exsolution phase. Such a texture, also observed in metallic and silicate systems, may be produced in several ways: in solid-liquid transformations as a result of an eutectic crystallization from the melt, and in the solid state as the result of an eutectoid reaction or of a discontinuous precipitation (e.g. Boland 1980). The close crystallographic relation between symplectitic calcite and the calcite from which it is growing, and the incorporation of old dolomite tablets in the growing symplectite, point to an origin in the solid state. Moreover, temperatures, at least in locations B and C, were probably too low to produce a melt. Little is known about phase transformations of high-temperature polymorphs of calcite, which could form eutectoid points in the phase diagram. Presumably they have not played a role in the temperature interval of about 800°C and lower (Goldsmith and Newton 1969), assumed for locations B and C. Also the aragonite field has presumably not been reached during the Rogaland cooling history (Swanenberg 1980). Therefore a discontinuous precipitation process is thought to have been responsible for the formation of the type 5 microstructures. The formation of the symplectite is accompanied by an extensive grain boundary mobility, characteristic of discontinuous precipitation. It is suggested here that Caledonian retrogressive M4b metamorphism could be the cause of such a recrystallization accompanied by dolomite exsolution. The coincidence of this type of microstructure with some retrogressive minerals seems to confirm this, as well as its spatial distribution: abundant in B and C, rare in A. However, the role of carbonate chemistry, notably the low original Mg content of the calcite at A, must also be taken into account. Type 6 symplectites seem to be the result of an advanced stage of grain boundary migration, rather than a new precipitation process. In this type of symplectite no new precipitates seem to have been formed, and no coarsening of type 5 symplectite has been observed (Scholten, 1982).

The following succession of calcite-dolomite microstructures is

proposed:

- 1) Formation of dolomite tablets in locations B and C during post-metamorphic cooling after M3. The relatively low Mg content of the calcites in location A (see the following paragraph) inhibited nucleation of a dolomite phase.
- 2) and 3) Lamellar coarsening and symplectitic coarsening in location B.
- 4) Formation of rhombohedral dolomite in locations A, B and C. Precipitation-free zones around types 1, 2 and 3. Presumably simultaneously with serpentinization of forsterite (M4a?).
- 5) Formation of fine-grained symplectite as result of discontinuous precipitation in locations A, B and C, minor in A. (M4b?).
- 6) Locally advanced grain boundary migration, mainly in location B, rarely in C. Presumably a continuous process from type 5 to 6.

CHEMISTRY OF THE CARBONATES

Microprobe analysis of the carbonate phases proved to be a difficult task. Within calcite grains differences in chemical composition were detected, which could be due either to the presence of very small dolomite rhombohedra or to real chemical inhomogeneities within the calcite. Damaging of the carbonates by the electron beam was another disturbing factor in carbonate analysis. Part of these difficulties could be avoided by analysis of a small area of about 30 μm^2 , instead of analysing a spot.

ANALYTICAL PROCEDURE

Electron microprobe analysis of the carbonate minerals were obtained using a TPD microprobe and a Cambridge Scientific Instruments Microscan M-9. Operating conditions were 15 and 20KV accelerating potential and 25nA beam current. Diopside, olivine, hematite and rhodonite were used as standards.

Table 2: Microprobe analyses of the carbonates.

	A164	BE24	C24	C235	(5)	non(4)	C236	
mole%	CD112	CD122	CD103	CD113	CD121	CD121	CD091	CD101
FeO ₂	0.2	0.3	0.2	0.2	0.2	0.3	0.2	0.4
MnO ₂	0.6	0.5	0.5	0.4	0.5	0.5	0.4	0.5
MgO ₂	4.7	4.6	4.2	4.7	7.3	7.0	6.9	7.3
CaO ₂	94.5	94.7	95.1	94.8	92.1	92.3	92.4	91.9
X _{Mg}	0.86	0.86	0.85	0.88	0.93	0.91	0.89	0.90
	C236	C267		C273	C236	C247	C272	
mole%	CD121	CD131	CD161	CD171	CD171	CD181	CD153	CD084
FeO ₂	0.3	0.1	0.4	0.4	0.5	0.3	0.3	0.9
MnO ₂	0.5	0.6	0.5	0.4	0.4	0.5	0.4	1.1
MgO ₂	8.1	2.9	5.5	8.6	8.4	7.5	7.8	6.1
CaO ₂	91.1	96.4	93.6	90.6	90.8	91.6	91.5	93.2
X _{Mg}	0.91	0.81	0.85	0.91	0.91	0.89	0.92	0.90
	C272	C283	C297	C480		H208		Q75
mole%	CD039	CD015	CD035	CD342	CD342	CD352	CD482	CD111
FeO ₂	0.3	0.2	0.2	0.4	0.3	0.3	0.2	0.1
MnO ₂	0.4	0.3	0.6	0.4	0.3	0.5	0.4	0.3
MgO ₂	5.7	5.9	3.2	7.9	7.0	7.1	5.5	5.1
CaO ₂	92.7	92.7	96.0	91.3	92.4	91.9	93.7	94.4
X _{Mg}	0.90	0.93	0.81	0.91	0.92	0.88	0.91	0.91
	Q75			Q138	Q159			
mole%	CD141	CD151	CD161	CD151	CD161	CD171	CD181	
FeO ₂	0.2	0.2	0.2	0.2	0.1	0.3	0.3	0.2
MnO ₂	0.4	0.3	0.3	0.3	0.4	0.3	0.3	0.8
MgO ₂	5.1	5.7	8.1	7.3	7.8	8.2	8.1	3.8
CaO ₂	94.3	93.8	91.4	92.1	91.8	91.2	91.3	93.2
X _{Mg}	0.90	0.92	0.94	0.93	0.93	0.94	0.90	
	C272		C283				H208	Q138
mole%	CD069	CD079	CD089	CD014	CD094	CD025	CD035	CD011
FeO ₂	0.6	0.9	0.6	0.8	0.7	0.7	0.8	0.8
MnO ₂	0.4	0.4	0.3	0.3	0.2	0.2	0.4	0.3
MgO ₂	47.8	47.4	47.8	48.5	49.3	46.6	38.7	48.3
CaO ₂	51.3	51.3	51.3	50.5	49.9	50.5	60.1	50.7
X _{Mg}	0.98	0.98	0.98	0.98	0.98	0.98	0.97	0.98

Each analysis is indicated by its sample number (A164 etc.) and by its spot code (CD112 etc.). Numbers in parentheses refer to microstructural types. non(microprobe acc.). X_{Mg}=Mg/(Mg+Fe+Mn).

SAMPLES AND RESULTS

Most carbonate minerals were analysed in forsterite-bearing marbles (A164, BE24, C336, C480 from location A; C372, C383, HS208, Q75, Q138 from location B; C24, C236, C267, C273 from location C), and some in diopside marbles (C235 (loc.C), Q159 (loc.B)). Carbonate from sample C347 (loc.A) was analysed at a tremolite-bearing contact zone between a diopside-forsterite-enstatite rock and a quartzite. C397 (loc.B) is a grossular-bearing diopside rock in which small calcite grains are enclosed. A list of mineral contents of these samples has been taken up in the Appendix. The microprobe analyses of the carbonate minerals are listed in Table 2 and, as far as the Mg-content is concerned, depicted in Fig. 4. Calcite shows an overall spread in Mg-content from about 2 to 11 mol% MgCO_3 . The highest Mg-contents, from 8 to 10 mol%, are analysed in samples from locations B and C (C235, C267, C236, Q75, Q159). The value of 10.6 mol% MgCO_3 in HS208 was obtained by scanning a fine-grained symplectitic calcite-dolomite intergrowth. Within a sample appreciable chemical variations may occur. These are mainly due to recrystallization (C236, Q159, Q75) or to retrograde formation of calcite in reaction rims around serpentinized forsterites (C372). Based on textures, it is also possible that the low Mg-calcites of samples C347 and C397 are of retrogressive origin. Dolomite exsolution too seems to produce chemical variations within a sample. A calcite in a fine-grained symplectite (type 5) in C235 has a much lower Mg-content

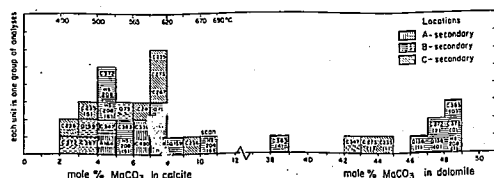


Fig. 4. Mg-content of calcite and dolomite. Analyses of the same carbonate type within one sample are averaged. Numbers in parentheses indicate microstructural types. Calcite contains some type 1, 2 or 4 dolomite, unless indicated otherwise. Temperature scale: calcite-dolomite geothermometry, according to Rice (1977).

than other calcites. Small differences have also been found between type 5 and type 6 symplectite in sample HS208. Qualitative data of Scholten (1982) also suggest a decreasing Mg content in calcites of later exsolution types. These compositional differences imply that large scale chemical reequilibration of the major elements has not taken place. The compositional differences observed are well explained, regarding the sequence of origin of the microstructures and the shape of the calcite-dolomite solvus (Fig. 5). Calcites belonging to early exsolution types will contain more Mg than later calcites.

The Fe content of the calcites mainly varies between 0.1 and 0.5 mol% FeCO_3 . In sample C347 an exceptionally high value of 0.9 mol% is encountered. The Mn content of the calcites generally is somewhat higher than the Fe content. MnCO_3 varies between 0.2 and 0.8. In C347 MnCO_3 is 1.1 mol%.

The data mentioned above refer to calcites from which a variable amount of dolomite has been exsolved. Only for samples from location A, where there is only a minor amount of dolomite exsolution, the analysed

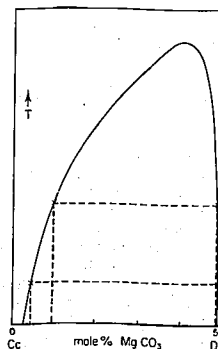


Fig. 5. Schematic drawing of the calcite-dolomite solvus, showing high Mg and, theoretically, high Ca contents of calcite and dolomite respectively during early exsolution stages, and low Mg and low Ca during later exsolution. Note that generally exsolution will take place somewhat below the equilibrium solvus.

compositions approximately represent the pre-exsolution chemistry. Samples from locations B and C however show a considerable amount of dolomite exsolution, mainly in the tablet form. Volumetrically the largest amount of exsolution has been observed in the lamellar exsolution type of sample C372 (maximum 25 vol%). Recalculation reveals an original MgCO_3 content of approximately 12 mol%. Recalculation of tablet exsolution types from both locations B and C, results in approximately 10 to 11 mol%. A microprobe scan over a fine-grained symplectitic exsolution type (HS208) gave the same MgCO_3 content of about 11 mol%.

The microprobe analyses of dolomite show a spread in MgCO_3 content from 42 to 49 mol% (Table 2, Fig. 4). The low value of 38 mol% in the rhombohedral exsolved dolomite in sample C383 is dubious because of its very small grain size. The composition of exsolved dolomite generally is more Ca-rich than the primary dolomite in the same sample (C372, Q138). The difference in composition between primary and exsolved dolomite, although small, is in contradiction with expectations (Fig. 5). The reason could be a more readily reequilibration of the larger dolomite grains to lower temperatures, in contrast to the smaller exsolved dolomite grains, enclosed in calcite. The Mn content of dolomite generally varies between 0.2 and 0.6 mol% MnCO_3 , the Fe content varies between 0.6 and 1.3. Dolomite in C347 shows exceptional FeCO_3 and MnCO_3 values of 4.0 and 2.1 respectively.

GEOOTHERMOMETRY

The Mg content of calcite in equilibrium with dolomite is dependent on temperature (Graf and Goldsmith 1955). The influence of pressure on the solubility of Mg is rather small (Goldsmith and Newton 1969). The equation given by Rice (1977) is used here to calculate the calcite-dolomite temperatures. In Rogaland the widespread dolomite exsolution from Mg-calcite presents a serious problem for the application of the calcite-dolomite geothermometer. In the only location (location A) where exsolved dolomite is only a minor constituent, primary dolomite is not present. Calculated temperatures for this location only represent minimum values. The highest Mg content found is 7.9 mol% MgCO_3 which corresponds to a minimum metamorphic temperature of 617°C. In locations B and C the recalculated Mg contents of exsolved Mg-calcites may give an indication of the temperature reached. Sample C372 with a recalculated mol% MgCO_3 of 12%

reveals a temperature of 710°C, samples from locations B and C with tablet exsolution types, recalculated to 10-11 mol%, give temperatures of 670 to 690°C. However, it has to be stressed here that these values are dependent on uncertainties in the microprobe analyses as well as in the recalculation of the Mg content from the amount of exsolved dolomite. The Mg content of calcite after exsolution shows a wide range, corresponding to calculated temperatures of about 500 to 600°C. In sample C372 the lowest amount of Mg, and thus the lowest calculated temperatures, around 500°C, are found in calcites very close to the coarse dolomite lamellae. Although this might give some indication about the temperature of exsolution, it could be questioned if exsolution took place according to the calcite-dolomite solvus. Therefore, temperatures of exsolution can not exactly be obtained. The amounts of Fe and Mn in the carbonates are low and they are not expected to change significantly the calculated temperatures (cf. Bickle and Powell 1977). The calculated temperatures for locations B and C (around 700°C) may represent minimum metamorphic temperatures. They are 70 to 100°C lower than Fe-Ti oxide and Opx-Cpx temperatures in the same region, obtained by Jacques de Dixmude (1978). This may be the result of post-metamorphic reequilibration in the carbonates. However, regarding the large spread in composition of the exsolved phases even within one sample, an overall reequilibration at lower temperatures has not taken place. A lower Mg content in high temperature calcites, not coexisting with dolomite, as in location A, has also been observed by Rice (1977) in the contact metamorphic marbles of the Marysville aureole. The Mg content of calcite in this case is not controlled by the calcite-dolomite solvus any more, but is fixed by the local mineral assemblage.

CARBON AND OXYGEN ISOTOPIES

SAMPLES

Carbon and oxygen isotope ratios were measured on several carbonate samples from the Rogaland area (see Fig. 1). The samples were mainly selected from the three marble locations A, B and C and some other samples were taken from an apatite marble (location E), from a calcite vein in retrograde augengneisses (location F), from the calcite matrix in explosion breccias near the Caledonian front (location G) and from

quartz marbles in a Caledonian unit close to the boundary with the Precambrian (location B).

The samples, with their isotopic composition, mode, extent of retrograde metamorphism, recrystallization and exsolution, are listed in Table 3.

Additionally the carbon isotopic composition of graphite from several samples from the garnetiferous migmatites was measured and also carbonaceous material from an explosion breccia close to the Caledonian front was analysed (see Fig. 1). Table 4 lists the samples with their carbon isotopic composition.

Calcite of samples with a large variety in modal composition and in extent of retrograde metamorphism was analysed from the marble locations A, B and C.

In location A all samples except A122 and C346 were collected in the same, 5 to 10 m, thick marble bed, within a distance of about 100 m. A164, C322 and C346 were collected from the basal parts of the marble, C481 from the middle, and C335 and C480 from the top. Samples A122 and C346 were taken from a marble layer in the same formation, several hundreds of meters away from the other samples. The samples A122, A164, C480 and C481 are fresh samples with varying amounts of the minerals calcite, forsterite, diopside, phlogopite and spinel. Calcite may form large or recrystallized, small grains. Sample C346, also fresh, contains only a small amount of silicate and oxide minerals. It represents a carbonate-rich zone between a diopside rock and a normal forsterite marble. Sample C322 contains a large amount of silicate minerals, mainly diopside. Forsterite is completely altered to serpentine. This sample forms the transition between a diopside rock and a forsterite marble. In the samples C324 and C335 forsterite is completely serpentinized. Calcite in C324 is fine grained and recrystallized, in C335 it is coarse grained. In samples from this location dolomite is only present as minute exsolved particles.

In location B samples C509, C510, C511 and Z52 were collected from the same marble lens, approximately 50 m long and 5 m thick. The first three samples were taken at 8, 17 and 24 cm distance from a small pegmatite. Q128 and Z177 were collected from two strongly retrogressive exposures. C372 and Z75 were taken from two more isolated marble lenses. The samples C372, C509, C510 and C511 contain varying amounts of calcite, dolomite, forsterite, diopside, phlogopite and spinel. Dolomite exsolution is volumetrically important especially in C372, where large dolomite lamellae occur. In C509, 510 and 511 dolomite

Table 3: Isotopic composition and modal composition (locations A, B and C) of the analysed carbonate samples.

Sample	NCU	coord	d ¹³ C (‰)	d ¹⁸ O (‰) (SMOW)	Cc	Pol	Fo	Di	Phl	Sp	total mole % silicates ¹⁾	recryst. calcite ²⁾	exsolution ³⁾
LOCATION A													
A122 Fo marble	337-070		-4.0	10.4	57	31	2	10			52	1	0
A164 Fo marble	336-076		-3.2	10.0	69	25	7	18			56	5	0
C322 Di marble	336-076		-4.3	16.6	27	(13)	60				77	15	0
C324 Fo marble	336-076		-3.6	16.3	53	(19)	8				57	85	x
C335 Fo marble	336-075		-4.2	19.6	53	(32)	3	12			56	70	a
C346 Fo marble	337-069		-4.2	21.5	85	13	3	<1			27	<1	
C480 Fo marble	336-076		-3.6	21.4	71	24	1	<1			40	<1	a
C481 Fo marble	336-076		-3.6	20.0	51	19	20	10			55	2	x
LOCATION B													
C372 Fo marble	268-260		-3.8	17.1	47	31 ⁴	19	<1	3		30	20	x
C372 dolomite			-3.6	18.2									
C509 Fo marble	255-273		-6.0	16.4	67	5	(23)	4	2		38	20	x
C510 Fo marble	255-273		-3.7	17.9	65	6	(21)	5	3		38	25	x
C511 Fo marble	255-273		-6.0	17.1	30	7	(21)	7	15		48	30	x
Q128 Tr marble	257-274		-4.7	16.9	60	205	176	37	36		100	a	
Z52 Fo marble	255-273		-5.9	14.9	66	4	(25)	(2)	4		40	25	x
Z75 Fo marble	274-261		-6.3	14.2	52	3	(34)	6	57		80	0	0
Z177 Di marble	261-270		-5.0	10.2	18				64	187	82	20	a
LOCATION C													
C143 Tr vein	192-316		-7.5	13.4	mainly calcite, some tremolite								
C236 Fo marble	192-316		-7.4	13.4	53	4	(27)	(39)	6	47	40	0	0
C264 Di marble	192-316		-7.4	14.4	40		(4)	39	17	65	10	0	0
C273 Fo marble	192-316		-7.4	13.5	61	2	(30)	(1)	6	66	35	x	0
C521 Di marble	192-316		-7.0	14.1	41		(4)	36	18	59	10	0	0
C522 DiFo marble	192-316		-8.2	13.3	37		(12)	24	28	64	25	0	0
C533 Fo marble	192-316		-7.9	13.1	53	3	(25)	8	11	52	45	0	0
LOCATION E													
A187 Ap marble	343-305		-3.5	12.5	Cc, Ap, Q, Fp, Ti								
H487 Ap marble	343-305		-2.8	12.2	Cc, Ap, Q, Fsp, Chl, Ep, Ti								
LOCATION F													
C76 Cc vein	189-361		-6.5	11.1	Cc (Q, Fsp)								
LOCATION G													
H4310 breccia	276-461		-3.3	10.2	Cc (matrix), Q, Fsp, Bt								
H4311 breccia	276-461		-4.6	11.4	Cc (matrix), Q, Fsp, Bt								
LOCATION H													
G160 Q marble	266-433		-1.7	11.0	Cc, Q, Bt, Fsp								
G210 Q marble	266-433		-1.2	10.2	Cc, Bt (both matrix), Q, Fsp								

Analysed carbonate phase is calcite, in C372 also dolomite has been analysed. 1) mainly primary dolomite. 2) proportion of silicates which has been retrograded. 3) recrystallization/exsolution for: a) abundant, b) moderate, c) minor. 4) 23% primary dolomite, 62% lamellar dolomite. 5) calc. 6) tremolite. 7) chlorite. 8) forsterite, Diopside, Calcite, Dolomite, Phlogopite, Spinel, Tremolite, Aegirine, Quartz, Epidote, Titanite, (K)Fsp (alkali)feldspar, Bt=green biotite. Numbers in parentheses: partly or wholly retrograded.

tablets and coarse-grained symplectitic dolomite are the predominant exsolution types. The samples Z52 and Z75 are more retrogressively altered, forsterite and diopside are largely serpentized, Z75 contains a large amount of clinohumite, overgrowing serpentine. In Q128 newly formed tremolite and talc have completely replaced forsterite and/or diopside. Calcite shows old, dusty cores, with new, clear rims. Some chlorite has replaced phlogopite. Z177 is a diopside marble in which phlogopite is almost completely retrotransformed to Mg-chlorite.

All samples from location C were taken within a distance of 20 m within this small exposure. The forsterite marbles C236, C273 and C533 have varying amounts of calcite, dolomite, forsterite, diopside and phlogopite. In C533 calcite has undergone extensive recrystallization. C264 and C521 are diopside marbles with a relatively high silicate content. C522 is intermediate between forsterite and diopside marbles, the result of a fine layering. Forsterite and diopside in the analysed Fo marbles samples from location C are partly serpentized. Dolomite exsolution is extensive in the form of tablets and of rhombohedral dolomite. G163 represents a small, coarse-grained, tremolite-calcite vein, which intersects a diopside rock. Along this vein diopside is altered to tremolite.

The grain size of the silicates in the forsterite marbles generally varies between 1 and 2 mm. In some samples it amounts to 4 mm. The grain size of the carbonates greatly varies. It may amount to 6 mm in several samples, but in those samples where recrystallization has played a role it does not exceed 1 mm. In the diopside marbles the overall grain size generally is not larger than 1 mm.

Apart from these marble locations other carbonate samples were collected. A187 and MA97 (location E) are apatite marbles from a 50 to 100 cm thick lens intercalated in garnetiferous migmatites. Showing a very different chemistry and occurring in a very different geological setting, these Precambrian marbles are not assumed to belong to the Faurefjell formation. The samples show coarse-grained, subhedral apatite crystals, in some cases exceeding 5 mm. They form 30 to 40% of the rock volume. The grain size of calcite occasionally is 5 mm, but most grains seem to have recrystallized to a grain size of 0.5 mm. Other minerals include chlorite, epidote, quartz and titanite.

C76 (location F) is a small calcite vein in retrograde augengneisses. Its location is close to the Caledonian overthrust. The

vein contains coarse-grained calcite (up to several centimeters large) and some quartz and feldspars. These latter minerals presumably are fragments from the country rocks. Locally fluorite is associated with this kind of calcite veins.

MA310 and MA311 (location G) are breccias, presumably the result of explosive volcanism (Maier, pers. comm.). These breccias occur in the Precambrian basement, mainly close to the Caledonian front. The fragments are angular and only represent material from the adjacent country rocks. The matrix is fine grained and often consists of small fragments of quartz, feldspars and green biotite. Occasionally (in samples MA310, 311) calcite forms the matrix. The grain size of the calcite varies from large (2 to 3 mm) to small (20 μ m). Textures indicate that the grain size reduction is the result of deformation and recrystallization. Some small quartz, feldspar and biotite grains may be found in the calcite matrix.

Samples G160 and G210 (location H) were collected from a mylonitized zone just above the Precambrian. They are supposed to be parautochthonous units of Cambro-Ordovician age (Tobi, pers. comm.), although Birkeland (1981) suggests a more allochthonous origin, of possible Precambrian age. These rocks mainly consist of calcite and quartz. G160 is a fine-grained rock (50 to 100 μ m), consisting of a polygonal texture of calcite and quartz. Locally streaks of green biotite are present. G210 contains semi-rounded, deformed and partly recrystallized quartz grains, with a size of 1 to 2 mm and some large,

Table 4: $\delta^{13}\text{C}$ of graphite in garnetiferous rocks and in a breccia.

Sample	NGU coord	$\delta^{13}\text{C}$ (‰)
A75 Ga granulite	384-033	-22.3
B51 Ga granulite	335-029	-23.2
G80 breccia matrix	263-418	-27.8
L156 Ga-Cord-Sill-Sp granulite	370-984	-22.2
Q96 Ga-Cord-Sill granulite	201-216	-23.8
Y33 Ga granulite	311-212	-24.7
Y121 Ga-Cord-Sill-Sp granulite	327-114	-23.9

Ga=garnet, Cord=cordierite, Sill=sillimanite,
Sp=spinel.

deformed alkali-feldspar grains, lying in a matrix of fine-grained calcite and quartz with a polygonal texture. Some alkali-feldspar and green biotite occur in the matrix.

The graphite-bearing samples from the garnetiferous migmatites are coarse-grained garnet granofelsens. They all contain the minerals quartz, alkali-feldspar, plagioclase and garnet, and additionally some of the minerals cordierite, sillimanite, spinel and biotite. Graphite is present as large, elongated flakes. The matrix of the explosion breccia G80, nearby location H, consists of very fine-grained quartz, feldspars, green biotite and carbonaceous material.

ANALYTICAL PROCEDURE

Carbon and oxygen isotope analyses were performed at the Vening Meinesz Laboratory for Geochemistry. Carbonates were reacted with 100% H_2PO_4 . Carbon and oxygen isotopic compositions are given in ‰, relative to PDB and SMOW respectively. The "d" notation is used for "delta". The reproducibility of the carbonate analyses is better than 0.1 ‰. Graphite was combusted with CuO . The reproducibility of the graphite analyses is better than 0.2 ‰.

Modal compositions of the samples used for isotope analysis were determined using a Swift & Son point counter. In order to estimate the amount of CO_2 released during decarbonation, for each mineral (silicates and spinel) the equivalent of CO_2 was calculated, starting with the components dolomite, quartz and alkali-feldspar and using the simple reactions: $2Do+1Q=1Fo+2Cc+2CO_2$, $1Do+2Q=1Di+2CO_2$, $3Do+1Kfs+1H_2O=1Phl+3Cc+3CO_2$, $13Do+2Kfs+6Fo+13Cc+1Sp+13CO_2+1K_2O$, $3Do+4Q+1H_2O=1Ta+3Cc+3CO_2$, $5Do+8Q+1H_2O=1Tr+3Cc+7CO_2$. This yields an equivalency of 2 mole CO_2 for each mole of forsterite, 2 CO_2 for each diopside, 3 CO_2 for each phlogopite, 13 CO_2 for 1Sp+6Fo, 3 CO_2 for each talc and 7 CO_2 for each tremolite. Using these CO_2 -equivalents a total mole% silicates+spinel is calculated.



PRECISION RESOLUTION TARGET™



RESULTS

The $\delta^{13}\text{C}$ and $\delta^{18}\text{O}$ values for the analysed carbonates are presented in Table 3 and in Fig. 6.

Samples from the three marble locations A, B and C, except one (Z177), define a trend in the $\delta^{13}\text{C}$ - $\delta^{18}\text{O}$ plot, from about $\delta^{13}\text{C} = -4$ and $\delta^{18}\text{O} = +21$ for samples from the southernmost location A to a value of about $\delta^{13}\text{C} = -7.5$ and $\delta^{18}\text{O} = +14$ for those of the northern location C. Most samples from location B define a value in between, about $\delta^{13}\text{C} = -5$ and $\delta^{18}\text{O} = +17$. There are some notable deviations from these mean values. Two samples from location A show a distinct depletion in the

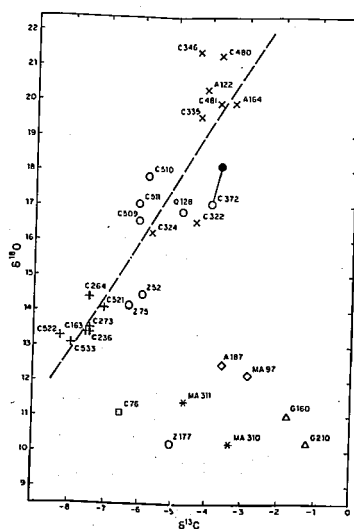


Fig. 6. $\delta^{13}\text{C}$ (PDB) versus $\delta^{18}\text{O}$ (SMOW) for the analysed calcites and dolomite. Crosses: location A, circles: B (black=dolomite), pluses: C, diamonds: E, square: F, asterisks: G, triangles: H. Broken line: best fit for calcite analyses of locations A, B and C, except for Z177. ($r=0.90$).

heavy isotopes, especially in ^{18}O , the silicate-rich rock C322 and the serpentized and recrystallized C324. Other samples which show either recrystallized calcite (A122, A164, C480) or strongly serpentized forsterite (C335) do not show significant depletion effects.

From location B the samples 252, 275 and 2177 are depleted mainly in ^{18}O with respect to the other samples from this location. These samples are moderately to strongly retrograde. The chloritized diopside marble 2177 has the lowest $d^{18}\text{O}$ value observed for samples from the three marble locations ($d^{18}\text{O} = 10.2$) and does not fit on the main trend. The tremolite- and talc-rich sample Q128 has isotopic ratios which fall in the range of not- or weakly-retromorphosed marbles of location B. The carbon and oxygen isotopic composition of dolomite was analyzed in sample C372. This sample contains a large amount of dolomite, partly as exsolution lamellae. The measured values are $d^{13}\text{C} = -3.6$, $d^{18}\text{O} = +18.2$.

All samples from location C show isotopic ratios closely falling in the same range. Two diopside-phlogopite marbles, C264 and C521, have somewhat higher $d^{13}\text{C}$ and $d^{18}\text{O}$ values than the forsterite marbles. The isotope ratios of the calcite-tremolite vein C163 do not deviate from those of the forsterite marbles.

Isotope ratios of calcite from all other locations do not show any systematic relation with the main trend (Fig. 6). The $d^{18}\text{O}$ ratios of these samples are all relatively low, from +10.2 to +12.5, while the $d^{13}\text{C}$ ratios show a wide spread, from -1.2 to -6.5. The quartz marbles C160 and C210 show the highest $d^{13}\text{C}$ values observed: -1.2 and -1.7 respectively. The calcite vein C76 has a relatively low $d^{13}\text{C}$ of -6.5.

The results of the carbon isotope determinations of graphite in rocks of the garnetiferous migmatites and in an explosion breccia are listed in Table 4 and are presented in Fig. 1. In the garnetiferous migmatites $d^{13}\text{C}$ shows a small spread from -22.2 to -24.7. The breccia shows a $d^{13}\text{C}$ of -27.8.

The results of the point counter analysis are listed in Table 3. The total mole% CO_2 equivalents of the silicate minerals and spinel (see analytical procedure for explanation) is plotted versus the $d^{13}\text{C}$ and $d^{18}\text{O}$ ratios of calcite from the marble locations A, B and C in Fig. 7. Most samples fall between about 40 to 60 total mole% (CO_2 equivalents), without systematic variation between the locations. However there seems to be a negative correlation between total mole% and $d^{18}\text{O}$ for samples

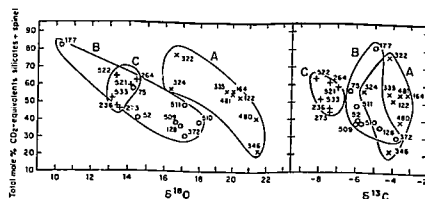


Fig. 7. $d^{18}\text{O}$ and $d^{13}\text{C}$ of calcite versus total mole% silicates and spinel (CO_2 -equivalents, see text for explanation) of samples from location A (crosses), B (circles) and C (pluses).

from location A as well as for those from location B. In location A the silicate-rich sample C322 has a relatively low $d^{18}\text{O}$, whereas the calcite-rich sample C346 has a high value. Equally in location B, the diopside marble 2177 shows a low $d^{18}\text{O}$ value, while other, silicate-poorer rocks from the same location have lower $d^{18}\text{O}$ values. These relations are not recognized in the $d^{13}\text{C}$ plot.

DISCUSSION

The isotopic composition of the calcites from the marble locations A, B and C covers a wide range, from values close to those reported for unmetamorphosed Precambrian sedimentary carbonate rocks (approximately $d^{13}\text{C} = 0 \pm 3$, $d^{18}\text{O} = 20 \pm 5$ (Schidlowski et al. 1975, Veizer and Hoefs 1976)), to much lower isotope ratios (Fig. 6). Such a depletion of ^{13}C and ^{18}O of calcite, resulting in a good correlation between $d^{13}\text{C}$ and $d^{18}\text{O}$, is a well-known phenomenon of metamorphism of siliceous dolomitic rocks (e.g. Deines and Gold 1969, Shieh and Taylor 1969, Kolodny and Gross 1974, Taylor and O'Neill 1977, Lattanzi et al. 1980) (Fig. 8). Several effects could be responsible for such a depletion process in the Rogaland marbles: 1) decarbonation reactions, 2) dolomite exsolution, 3) exchange with external fluids. The possibility of original isotopic differences between the locations can not totally be excluded. However, it is unlikely to assume that original differences would define such a large-scale trend in $d^{13}\text{C}$ and $d^{18}\text{O}$.

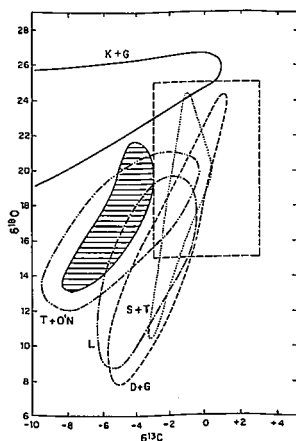


Fig. 8. Isotopic variation of carbonates from several localities. Horizontally hatched area: Rogaland, this work. D+G: Deines and Gold (1969). S+T: Shieh and Taylor (1969). K+G: Kolodny and Gross (1974). T+O'N: Taylor and O'Neil (1977). L: Lattanzi et al. (1980). Rectangle: approximate compositional field for unmetamorphosed Precambrian carbonates, after Schidlowski et al. (1976) and Veizer and Hoefs (1976).

1) Decarbonation reactions in siliceous dolomitic rocks produce isotopically heavy CO_2 , leaving carbonates which are depleted in ^{13}C and ^{18}O (Shieh and Taylor 1969). With a continuous removal of CO_2 the isotopic composition of the remaining carbonates can reach fairly low values with respect to the unmetamorphosed dolomitic limestones. Such a process can be described as a Rayleigh distillation process (Lattanzi et al. 1980) and it is supposed to be the main process to have occurred in several contact metamorphic aureoles (Deines and Gold 1969, Lattanzi et al. 1980).

The observed large-scale trend in the isotopic composition of the Rogaland calcites however, cannot be the result of prograde decarbonation. Firstly, in the siliceous dolomite system most decarbonation reactions take place at much lower temperatures than the maximum temperatures reached in locations A to C. So when in the prograde metamorphic sequence temperatures reached the maximum value for location C observed now, the largest part of isotopic shift as a

result of decarbonation would have already taken place in all locations. The extra granulite facies heat, especially felt at location A, caused only a minor amount of decarbonation (Sauter 1980) and the result would be a slightly more ^{18}O and ^{13}C depleted marble. This is exactly the reverse of what is observed in this study.

Secondly, there is no evidence of differences between the locations in the amount of decarbonation as a result of variable initial carbonate-silica ratios. These variations should be reflected in the now observed carbonate-silicate ratios, and, as is shown in Fig. 7, there is no consistent trend in these ratios between the locations. On a local scale however, decarbonation might have influenced the isotope ratios. Some extreme silicate-poor (C346) or silicate-rich samples (C322, Z177) show relatively high, respectively low $\delta^{18}\text{O}$ values (Fig. 7) but the absence of such a correlation for $\delta^{13}\text{C}$ excludes a pure, prograde, decarbonation effect.

The slope of the $\delta^{13}\text{C}$ - $\delta^{18}\text{O}$ line is often used to determine whether decarbonation is the only process involved in shifting the isotope ratios of calcite during metamorphism (Taylor and O'Neil 1977, Lattanzi et al. 1980). The slope of the depletion trend for the Rogaland marbles is about 1.6. This is much lower than the calculated slopes for calcite in equilibrium with CO_2 , which are between 3.1 and 2.5 for temperatures between 400°C and 900°C. Due to extrapolation of the fractionation factors (given by Bottinga 1968) above 700°C, the slopes for higher temperatures must be regarded with caution, but presumably they will not reach much lower values than those quoted here. Relatively large depletions in ^{13}C and therefore small slope values are reported by Kolodny and Gross (1974) and by Taylor and O'Neil (1977) (Fig. 8). These small slopes are supposed to be the result of exchange with CO_2 derived from oxidation of carbonaceous material. Thus, as additional evidence, the slope of the depletion line of the Rogaland calcites indicates that decarbonation was not a main process in the depletion of the isotope ratios.

2) Dolomite exsolution is widespread in the marbles of locations B and C, while the samples from location A only show a small amount of exsolved dolomite, such as the rhombohedral type and as the fine-grained symplectitic type. It is likely to assume that dolomite exsolution from Mg-calcite causes an isotopic exchange. Regarding the carbon and oxygen fractionation factors between dolomite and calcite (Sheppard and Schwarz 1970), dolomite will be enriched in ^{13}C and ^{18}O

with respect to calcite. However, the fractionation factors are so small that exsolution of relatively small amounts of dolomite could never result in such large shifts in the oxygen and carbon isotope composition of calcite. In sample C372 the bulk isotopic composition of dolomite, which consists for about 25% of exsolution lamellae, indeed deviates only slightly from the composition of calcite (see Fig. 6). Apart from the fact that the analysed dolomite is a mixture of primary and exsolved dolomite, the calcite-dolomite fractionations, pointing to temperatures above 1000°C for the carbon- and about 2800°C for the oxygen fractionation (Sheppard and Schwarz 1970), clearly indicate non-equilibrium conditions for the bulk dolomite-calcite exchange.

3) The rejection of these two possibilities, decarbonation and exsolution, as the main factors for the origin of the depletion trend, suggest a major role for exchange with external fluids. Assuming that there were no significant original isotopic differences between the three marble locations, interaction of isotopically light CO_2 with marbles with a composition close to that of location A is needed to shift the isotopic composition to that of locations B and C. Such an interaction could have taken place at several stages: a) a prograde metamorphic-migmatitic stage, b) a low-grade retrogressive stage.

a) High-temperature marbles undergo more isotopic exchange than low-temperature marbles. Such a behaviour has been demonstrated in the marbles at Naxos, Greece (Rye et al. 1976). At high temperatures however, such as in Rogaland, differences in exchange as a result of temperature variation presumably are not significant, as is also pointed out by Rye et al. (1976). The Rogaland marbles of location A apparently show a limited exchange only. Regarding the isotopic composition of unmetamorphosed Precambrian carbonate rocks (Schidlowski et al. 1975, Veizer and Hoefs 1976) they remained relatively closed for isotopic exchange, as is also observed in high-grade marbles of the Grenville Province (Sheppard and Schwarz 1970, Shieh and Schwarz 1974). The difference in exchange between locations A and C might also be the result of regional differences in the availability of fluids. During granulite facies metamorphism at least compositional differences in the fluid have existed (Swanenberg 1980), but nothing is known of variations in the amount, which could have caused a limited isotopic exchange between country rocks and marbles in location A. Besides that, the largest part of isotopic exchange is expected to have already taken place at lower temperatures, and there is no reason to assume a

large difference in the amount of fluid available for exchange, between locations A and C at that metamorphic stage. Locally the amount of exchange can also be controlled by the accessibility of fluids which is for instance dependent on the thickness of the marble layers. On Naxos, Greece, (Rye et al. 1976) and in the Austrian Alps (Schoell et al. 1975), the margins of marble lenses are more susceptible for exchange than the inner parts. In the Rogaland marbles however, no clear relation between position in the layers and isotopic composition has been found in any of the locations. Sample C324 from the bottom contact of a marble and a diopside rock in location A indeed shows a low isotopic composition, but strong calcite recrystallization and strong serpentinization of forsterite also suggest a retrogressive influence.

Little is known about the isotopic composition of prograde metamorphic fluids. Swanenberg (1980) reported three $\delta^{13}\text{C}$ values of -3.1 to -8.7 for CO_2 in fluid inclusions in quartz from several Rogaland rocks which are not associated with the marbles. Quartzites close to or in the marbles of location B show values of -3.3 and +0.0. Especially this last value, from a small quartz pod in the marble, containing primary fluid inclusions (Swanenberg 1980), could well represent CO_2 derived from decarbonation reactions. The $\delta^{13}\text{C}$ of a fictitious calcite in equilibrium with this CO_2 is about -2, a value even higher than that of the calcites of location A. This might indicate an original isotopic composition of the marbles from location B, and it supports the idea of a common origin of all the marbles. Isotope ratios from CO_2 -rich inclusions from quartzites at location A (-6.0 and -7.4), however, are far too low to represent decarbonation CO_2 . They possibly reflect the composition of a prograde metamorphic fluid, which however apparently did not equilibrate with the isotopic composition of the calcites in location A. The low $\delta^{13}\text{C}$ of this CO_2 could be derived from deep-seated CO_2 or from exchange with the light graphite in the garnetiferous migmatites. However, the $\delta^{13}\text{C}$ values for the graphite analysed here are low (see Table 4) and comparable with the values reported for graphites in metasedimentary rocks in the Arendal area (Andreane 1974) and in the Grenville Province (Weis et al. 1981). These values suggest an organic origin for this graphite without a later large-scale exchange with fluids (Weis et al. 1981). Oxygen isotope ratios for Rogaland rocks are reported by Demalffe and Javoy (1980). Some noritic, granitic and charnockitic gneisses show whole rock $\delta^{18}\text{O}$ values from +4.3 to +9.8.

Combination of these data leads to the suggestion of a prograde metamorphic fluid with relatively low oxygen and carbon isotope ratios, theoretically capable of producing an isotopic shift in the marble carbonates. It is not clear however how exchange with such a fluid could cause such a gradual and regional isotopic shift in the marbles. Therefore the retrograde metamorphism, from which it is known that at least a part of its effects are distributed in a gradual way from north to south in the Precambrian basement, (Sauter et al., 1983) needs to be taken into consideration too.

b) Investigations of thin sections of some 200 marble samples from locations A, B and C has shown that generally the marbles from locations B and C show more retrograde effects than those from location A. These effects include the formation of serpentine, chlorite, tremolite, talc and clinohumite. Also dolomite exsolution from calcite is more widespread in B and C than in A. In Table 2 a rough measure for the retrogradation is listed, indicating in each thin section the proportion of the silicate minerals which retrogressively has been altered.

In other rocks of the Precambrian basement generally two low-grade retrogressive stages can be recognized: the very low-grade metamorphism mainly in the prehnite-pumpellyite facies (M4a), over a large part of S Norway, and the mainly greenschist metamorphism (M4b) in a zone along the Caledonian front (Verschure et al. 1980, Sauter et al. 1983). In the marbles, a part of serpentine is attributed to the M4a, while clinohumite, tremolite and talc overgrowths on serpentine are supposed to belong to the M4b phase (Chapter 4).

The general increase of retrograde metamorphism from south to north and the depletion in heavy isotopes in the calcites in the same direction suggests a relationship in itself. Moreover, several retrograde samples from locations A and B (C324, Z52, Z75) show an isotopic depletion with respect to the bulk composition of their locations in more or less the same direction as the large-scale trend (Fig. 6). The most significant isotopic depletion in these samples is in $\delta^{18}\text{O}$. Sample Z177 even shows such a large depletion, that it does not fit on the main trend any more. The $\delta^{18}\text{O}$ falls in the range of samples which lie close to or just above the Caledonian boundary. The isotopic composition of the quartz marbles from location H, C160 and C210, indicates an extreme depletion only in $\delta^{18}\text{O}$, assuming an original Palaeozoic isotopic composition of $\delta^{13}\text{C}$ between -2 and +1 and $\delta^{18}\text{O}$

between 20 and 25 (Veizer and Hoefs 1976). Also the isotopic composition of other samples in this group, MA310, MA311 and C76 indicate the existence of low $\delta^{18}\text{O}$ fluids associated with a Caledonian event. This event presumably involved the thrusting and M4b metamorphism, which induced the greenschist facies metamorphic overprint in the Precambrian basement. The role of the carbon isotopes is less clear. The range of $\delta^{13}\text{C}$ in the samples associated with the Caledonian front is large, the most negative value is found in the calcite vein C76 (Fig. 6). However, fluids with still more negative $\delta^{13}\text{C}$ values are needed to induce the isotopic shift observed in the Precambrian marbles. Strongly negative $\delta^{13}\text{C}$ values possibly could be obtained by exchange of Caledonian fluids with the graphite-rich phyllites which form the lowest nappe in the Caledonian nappe system in the Stavanger area (Birkeland 1981).

The tremolite bearing samples C163 and Q128 do not show an isotopic depletion relative to other samples of locations C and B respectively. Tremolite in C163 could have formed in the M3 stage, before the isotopic depletion, but tremolite in Q128 clearly indicates a M4b formation. Apparently no extra isotopic depletion of calcite in this sample has taken place. The apatite marbles from location E show retrograde metamorphism (chlorite, epidote) which could have caused their low oxygen isotopic composition. However, their complete different chemistry could also point to a different original isotopic composition.

No examples are known in which such a large isotopic shift in calcite is caused by exchange with low-grade retrogressive fluids. Only the isotopic data of carbonate samples retrograde in the staurolite-kyanite zone of southeastern Vermont (Sheppard and Schwarz 1970) suggest perhaps a retrogressive influence, apart from decarbonation effects. In burial metamorphic rocks massive oxygen isotopic exchange at relatively low temperatures (225-310°C) has been demonstrated by Esslinger and Savin (1973), while disequilibrium between carbonates and quartz suggests that the carbonate is much more subject to retrograde exchange than the silicates (Esslinger and Savin 1973, Magaritz and Taylor 1976).

More research is needed to fully establish the effect of retrograde metamorphism on the isotopic composition of the Rogaland carbonates. A study of fluid inclusions and of the isotopic composition of carbonate veins and rocks close to or in the Caledonian front deserves herein much attention. Oxygen isotope compositions of the silicate phases in

the marbles could also attribute to a better understanding of the isotope chemistry of these rocks. The results thusfar show that interpretation of isotopic data of such polymetamorphic rocks is difficult, and that such a study always has to be accompanied by extensive field and petrographic studies.

REFERENCES

- Andreas, M.O. 1974: Chemical and stable isotope composition of the high-grade metamorphic rocks from the Arendal Area, Southern Norway. *Contrib. Mineral. Petrol.* 47, 299-316.
- Bickle, M.J. and Powell, R. 1977: Calcite-dolomite geothermometry of iron-bearing carbonates. The Glockner area of the Tauern Window, Austria. *Contrib. Mineral. Petrol.* 59, 281-292.
- Birkeland, T. 1981: The geology of Jaeren and adjacent districts. A contribution to the Caledonian nappe tectonics of Rogaland, southwest Norway. *Norsk Geol. Tidsskr.* 61, 213-235.
- Boland, J.N. 1980: Electron microscopy of mineral phase transformations in metamorphic reactions. *Electron Microscopy 1*, 444-451.
- Bottings, Y. 1968: Calculation of fractionation factors for carbon and oxygen isotopic exchange in the system calcite-carbon dioxide-water. *J. Phys. Chem.* 72, 800-808.
- Coomaraswamy, A.K. 1902: The crystalline limestones of Ceylon. *Quat. J. Geol. Soc. London* 58, 399-424.
- Deines, P. and Gold, D.P. 1969: The change in carbon and oxygen isotopic composition during contact metamorphism of Trenton limestone by the Mount Royal pluton. *Geochim. Cosmochim. Acta* 33, 421-424.
- Demaiffe, D. and Javoy, M. 1980: $^{18}\text{O}/^{16}\text{O}$ ratios of anorthositic and related rocks from the Rogaland Complex (SW Norway). *Contrib. Mineral. Petrol.* 72, 311-317.
- Eislinger, E.V. and Savin, S.M. 1973: Oxygen isotope geothermometry of the burial metamorphic rocks of the Precambrian Belt Supergroup, Glacier National Park, Montana. *Bull. Geol. Soc. Am.* 84, 2549-2560.
- Goldsmith, J.R. 1960: Exsolutions of dolomite from calcite. *J. Geol.* 68, 103-109.
- Goldsmith, J.R., Graf, D.L. and Joensuu, O.I. 1955: The occurrence of magnesian calcites in nature. *Geochim. Cosmochim. Acta* 7, 212-230.
- Goldsmith, J.R. and Newton, R.C. 1969: P-T-X relations in the system $\text{CaCO}_3\text{-MgCO}_3$ at high temperatures and pressures. *Am. J. Sci.* (Schairer vol.) 267-A, 160-190.
- Graf, D.L. and Goldsmith, J.R. 1955: Dolomite-magnesian calcite relations at elevated temperatures and pressures. *Geochim. Cosmochim. Acta* 7, 109-128.
- Hermans, G.A.E.M., Tobé, A.C., Poorter, R.P.E. and Majer, C. 1975: The high-grade metamorphic Precambrian of the Sirdal-Ørdsdal area, Rogaland/Vest-Agder, South-west Norway. *Norges Geol. Unders.* 318, 51-74.
- Hörmann, P.K. and Morteani, G. 1972: Mineralogical and chemical composition of some carbonate minerals from the Zillertal Alps, Tyrol (Austria). *Tscherm. mineral. petrogr. Mitt.* 17, 46-59.
- Hutchison, C.S. 1974: Laboratory handbook of petrographic techniques. J. Wiley and Sons, New York-London-Sydney-Toronto. 527 pp.
- Jacques de Dixmude, S. 1978: Géothermométrie comparée de roches du faciès granulite du Rogaland (Norvège méridionale). *Bull. Minéral.* 101, 57-65.
- Joplin, G.A. 1935: The exogenous contact-zone at Ben Bullen, New South Wales. *Geol. Mag.* 72, 385-400.
- Kolodny, Y. and Gross, S. 1974: Thermal metamorphism by combustion of organic matter: isotopic and mineralogic evidence. *J. Geol.* 82, 489-506.
- Kretz, R. 1980: Occurrence, mineral chemistry and metamorphism of Precambrian carbonate rocks in a portion of the Grenville province. *J. Petrol.* 21, 573-620.
- Lattanzi, P., Rye, D.M. and Rice, J.M. 1980: Behavior of ^{13}C and ^{18}O in carbonates during contact metamorphism at Marysville, Montana: Implications for isotope systematics in impure dolomitic limestones. *Am. J. Sci.* 280, 890-906.
- Legrand, J.-M. 1976: Etude pétrologique des séries gneissiques et anastectiques catazonales du dôme de Sandnes-Håle. - Les équilibres minéralogiques. Thèse Bruxelles, 219 pp.
- Magaritz, M. and Taylor, H.P. 1976: Oxygen, hydrogen and carbon isotope studies of the Franciscan formation, Coast Ranges, California. *Geochim. Cosmochim. Acta* 40, 215-234.
- Puustinen, K. 1974: Dolomite exsolution textures in calcite from the Siilinjärvi carbonatite complex, Finland. *Bull. Geol. Soc. Finland* 46, 151-159.
- Rice, J.M. 1977: Progressive metamorphism of impure dolomitic limestone in the Marysville aureole, Montana. *Am. J. Sci.* 277, 1-24.
- Rye, R.O., Schilling, R.D., Rye, D.H. and Jansen, J.B.H. 1976: Carbon, hydrogen and oxygen isotope studies of the regional metamorphic complex at Naxos, Greece. *Geochim. Cosmochim. Acta* 40, 1031-1049.
- Sauter, P.C.C. 1981: Mineral relations in siliceous dolomites and related rocks in the high-grade metamorphic Precambrian of Rogaland, SW Norway. *Norsk Geol. Tidsskr.* 61, 35-45.
- Sauter, P.C.C., Hermans, G.A.E.M., Jansen, J.B.H., Majer, C., Spits, P. and Wegelin, A. 1983: Polyphase Caledonian metamorphism in the Precambrian basement of Rogaland/Vest-Agder, SW Norway. *Nor. Geol. Unders.* in press.
- Schidlowski, M., Eichmann, R. and Junge, C.E. 1975: Precambrian sedimentary carbonates: carbon and oxygen isotope geochemistry and implications for the terrestrial oxygen budget. *Prec. Res.* 2, 1-59.
- Schoell, M., Morteani, G. and Hörmann, P.K. 1975: $^{18}\text{O}/^{16}\text{O}$ and $^{13}\text{C}/^{12}\text{C}$ ratios of carbonates from gneisses, serpentinites and marbles of the Zillertal Alps, western Tauern area (Austria). *N. Jb. Miner. Mh.* 10, 444-459.
- Scholten, D. 1982: Exsolution in Mg-calcite. Internal report, Rijksuniversiteit Utrecht. 37 pp.

- Sheppard, S.M.F. and Schwarcz, H.P. 1970: Fractionation of carbon and oxygen isotopes and magnesium between coexisting metamorphic calcite and dolomite. *Contrib. Mineral. Petrol.* 26, 161-198.
- Shieh, Y.N. and Schwarcz, H.P. 1974: Oxygen isotope studies of granite and migmatite, Grenville province of Ontario, Canada. *Geochim. Cosmochim. Acta* 38, 21-45.
- Shieh, Y.N. and Taylor, H.P. 1969: Oxygen and carbon isotopic studies of contact metamorphism of carbonate rocks. *J. Petrol.* 10, 307-331.
- Swanberg, H.E.C. 1980: Fluid inclusions in high-grade metamorphic rocks from S.W. Norway. *Geol. Ultralect.* 25, 147 pp.
- Taylor, B.E. and O'Neill, J.R. 1977: Stable isotope studies of metasomatic Ca-Fe-Al-Si skarns and associated metamorphic and igneous rocks, Osgood mountains, Nevada. *Contrib. Mineral. Petrol.* 63, 1-49.
- Valley, J.W. and O'Neill, J.R. 1981: $^{13}\text{C}/^{12}\text{C}$ exchange between calcite and graphite: a possible thermometer in Grenville marbles. *Geochim. Cosmochim. Acta* 45, 411-419.
- Veen, A.R. van der 1965: Calcite-dolomite intergrowth in high temperature carbonate rocks. *Am. Min.* 50, 2070-2077.
- Veizer, J. and Hoefs, J. 1976: The nature of $\text{O}^{18}/\text{O}^{16}$ and $\text{C}^{13}/\text{C}^{12}$ secular trends in sedimentary carbonate rocks. *Geochim. Cosmochim. Acta* 40, 1387-1395.
- Verschure, R.H., Andriessen, P.A.M., Boelrijk, N.A.I.M., Hebeda, E.H., Majer, C., Priem, H.N.A. and Verdurmen, E.A.Th. 1980: On the thermal stability of Rb-Sr and K-Ar biotite systems: evidence from coexisting Sveconorwegian (ca 870 Ma) and Caledonian (ca 400 Ma) biotites in SW Norway. *Contrib. Mineral. Petrol.* 74, 245-252.
- Weis, P.L., Friedman, I. and Gleason, J.P. 1981: The origin of epigenetic graphite: evidence from isotopes. *Geochim. Cosmochim. Acta* 45, 2325-2332.
- Wielens, J.B.W., Andriessen, P.A.M., Boelrijk, N.A.I.M., Hebeda, E.H., Priem, H.N.A., Verdurmen, E.A.Th. and Verschure, R.H. 1981: Isotope geochronology in the high-grade metamorphic Precambrian of Southwestern Norway: New data and reinterpretations. *Nor. Geol. Unders.* 359, 1-30.

CHAPTER 4

MINERALOGY AND PETROGENESIS OF THE MARBLES

INTRODUCTION

In this chapter the occurrence, chemistry and petrogenesis of the minerals in the marbles will be treated, except for diopside and carbonates. Diopside is described in Chapter 2: Zoning in diopside from granulite facies marbles from Rogaland, SW Norway. The carbonates are described in Chapter 3: Exsolution, major element and isotope chemistry of Rogaland carbonates. Firstly the main minerals forsterite, phlogopite and spinel will be described, followed by the more rarely occurring minerals and the retrogressive minerals. Representative mineral analyses and a list of mineral contents of the samples mentioned in the text are given in the Appendix.

At the end of this chapter element distribution between the minerals and geothermometry will be discussed. A general petrogenesis will be given in the last section of this chapter.

ANALYTICAL PROCEDURE

Most electron microprobe analyses of the minerals were performed at the Cambridge Scientific Instruments Geoscan and Microscan M-9, at the Vrije Universiteit in Amsterdam. Both instruments were equipped with wave-length dispersive systems. Operating conditions were 20 kV accelerating voltage and 25 nA beam current. Various natural and synthetic oxide and silicate minerals were used as standards. Data were corrected with the M-9 correction program. Some analyses were made with the electron microprobe at the Vening Meinesz Laboratory for

Geochemistry in Utrecht. This microprobe, constructed by the Technisch-Physische Dienst TH/TNO-Delft, is also equipped with a wave-length dispersive system. Operating conditions were 15 kV and 40 nA sample current for a periclase standard. Various oxide and silicates were used as standard. Data were corrected with the Springer correction program.

MAIN MINERALS

Forsterite

Forsterite is the most abundant non-carbonate phase in the forsterite marbles, with a modal amount up to about 40%. Generally forsterite forms rounded grains with a maximum grain size of about 3 mm. (Fig. 1). Often irregular grain forms are observed. Small calcite inclusions in forsterite are common, in some samples spinel or phlogopite inclusions are present. Forsterite often shows



Fig. 1. Forsterite-phlogopite marble. Photomicrograph, A122. Crossed polarizers. Abbreviations in all photomicrographs: Fo = forsterite, Phl = phlogopite, Ce = calcite, Sp = spinel, Do = dolomite, Chl = chlorite, Hbl = Magnesian-hornblende, Chu = clinohumite, Cho = chondrodite, Tr = tremolite, Ht = hydrocalcite.

serpentinization, beginning as thin networks, developing through the whole crystal. In some samples (e.g. Q75) forsterite may be replaced by clinohumite. In one sample forsterite is replaced by diopside + calcite. Forsterite-spinel contacts have become unstable, invariably a zone of fine-grained chlorite is found between these minerals. Besides the abundant occurrences of discrete forsterite grains, forsterite may also occur as massive zones along contacts of marbles and diopside rocks, with a thickness of several millimetres. (e.g. C347). In several samples such a zone has completely been serpentinized. Poikiloblastic forsterite grains are found around a diopside aggregate in sample C336 (see Fig. 8 in Chapter 2). They seem to be an equivalent of the above mentioned forsterite zones. No forsterite zones are found around single diopside grains.

Chemistry

The forsterite compositions lie very close to the Mg-end member, X_{Mg} varying only between 0.92 and 0.96. The amount of Mn falls mainly between 0.45 and 0.77 wt% MnO. Forsterite in an amphibole-bearing marble (C383) has a low Mn content of 0.29 wt% MnO. Fig. 2 shows X_{Mg} plotted versus MnO. Although Mn is incorporated in the X_{Mg} term, the trend of decreasing Mn content with increasing X_{Mg} is only slightly the result of this calculation. It indicates a substitution of Mn preferentially in olivines richer in Fe. Sinkin and Smith (1970)

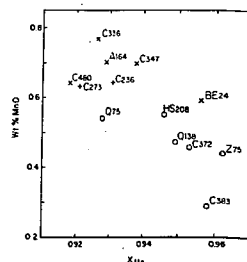


Fig. 2. Mn content versus X_{Mg} in forsterite. $X_{Mg} = Mg/(Mg+Fe+Mn)$. Crosses: location A, circles: location B, pluses: location C.

reported the same trend in olivines of igneous origin. The Mn content of the Rogaland forsterites is much higher than in the igneous forsterites and also higher than in the metamorphic olivines in siliceous dolomites described by e.g. Glassley (1975) and Rice (1977a). Within a sample the composition of forsterite is remarkably constant and even the compositional spread between several samples is small. The forsterite rim around diopside aggregates in C336 shows the same composition as the normal forsterites in the same sample. Also the forsterite zone in C347 does not deviate from the general compositional trend (Fig. 2). The Ca content of the forsterite generally is below the detection limit, traces do not exceed 0.07 wt% CaO. The high Ca contents mentioned in Sauter (1981) (Chapter 1) could not be reproduced. They were possibly due to interferences of surrounding calcites at the rim of the forsterites.

Petrogenesis

As already pointed out by Sauter (1981) (Chapter 1), in a prograde sequence forsterite can be formed by tremolite- and diopside-consuming

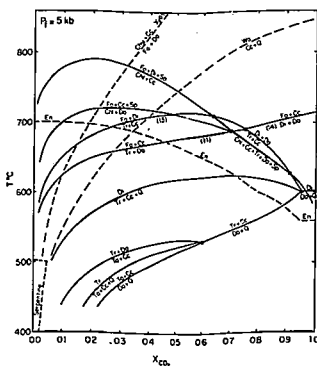


Fig. 3. T-XCO₂ diagram for reactions in the Rogaland marbles, at $P_f = 5$ kb. Partly after the review of Winkler (1979), with additional data of Johannes (1969), Rice (1977a, 1980a), Kise and Metz (1980), Bucher-Nurminen (1982).

reactions. In the Rogaland marbles no textural indications for the reactions are found. The lower stability of forsterite in the siliceous dolomite system is limited by the reactions: $1Tr + 11Do = 8Fo + 13Cc + 9CO_2 + 11H_2O$ (11) and $1Di + 3Do = 2Fo + 4Cc + 2CO_2$ (14) (Fig. 3) (reaction numbers after Winkler 1979). For Fig. 3, a fluid pressure of 5 kb has been chosen, being a reasonable estimate for the conditions of the high-grade metamorphism in Rogaland (Hermans et al. 1976). Experiments by Kise and Metz (1980) show that at a pressure of 5 kb and at high X_{CO_2} values (>0.7) this lower stability limit is about 700°C. Jacobs (in Eggert and Kerrick 1981) places reaction (14) about 50° lower. This could be due to the use of natural minerals in the experiments of Jacobs, in contrast to the synthetic starting materials used by Kise and Metz (1980). However, calculations by Rice (1977a) and by Bucher-Nurminen (1981) predict only an insignificant temperature change of forsterite-forming reaction (11) when a considerable amount of Al substitution in tremolite is taken into account. For the Al substitution in diopside the same small effect may be assumed for reaction (14). Basically the forsterite rims at marble-diopside rock contacts can be thought to have been formed by reaction (14): $1Di + 3Do = 2Fo + 4Cc + 2CO_2$, in which Do may represent the dolomite fraction in the calcite solid solution. The diopside-forsterite zones between a quartzite and a marble also reflect decreasing Si and increasing Ca and Mg activities across the contact.

Phlogopite

Phlogopite is very common in the Rogaland marbles, both in the forsterite and the diopside marbles. Furthermore it occurs in diopside rocks, in minor as well as in major amounts. In the marbles phlogopite occurs as subhedral, elongate grains with a maximum grain size of about 2 mm (Fig. 1). Generally no preferred orientation is present, except in the diopside-phlogopite marbles. In most spinel-bearing marbles phlogopite only occurs as small grains enclosed in forsterite. In some of these marbles however, phlogopite may also be present as large grains (Fig. 4). In the forsterite-spinel marble C480 this phlogopite has a very pale-brown pleochroic dark colour, n_o -red-brown, n_e -light brown, in contrast to the very pale-brown pleochroic colours normally observed in the phlogopites. Frequently chloritization of phlogopite is observed, especially in samples from retrograde exposures in location B.



Fig. 4. Phlogopite as small inclusions in forsterite and as large grain of Ba-phlogopite (lower left). Forsterite also contains spinel inclusions. Calcite dark by staining with Alizarin. Photomicrograph, C480. Plane polarized light. Abbr.: see Fig. 1.

Chemistry

A characteristic feature of the phlogopites is their Ba content (Fig. 5). The range encountered in the analysed "normal" phlogopites, (except the coarse phlogopite in C480) is from 0 to 4.8 wt% BaO. The Ti content generally is low, 0.4 to 0.8 wt% TiO₂, but phlogopite, enclosed in forsterite, in spinel-bearing marbles C372 and C480 have higher amounts, up to 2.7 wt%. Phlogopites in spinel-bearing marbles show high Al contents, up to 18.5 wt% Al₂O₃ in BE24. Na and Mn are only present in minor amounts, Ca only as a trace. The X_{Mg} ratio varies from about 0.91 for phlogopite in a Di-Phl rock to 0.97 in Fo marbles Q75 and Q138. Most values fall in the range 0.94 to 0.97. Fluorine, not analysed in all samples, is present up to 3.3 wt%, (in Q75, a clinohumite-bearing sample), corresponding to a F/(F+OH) ratio of 0.37. Except for its Ba content, the composition of phlogopite is comparable with phlogopites from similar occurrences, for instance those reported by Glassley (1975), Rice (1977b), Kretz (1980) and Bucher-Nurminen (1982).

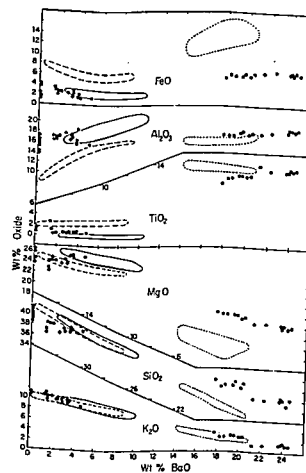


Fig. 5. Chemical variation in phlogopites. Dots: Rogaland phlogopites, this work. Stippled line (right): Mansker et al. (1979). Solid line: Gaspar and Wyltie (1982). Broken line: Wendlandt (1977).

Coarse phlogopite not enclosed in forsterite, in sample C480, shows exceptionally high Ba contents up to 24 wt% BaO, high Ti contents up to 14 wt% TiO₂ and low K and Si contents, down to 1.2 and 23.3 wt% respectively. For unknown reasons the oxide totals of the analyses generally are too high. Therefore the absolute values for the oxide wt% have to be regarded with caution although the Ba contents remain among the highest ever recorded. Such extreme compositions have not been described earlier from metamorphic environments. The Ba-biotites from Hawaiian nephelinites (Mansker et al. 1979) have a composition very much alike, except for their Mg/Fa ratio, which is lower in Hawaii. Wendlandt (1977) described Ba-phlogopites from peridotite and turjaite, which have a composition close to that of the low-Ba phlogopite group, except for their somewhat lower Al and higher Ti

content. The Ba-phlogopite from Jacupiranga carbonatite (Gaspar and Wyllie 1982) has lower Ti contents than the Rogaland phlogopites.

The compositional variation of the Rogaland phlogopites, together with compositional data of the Ba-phlogopites of Wendlandt (1977), Mansker et al. (1979) and Gaspar and Wyllie (1982), is shown in Fig. 5. Comparing the high-Ba phlogopite of C480 with the low-Ba group, there is a decrease of K, Si and Mg, and an increase of Ti and Fe with increasing Ba. Within the group of low-Ba phlogopites these trends are not always clear and sometimes even reversed. Ti is variable within this group, with high Ti contents especially in C480. The behaviour of Mg and Fe just seems to be the reverse of the large-scale trend: an increase of the Mg/Fe ratio in the low-Ba phlogopites, and a decrease in the high-Ba phlogopites with increasing Ba.

The decrease of K with increasing amount of Ba illustrates the Ba substitution for K on the phlogopite interlayer sites. Charge balance is restored by Al^{IV} substitution for Si on the tetrahedral sites, according to the substitution scheme: Ba+Al^{IV}-K+Si (1) (Wendlandt 1977). In all phlogopites the amount of Al^{IV} substituting for Si is more than sufficient to achieve this charge balance. In the low-Ba phlogopites, where Si+Al>8 (Fig. 6), Al^{IV} compensates also for Al^{VI} and Ti substitutions for Mg and Fe on the octahedral sites. The substitutions playing a role here are the phlogopite-eastonite substitution: Mg+Si=Al^{IV}+Al^{VI} (2) and the substitution Ti+2Al^{IV}-Mg+2Si (3) (Robert 1976). The high-Ba phlogopites show, despite their high Al

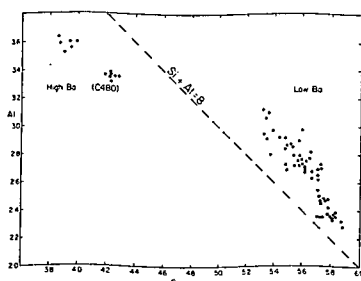


Fig. 6. Si versus Al plot (per 22 O) of Rogaland phlogopites.

content, Si+Al<8 (Fig. 6). The Ti content of these phlogopites is so high that Ti can not be sufficiently compensated by Al^{IV} according to substitution scheme (3). Therefore the extra Ti will substitute according to 2Mg=Ti+vacancy (4) (Forbes and Flower 1974). The octahedral vacancies, induced by this substitution, are reflected in the low cation sums (about 15) observed in the high-Ba phlogopites from Rogaland. The same is observed in the high Ba-Ti biotites from Hawaiian nephelinites (Mansker et al. 1979). For these biotites Mansker et al. suggested the substitutions scheme Ba+2Ti+3Al=K+3Mg+3Si, as a combination of the substitutions (1), (3) and (4). When calculating and plotting these values for the Rogaland phlogopites (Fig. 7), it is obvious that the high-Ba phlogopites of C480 and the low Ba group did not substitute following the same scheme. The low-Ba phlogopites plot close to the stoichiometric line (Ba+2Ti+3Al=K+3Mg+3Si=44). The Ba-phlogopites of Wendlandt (1977) and Gaspar and Wyllie (1982) also fall on the same line approximately. Phlogopites in this group with higher Ti contents (Rogaland: C480, samples of Wendlandt) show a slight deviation from the stoichiometric line, indicating a small number of vacancies introduced by substitution scheme (4). The high-Ba phlogopites approximately fall on the same line as the Ba-biotites of Mansker, both at a larger distance from the stoichiometric line, illustrating the octahedral vacancies.

Fe³⁺ may account for the tetrahedral Si+Al deficiency in the high-Ba phlogopites, although the substitution of Ti may not be excluded. The incorporation of tetrahedral Ti in silicates is controversial (Hartman 1969). High-Ti micas do not seem to contain tetrahedral Ti (Robert 1976), although Farmer and Boettcher (1981) suggest the occurrence of tetrahedral Ti in their "normal" pleochroic Ti-phlogopites which contain tetrahedral Fe³⁺. Similarly, the lowest Ba-phlogopites of

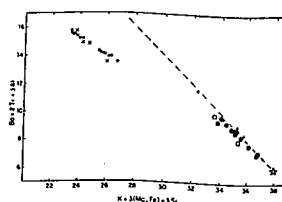


Fig. 7. Substitution in phlogopites. (See text). Heavy dots: Low-Ba Rogaland phlogopites, small dots: high-Ba phlogopite C480. Crosses: Mansker et al. (1979), Gaspar and Wyllie (1982), Wendlandt (1977). Asterisk: stoichiometric Ba- and Ti-free phlogopite composition. Broken line: stoichiometric line for increasing Ba and Ti compositions (see text).

Wendlandt (1977), also showing a reversed pleochroic scheme, have strong indications for Fe^{3+} . The increase of Ti with increasing Ba in his "normal" phlogopites, as well as the high Ti contents of the Ba-biotites of Mansker et al. (1979) and of the Rogaland phlogopites suggest the existence of tetrahedral Ti.

Petrogenesis

The formation of phlogopite in the siliceous and potassic/aluminous dolomite system may take place by alkali-feldspar-consuming reactions at temperatures slightly below the upper stability of dolomite + quartz (Rice 1977b). In the Rogaland marbles no evidence for certain reaction types have been preserved. The phlogopites in the spinel-bearing marbles, especially in BE24, have a notably high Al content (Al=3.1 cations in formula). Besides the crystal-chemical factors related with the Ba substitution, high temperatures must also be responsible for these high amounts of Al. Glassley (1975) also found high Al contents in a spinel-bearing marble (Al=2.9) in the granulite facies, while Bucher-Nurminen (1981, 1982) reported Al contents of 2.6 to 2.7 at temperatures of 600-630°C. In lower grade marbles of the tremolite zone Sanford (1980) found phlogopites with Al=2.4.

The difference in chemistry and in substitution mechanisms between the low- and high-Ba phlogopites of the Rogaland marbles indicates an origin under different conditions. Textural evidence in forsterite-spinel marble C480, where low-Ba phlogopites only occur as small grains enclosed in forsterite, while the high-Ba phlogopites occur as large, individual grains (both types being very scarcely distributed in the rock), indicates a difference in age. The low-Ba phlogopites apparently survived the spinel-forming reaction from phlogopite. Cations released by this reaction, which could not be incorporated in the reaction products, may have been transported away, but locally a new growth of phlogopite seems to have taken place, concentrating especially Ba and Ti in the Ba-phlogopite.

Spinel

Spinel sporadically occurs in forsterite marbles of locations A and B. Rarely it is found in diopside rocks. Its colour varies from almost colourless - pale green, to deep green, dependent on the Fe content. In the marbles spinel occurs as subhedral grains, with grain sizes up to 3 mm (Fig. 8). Occasionally spinel is enclosed in forsterite. At the



Fig. 8. Spinel in forsterite marble. Zone of fine-grained Mg-chlorite at forsterite-spinel contact. Photomicrograph, C372, plane polarized light. Abbr.: see Fig. 1.

contacts with forsterite a very fine-grained Mg-chlorite is formed (Fig. 8), in some cases consuming the whole spinel. Another alteration product of spinel is hydrotalcite (Fig. 17). Small opaque exsolution lamellae in spinel are observed in a few samples. Rarely phlogopite inclusions are found.

Chemistry

Spinel in the Rogaland marbles have the lowest observed X_{Mg} ratio of all the primary minerals. X_{Mg} is down to 0.84, the range is from 0.84 to 0.91. Spinel from a diopside zone in sample C397 still is richer in Fe+Mn and has a X_{Mg} ratio of about 0.8. The colour of the spinels seems to be related with the Fe content, the low-Fe spinels being almost colourless. Zn may be present in fairly large amounts, up to 2.4 wt% ZnO in marble C480 and up to 3.1 wt% in diopside rock C397. The $\text{Fe}^{3+}/(\text{Fe}^{3+}+\text{Fe}^{2+})$ ratio varies between 0 (BE24) and 0.5 (C383). The Mn content has a fairly constant value of 0.3 wt% MnO, except for C397, where spinel contains about 0.7 wt% Cr. Cr is only present as a trace in BE24, it does not exceed 0.1 wt% Cr_2O_3 .

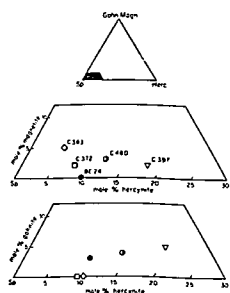


Fig. 9. Compositional variation of spinel in terms of molar proportions of spinel, hercynite, magnetite and gahnite.

Within a sample spinel shows a fairly constant composition. Only at the outer rims (max. 50 μ m) in contact with carbonates is a small decrease of Fe^{3+} , coupled with an increase of Al, observed. The compositional spread between the samples, in terms of mole % spinel, hercynite, gahnite and magnetite, is shown in Fig. 9. The composition of the spinels is close to that of the Mg-endmember. The gahnite content increases with hercynite, but no relation is found between magnetite and gahnite.

In many impure dolomites (e.g. Glassley 1975, Rice 1977a, Bucher-Nurminen 1981, 1982) spinel is the most Fe-rich phase observed, Zn in spinel is only reported by Rice (1977a), with low amounts of about 0.2 wt% ZnO.

Petrogenesis

In Al-containing siliceous dolomites spinel may be formed by chlorite consuming reactions (Rice 1977a, Bucher-Nurminen 1976, 1981, 1982, Widmark 1980, 1981). Chlorite is present in some spinel-bearing marbles in Rogaland, but it is considered as a retrogressive product (see section chlorite). The common observation that phlogopite in spinel-bearing marbles only occurs as inclusions in forsterite, suggest a spinel-forming reaction out of phlogopite. The same kind of relationships were observed by Glassley (1975) in granulite facies

marbles from the Lofoten region. He suggested the reactions: $2Phl + 7Do = 6Fo + 7Ct + 1Sp + 7CO_2 + 2H_2O + 1K_2O$ or $6Phl + 7Cc = 7Di + 4Fo + 3Sp + 7CO_2 + 6H_2O + 3K_2O$, which could also be applicable for the Rogaland situation. The topology in T-XCO₂ space of the system including K is about the same as in the K-free system (Glassley 1975, Bucher-Nurminen 1981, 1982, Widmark 1981) although the exact location of these reactions in T-XCO₂ space is not known. In the K-free system the assemblage Fo+Sp is stable above about 700°C at 5 Kb for a large range of XCO₂ (Fig. 3). The absence of spinel in location C might be due to a temperature effect, although the spinel inclusions in forsterite in locations A and B suggest an earlier spinel formation already at lower temperatures, also prevailing in location C. Therefore the absence of spinel in location C is mainly considered to be a bulk rock effect, the formation of spinel being favoured by low K/Al ratios and low Si activities.

MINOR AND SECONDARY MINERALS

In this section minerals will be described which are only rarely observed or which are secondary products of earlier described minerals. The minerals involved are: enstatite, magnesio-hornblende, humite-group minerals, tremolite, chlorite, serpentine and hydrotalcite. Representative microprobe analyses of these minerals are given in the Appendix. Finally, the occurrence of wollastonite in the quartz-diopside gneisses is described.

Enstatite

This mineral is only observed in one sample from location A, C347, which contains a reaction zone between a forsterite marble and a quartzite. In this reaction zone several parallel layers of medium-grained (0.5-2 mm) forsterite and diopside are observed. Discordantly within layers close to the quartzite contact aggregates of fine-grained (0.3 mm) enstatite occur (Fig. 10). The enstatite shows a well-defined polygonal texture. The relations between enstatite and the forsterite-diopside zones indicate a replacement of forsterite or diopside by this mineral. Enstatite contains fine clinopyroxene exsolution lamellae // (100). The amount of lamellae is fairly large, so that a pigeonitic origin of these enstatites may not be excluded (Rietmeijer, pers. comm.).



Fig. 10. Enstatite in diopside-enstatite-forsterite rock. Photomicrograph, C347, crossed polarizers. Abbr.: see Fig. 1.

Chemistry

Enstatite found in C347 is nearly pure enstatite ($\text{En}_{93}\text{Fs}_6\text{Wo}_1$), a composition not found earlier in the Rogaland/Vest-Agder region. The amount of Mn is fairly high, approximately 1 wt% MnO.

Petrogenesis

The forsterite and diopside zones in sample C347 are the normal, often observed, reaction products between quartzites and marbles. The enstatite seems to have formed from diopside and forsterite, at a later stage of metasomatism. The formation of enstatite by disequilibrium reactions of the type: $\text{Fo} + \text{SiO}_2 = 2\text{MgSiO}_3$ can take place anywhere in its stability field. The lower stability of enstatite is bounded by several anthophyllite and magnesite involving reactions. At 5 kb minimum temperatures for the stability of enstatite are approximately 700°C at $X_{\text{CO}_2}=0$ and 570°C at $X_{\text{CO}_2}=1$ (Johannes 1969) (Fig. 3). A similar metasomatic origin of orthopyroxene has been observed by Carswell et al. (1974) and by Sack (1982). In these cases an orthopyroxene reaction zone was described between a peridotite and a quartz-rich vein.

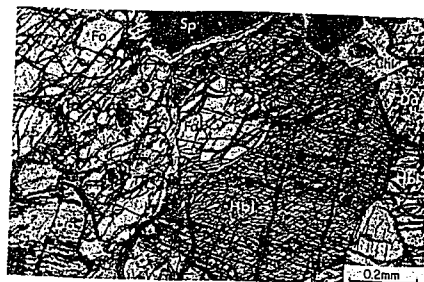


Fig. 11. Magnesio-hornblende in forsterite-spinel-dolomite marble. Photomicrograph, C383, plane polarized light. Abbr.: see Fig. 1.

Magnesio-hornblende

This mineral has only been found in one sample, a forsterite-spinel-dolomite marble C383 (location B) (Fig. 11). The pale-green amphibole in this sample forms a small zone within the rock. It has a grain size up to 4 mm and it shows primary textures, in contrast to the more frequently occurring tremolite in other samples, which clearly is a retrogressive product. The magnesio-hornblende may contain inclusions of forsterite, phlogopite or spinel. This sample has a unique mineral content, not found elsewhere in the Rogaland marbles. It contains large amounts of forsterite and spinel, while dolomite is the main carbonate phase. Chlorite occurring in this sample is interpreted to be a retrogressive product.

Chemistry

According to Leske (1978) the amphibole in sample C383 is a magnesio-hornblende; Na+K+Ba and Ti are low, X_{Mg} is high (0.89) and Al^{IV} is moderate. The total Al and Al^{IV} contents lie just between the values found for tremolitic and pargasitic amphiboles in lower grade

aluminous dolomites (Rice 1977a, Bucher-Nurminen 1981, 1982). The compositions of amphiboles in lower grade rocks indicate a compositional gap between tremolitic and pargasitic amphiboles (Misch and Rice 1975), while at amphibolite grade Misch and Rice found a continuous tremolite-hornblende series. The amphibole described here (C383) and those from the granulite facies terrain in the Lofoten area (Glassley 1975) form part of this continuous series.

Petrogenesis

Pargasitic amphiboles are frequently observed in aluminous marbles, often associated with spinel (Glassley 1975, Rice 1977a, Bucher-Nurminen 1982). Their scarcity in the Rogaland marbles might be due to special bulk chemical factors. The sample in question is very rich in spinel, forsterite and dolomite, and thus in Mg and Al, and relatively poor in Ca, compared with other forsterite marbles. There are no clear textural indications for reactions involving the amphibole. A theoretical reaction in the system is given by Rice (1977a): $8\text{Chi} + 23\text{Cc} + 11\text{CO}_2 = 3\text{Tr} + 17\text{Do} + 8\text{Sp} + 29\text{H}_2\text{O}$ (Fig. 3), placing the occurrence of tremolite+spinel at medium to high temperatures and high X_{CO_2} values. However, at higher temperatures tremolite+dolomite is unstable with respect to forsterite+calcite. The deviation from ideal tremolite chemistry might enlarge the stability field for Mg-hornblende, although Rice (1977a) and Bucher-Nurminen (1981) calculated only a very small temperature difference for the forsterite-forming reaction from an Al-rich tremolite. Bucher-Nurminen (1982) describes pargasite + dolomite forming reactions at the expense of spinel + forsterite+calcite as a result of introduction of Na to the rock system, forming an edenitic component in the pargasite. The inclusions of forsterite and spinel in the hornblende of C383 and the abundance of dolomite make such a type of reaction possible. The very limited occurrence of the magnesio-hornblende makes a detailed study of phase relations and chemistry not possible however.

Humite-group minerals

The minerals of this group are rarely present in the Rogaland marbles. They are mainly found in location B, sporadically in C and only very rarely in location A. The humite minerals occur in two ways: 1) as a replacement of forsterite, often epitaxially overgrowing this



Fig. 12. Clinohumite overgrowth on forsterite. Photomicrograph, C382, plane polarized light. Abbr.: see Fig. 1.

mineral (Fig. 12), and 2) as an overgrowth on serpentine, a retrogressive product of forsterite or diopside (Fig. 13). The pleochroic α_a -colour of the humite minerals ranges from colourless to yellow. In some samples colourless rims along yellow cores are observed. The grain size is variable, the size of large humite minerals overgrowing serpentine may amount to several mm.

Chemistry

The humite group has the general formula $n\text{Mg}_2\text{SiO}_4 \cdot \text{Mg}_{1-x}\text{Ti}_x(\text{OH},\text{F})_{2-2x}\text{O}_{2x}$, where $n=2$ for chondrodite and $n=4$ for clinohumite. Replacement of $\text{Mg}+2(\text{OH},\text{F})$ by $\text{Ti}+2(\text{O})$ and of Mg by Fe or Mn can occur. In the Rogaland marbles the humite group shows a range in composition in terms of the tetrahedral/octahedral ratio from about chondrodite to close to forsterite (Fig. 14). The Ti and Mn contents also show a considerable variation.

Chondrodite-like compositions are observed in sample 275. They generally are Ti-poor (TiO_2 about 0.15 wt%) and Mn-rich (MnO about 1.2%). Some chondrodites in this sample show much higher Ti contents, (up to 2.3 wt%), compensated by lower Mg contents. Clinohumite-like compositions are found in samples C236, C372, Q75 and 275. They show a

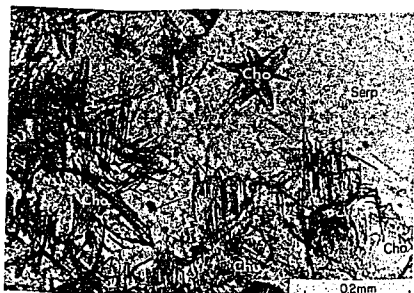


Fig. 13. Overgrowth of chondrodite and clinohumite on serpentine. Photomicrograph, 278, plane polarized light. Abbr.: see Fig. 1.

Ti content up to 3.2 wt% TiO_2 and a Mn content of 0.4 to 2.4 wt% MnO. In sample 275 chondrodite and clinohumite can be found epitaxially intergrown, with colourless chondrodite as rims along yellow clinohumite. Unlike other reported occurrences, where chondrodite and clinohumite contain the same amount of Ti in formula (Aoki et al. 1976, Franz and Ackermann 1980), chondrodite usually contains less Ti than clinohumite. This throws some doubt on the ordering of Ti at the M3 octahedral sites (Ribbe 1979) in the Rogaland humite group.

In sample C372 a spread in tetrahedral/octahedral ratios is observed from clinohumite to forsterite compositions. The Ti and Mn content is much higher than in the associated forsterite (TiO_2 : humites 0.29 to 3.24, forsterite nihil; MnO: humites 1.4 to 2.4, forsterite 0.4 to 0.5). The highest tetrahedral/octahedral ratios are found in minerals overgrowing serpentine, which presumably is a retrogressive product of diopside. These humite-like minerals also contain a small amount of Al. The cause of the compositional range of the humite minerals is not known. Possibly very fine-scale intergrowth of different members of the humite group and forsterite itself are present at forsterite-humite contacts.

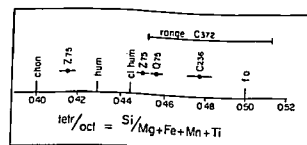


Fig. 14. Chemical variation of humite minerals in terms of tetrahedral/octahedral ratio. Shown are average values and standard deviation, except for C372: range. Stoichiometric ratios for humite minerals and forsterite are indicated.

Fluorine was analysed in the clinohumites of samples C236 and Q75. In the low-Ti clinohumites of Q75 F is higher (about 2.9 wt%) than in the higher-Ti clinohumites of C236 (about 2.0 wt%). These differences are a reflection of the substitution $\text{Mg}+2(\text{F})=\text{Ti}+2(\text{O})$.

Petrogenesis

Formerly, minerals of the humite group were thought to originate solely as a result of low-pressure contact metamorphism and the metasomatic introduction of fluorine. Rice (1980a) showed that these minerals also can form as a normal product of regional, isochemical metamorphism. The T-XCO₂ stability field of the humite minerals extends to high XCO₂ values with an increasing amount of F substitution in the mineral. The substitution of Ti has the same effect, while an increase of pressure decreases the stability field again to low XCO₂ values (Rice 1980a). In the Rogaland marbles textures of clinohumite replacing forsterite indicate the following reaction: $4\text{Fo} + 10\text{H}_2\text{O} + 1\text{Chut} + \text{Cct} + \text{CO}_2$ (Rice 1980a). In sample Q75 the F/(F+OH) ratio (X_F) is about 0.5. At 5 kb the T-XCO₂ stability field for such a clinohumite+calcite relative to forsterite+dolomite lies at low XCO₂ values for a large range of temperatures (approximately <0.2 at 700°C, <0.05 at 500°C) (Fig. 3). So, most likely the clinohumites replacing forsterite were formed at a retrogressive stage of metamorphism in H₂O-rich fluids. If, as is the case in sample Q75, the sample shows hardly any signs of retrogradation to serpentine or chlorite, this seems to have happened at temperatures high enough to prevent forsterite from serpentinization (about 400–500°C). On textural grounds it is not possible to establish the time relationship between clinohumite and diopside rims which occur in the same sample, but both could have formed at the M3 stage.

The clinohumites and chondrodites of the second group are more clearly related with retrogradation. The overgrowing of these minerals on serpentine indicates that they were formed at a late or second stage of retrograde metamorphism. Trommsdorff and Evans (1980) place the stability field of Ti-hydroxyl clinohumite inside that of antigorite, at very low X_{CO_2} values, but a small amount of F substitution would certainly enlarge the stability field for the clinohumites. Unfortunately no F analyses are available for clinohumite and chondrodite in sample 275, but the presence of chondrodite suggests a certain amount of F substitution (Rice 1980b). In that case the formation of clinohumite and chondrodite can have taken place at a second stage of retrograde metamorphism (M4b), for instance as a result of an introduction of some fluorine.

Tremolite

Locally, colourless tremolite is a fairly common retrogressive product in the Rogaland marbles, occurring mainly in locations B and C. In location A it is only rarely observed, for instance in the diopside-forsterite-enstatite rock C347, where it replaces diopside. Such replacements of diopside are more common in locations B and C, as well as in forsterite marbles, diopside marbles and diopside rocks. Generally, tremolite forms small rims around diopside and locally large parts of diopside may be altered to tremolite (Fig. 15). In some samples tremolite grows into serpentine pseudomorphs after forsterite. Generally tremolite only has a small grain size, but in strongly retrograded rocks the size may amount to several centimeters. In the strongly retrogressive marbles, mainly in location B, tremolite may form euhedral to subhedral crystals, while virtually no relics of diopside or forsterite are present. Talc may be associated with tremolite. In location C some small (a few cm.) tremolite-calcite veins are observed in which tremolite forms large elongated grains. The diopside rock, which this vein intruded, is altered into tremolite along the border of the vein.

Chemistry

According to the nomenclature of Leake (1978), the amphibole of sample C347, amphiboles of sample Q159 and amphibole analyses of Teske (1977) represent true tremolites. They all contain a low amount of non-quadrilateral components. In C347 Al is somewhat higher (0.2 wt%



Fig. 15. Tremolite overgrowth on diopside. Photomicrograph, Q128, crossed polarizers. Abbv.: see Fig. 1.

oxide) than in the associated diopside (<0.1), Mn is lower. X_{Mg} is about the same in tremolite and diopside, a feature also observed in prograde metamorphic sequences. No fluorine was detected in the tremolite of sample Q159. The Al content of tremolite in prograde metamorphic sequences generally is higher (Glassley 1975, Rice 1977b).

Petrogenesis

The absence of tremolite as a primary phase in the marbles places the high-grade metamorphic conditions of the Rogaland marbles above reactions (7) and (13) (upper stability of tremolite+calcite) in T- X_{CO_2} space (Fig. 3). The retrogressive formation of tremolite may have taken place under a large range of T- X_{CO_2} conditions and, therefore, over a long time span during the cooling and retrogressive history of Rogaland. The occurrence of tremolite mainly at locations B and C suggests a relation with Caledonian metamorphism. In particular, tremolite growing in the serpentine pseudomorphs is regarded as a late retrogressive product, presumably formed during the M4b phase of metamorphism (Sauter et al. 1983). In H₂O-rich fluids its formation can take place at relatively low temperatures. For tremolites where such textural relations are not present a higher temperature M3 age of formation can not be excluded.

Chlorite

Chlorite is, like tremolite, fairly common as a retrogressive mineral in the Rogaland marbles. Several types of formation of chlorite can be recognized: 1) decomposition of phlogopite, 2) decomposition at the contact of spinel and forsterite, 3) decomposition of spinel.

1) Phlogopite can be partly or totally retrograded into chlorite. The chlorite can be a pennine, with negative optical sign, or a Mg-chlorite with a positive optical sign and a high birefringence. In some samples a relic phlogopite core can successively be rimmed by chlorite and Mg-chlorite. The chloritization of phlogopite is mainly observed in locations B and C.

2) At all forsterite-spinel contacts observed in locations A and B (no spinel is present in location C), a very fine-grained Mg-chlorite aggregate has been formed (Fig. 8). In some cases it seems to have consumed the whole spinel, but also forsterite is partly consumed.

3) In spinel-bearing marbles of location B (e.g. C372, C383) a coarse-grained Mg-chlorite is observed with positive optical sign and high birefringence. At first glance it has a primary appearance, but corroded spinel in contact with this chlorite suggests a retrogressive reaction between these two minerals (Fig. 16). In some cases the coarse-grained chlorite seems to grow from the fine-grained Mg-chlorites of type 2.

Chemistry

Chlorites were analysed in marbles C372 and C383. In the two samples the three types of chlorite have an almost similar composition. In the nomenclature used by Deer et al. (1962) the composition falls just at the boundary between the sheridanite and clinocllore fields, with tetrahedral Al ranging from 2.1 to 2.6 (per 28 O). In both samples chlorite at forsterite-spinel contacts has a somewhat higher X_{Mg} ratio (0.98) than the two other types of chlorite (0.96 to 0.97). Chlorite forming from phlogopite has the same X_{Mg} as phlogopite. Qualitative data available for chlorite retrogressive after phlogopite in the spinel-lacking sample Q159, show much lower Al contents, Al^{IV} being about 1.3. This points to a pennine composition. No fluorine is detectable in this chlorite.

The composition of the chlorites in the spinel-bearing marbles in Rogaland, notably the Al^{IV} content, is close to that observed in the prograde sequences of Rice (1977a) and Bucher-Nurminen (1981, 1982).

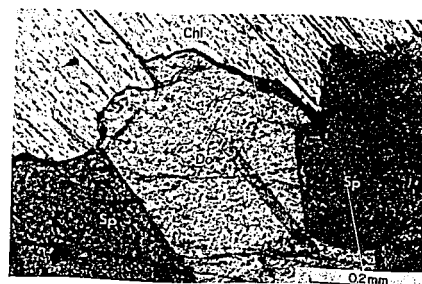


Fig. 16. Mg-chlorite-spinel-dolomite contacts. Photomicrograph, C383, plane polarized light. Abbr.: see Fig. 1.

Petrogenesis

In the Al-containing siliceous dolomite system, chlorite is stable over a large range of T-XCO₂ conditions (Rice 1977a, Bucher-Nurminen 1981, 1982). Chlorite+calcite even has a higher temperature stability than tremolite+calcite up to high XCO₂ values (Fig. 3). Chlorite+calcite is unstable, forming spinel, in a part of the tremolite+calcite stability field, only at XCO₂ values higher than about 0.6. Because of this large stability field it is difficult to pinpoint the conditions of the retrograde formation of chlorite in the Rogaland marbles. Rice (1977a) noted an increase of Al^{IV} in chlorite with increasing grade of metamorphism. In the same kind of rocks (spinel marbles) Bucher-Nurminen (1981, 1982) found the same amount of Al^{IV} at higher pressures. The similar range of Al^{IV} in the Rogaland chlorites suggests this retrograde formation of chlorite in the spinel marbles to have occurred at relatively high temperatures (M37), close to the upper stability of chlorite+carbonate.

Serpentine

Serpentine in the Rogaland marbles is the retrogressive product of forsterite as well as diopside. Serpentinization of cracks in forsterite is common in all forsterite marbles, and in several samples complete serpentinization can be observed. If so, only the outer form of the pseudomorphs may indicate an origin from forsterite or diopside. In locations B and C a later overgrowing of serpentine by tremolite, talc and clinohumite or chondrodite is observed. In a strongly retrograded exposure in location B some chrysotile fibre veins are present.

Chemistry

Some analyses of serpentine show a variation in composition notably in Al. A low amount of Al is present in serpentine retrogressive after forsterite, and up to 3.2 wt% Al is present in serpentine retrogressive after diopside. The X_{Mg} ratio of serpentine is about the same as in the associated forsterite.

Petrogenesis

Serpentine is a common alteration product of forsterite. The serpentinization of forsterite in a pure H_2O fluid takes place at about 400°C. In fluids somewhat richer in CO_2 , serpentinization may begin at 500°C, but the stability field of serpentine is confined to very low X_{CO_2} values (Johannes 1969) (Fig. 3). The T- X_{CO_2} conditions of serpentinization of diopside are not known, but the extension of the Al-rich serpentine towards the compositional fields of chlorite or septechlorite, suggest an enlargement of its stability field with respect to pure Mg-serpentine.

The formation of serpentine possibly can have taken place during the post M3 cooling stage, but a great part will have been formed during Caledonian M4a and M4b metamorphic phases, when temperature was low enough and fluids were available to form serpentine.

Hydrotalcite

The mineral hydrotalcite was recognized with the aid of microprobe analysis of some spinel marbles. This Mg-Al hydroxycarbonate occurs in

aggregates rimming spinel (Fig. 17), while in some cases complete consumption of spinel has taken place. Strongly bent crystals may occur in an otherwise undeformed rock, the strong bending apparently being the result of the replacement of spinel. The mineral has an appearance much like serpentine or chlorite. It is optically negative, uniaxial, it has a refractive index of about 1.5 and a birefringence of about 0.01. The grain size is less than about 0.3 mm. In some cases hydrotalcite is observed between spinel and fine-grained Mg-chlorite, indicating that it was formed later than the formation of Mg-chlorite at the expense of spinel+forsterite.

Chemistry

The microprobe analyses showed a composition close to the theoretical formula: $Mg_3Al_2(OH)_6CO_3 \cdot 4H_2O$. Only a small amount of Fe has replaced Mg. No other elements were detected. XRD analysis confirmed the chemical determination and showed that the mineral is a mixture of the rhombohedral (hydrotalcite) and hexagonal (manasseite) polymorphs of this hydroxycarbonate. This is a common feature in this group of minerals (Fronzel 1941, Struve 1959).

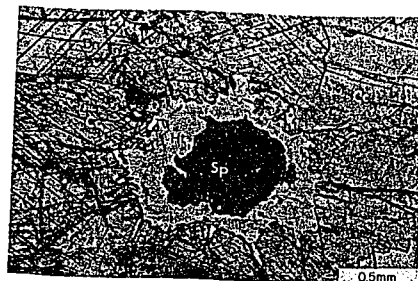


Fig. 17. Aggregate of hydrotalcite around spinel. Photomicrograph, BLOBS, plane polarized light. Abbr.: see Fig. 1.

Petrogenesis

Hydrotalcite is an alteration product of Mg-spinel in aluminous dolomites, not frequently described. Possibly it often is overlooked and mistaken as chlorite. Struve (1959) described hydrotalcite and manasseite as an alteration of spinel in contact-metamorphic dolomites in the French Pyrenees, while Trommsdorff and Schwander (1969) found hydrotalcite in brucite marbles from the Bergell Alps. The conditions of formation of hydrotalcite in metamorphic rocks are not known. In other environments for instance it is observed as a very low-temperature (90°C) alteration product of basaltic glasses, interacting with sea water (Thomassin and Touray 1982).

Accessory minerals

Accessory phases in the marbles are scarce. Barite is among the most conspicuous accessories, occurring in forsterite marbles from locations A and B. Apatite can be present in marbles from all locations. It is rich in chlorine. Zircon is very scarce in the marbles. Sphene is mainly present in the diopside marbles. Most of the opaques are Fe oxides, retrogressively formed during serpentinization of forsterite. In strongly retrograde marbles pyrite can occur.

Wollastonite

The occurrence of wollastonite in the quartz-diopside gneisses is treated here too, as it is in contrast to the absence of this mineral in the marbles. Recently Venhuis (1982) reported the occurrence of wollastonite in a quartz-diopside gneiss of location A. Until then, no wollastonite was reported from rocks of the Faurefjell formation. No exact fluid data are available for the wollastonite-bearing rock, but the occurrence of a high proportion of carbonic inclusions in the quartz-diopside gneisses (Swanenberg 1980) suggests a high temperature formation of wollastonite (Fig. 3). Despite the high temperatures inferred for the marbles of location A, close to the intrusive complexes, no wollastonite has been found in these marbles. This is due to the relatively high Mg activity in the marbles which favours the formation of Mg-silicates such as diopside, forsterite or even enstatite at any metamorphic or metasomatic SiO_2 -introducing phase. The widespread occurrence of wollastonite in the high-temperature marbles

of the Bergell area in the Alps (Trommsdorff 1966) and the Morin anorthosite-granulite terrain in the Grenville Province (Martignole 1975) indeed is the result of different bulk compositions: these marbles generally contain quartz, plagioclase or scapolite, and diopside, in contrast to the Rogaland marbles.

ELEMENT DISTRIBUTION AND GEOTHERMOMETRY

As already pointed out by Sauter (1981) (Chapter 1), the order of preference for Mg over Fe and Mn in the minerals of the Rogaland marbles grossly is the same as in other studied siliceous dolomite occurrences (Glassley 1975, Rice 1977a, b, Bucher-Nurminen 1981, 1982). The order of increasing X_{Mg} in the Rogaland marbles is: $\text{Sp} > \text{Cc} > \text{Fo} > \text{Phl} > \text{Di} > \text{Do}$ (Fig. 18). In the studies of Rice (1977a, b) and Bucher-Nurminen (1981, 1982) tremolite and pargasitic amphiboles fall in the high X_{Mg} range, with X_{Mg} values larger than that of forsterite or spinel. In the higher temperature marbles of the Lofoten (Glassley 1975) and of Rogaland pargasite and magnesio-hornblende are among the most Fe-rich phases, together with spinel. The higher Al content in these amphiboles apparently is correlated with a high Fe content, possibly partly in the form of Fe^{3+} .

The order of X_{Mg} ratios of retrograde minerals such as tremolite, chlorite and clinohumite is the same as in prograde sequences (Rice 1977a, b, Bucher-Nurminen 1981, 1982): tremolite approximately shows the same ratio as diopside, chlorite about the same as phlogopite and

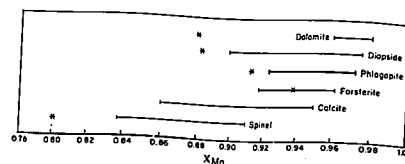


Fig. 18. Range of X_{Mg} of minerals in marbles and in diopside rocks (astorite). X_{Mg} calculated with total Fe as Fe^{2+} , except for spinel: corrected for Fe^{3+} . X_{Mg} of calcite in diopside rock: 0.68 (not shown).

the value for clinohumite lies between that of forsterite and phlogopite.

The element distribution between several minerals in the Rogaland marbles shows a fairly complicated pattern, mainly because of the compositional variation in diopside. The Mg, Fe and Mn distribution, in terms of $X_{Mg} = Mg/(Mg+Fe+Mn)$, between forsterite and diopside is shown in Fig. 19. This is a refinement and an extension of Fig. 5 in Chapter 1 (Sauter 1981), mainly because of the addition of data from some spinel-bearing rocks. As is apparent from Fig. 19, a fact already mentioned in preceding sections, the X_{Mg} of forsterite in a sample is nearly constant, while there is a large variation in X_{Mg} of diopside. The data show a tendency to spread towards lower K_D values, i.e. farther away from the $K_D=1$ line, for samples from locations B and C. One of the possible reasons for such a K_D shift is temperature variation, the marbles from locations B and C having experienced lower metamorphic temperatures than those of location A. However, new data on the Al-rich diopsides from spinel-bearing marbles show that also a compositional factor has to be taken into account: the X_{Mg} of diopside is strongly correlated with its Al content. In Chapter 2 it is shown that in Al-rich diopsides the larger total Fe content partly is due to a larger Fe^{3+} content. A direct correction of X_{Mg} of diopside for Fe^{3+} is not appropriate, due to large errors in the Fe^{3+} calculation, but the compositional effects on K_D can be studied in the K_D versus Al_2O_3 (diopside) plot of Fig. 20. Because of the constant forsterite composition within a sample, the good correlation in several samples

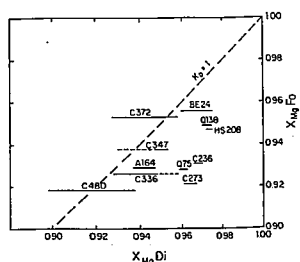


Fig. 19. X_{Mg} of forsterite versus range of X_{Mg} of diopside in each sample. Stippled: clearly not in co-existence with forsterite. BE24, C347, A164, C336, C480: Loc. A, C372, Q138, H5208, Q75: Loc. B, C236, C273: Loc. C.

between K_D and Al_2O_3 is directly related to the X_{Mg} -Al correlations in diopside. When the K_D - Al_2O_3 lines for the high-Al samples BE24, C336, C372 and C480 are extrapolated to an Al_2O_3 content of 0.5 wt%, a value equal to the lowest Al content in BE24 and equal or close to the low-Al diopsides of locations B and C, all K_D values fall in a narrow range, except for samples C347 and C372. This feature suggests a major control of the Al and Fe^{3+} content in diopside on the K_D values between diopside and forsterite. The temperature effects K_D only indirectly: in the same assemblage the Al content in diopside is temperature-dependent (see next paragraphs) and in that way the Mg distribution between forsterite and diopside is dependent on temperature. Only the distributions in C372 (a forsterite-spinel marble from location B) and C347 (a forsterite-diopside-enstatite rock from location A) are significantly different from other samples. The reason for the relatively high extrapolated K_D value for sample C372 is unknown. In C347 the formation of the forsterite-diopside-enstatite rock, as a metasomatic product between a quartzite and a marble, perhaps suggests non-equilibrium conditions. The occurrence of tremolite in this rock could also point to different late-metamorphic re-equilibration conditions, relative to other samples from location A.

For the reasons mentioned above, geothermometry based on the Mg-Fe distribution between diopside and forsterite is not possible in the Rogaland marbles. For instance, the temperatures obtained applying the Powell and Powell (1974) olivine-clinopyroxene geothermometer are

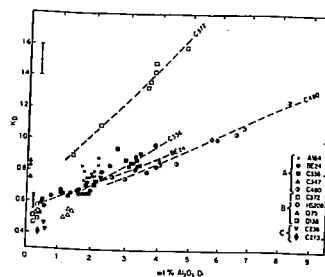


Fig. 20. Variation of K_D (Fo-Di) as function of Al content in diopside. $K_D = X_{Fo}^{Mg} (1 - X_{Di}^{Al}) / X_{Di}^{Mg} (1 - X_{Fo}^{Al})$. Error bars: maximum estimated error in K_D .

strongly variable and they depend more on the Al content in diopside than on the Mg-Fe distribution between forsterite and diopside (Sauter 1978). The use of this geothermometer must be also rejected for other reasons (Wood 1976).

Virtually no Al is present in the only clinopyroxene-orthopyroxene pair found, but the problem in this sample is equilibrium: enstatite in this sample presumably formed metasomatically, as a result of disequilibrium reactions involving forsterite and diopside (see section on enstatite). Therefore, the calculated temperatures using the opx-cpx geothermometer of Wood and Banno (1973) (989°C) and of Wells (1977) (850°C) must be regarded with caution. The Ca and Mg contents in diopside and enstatite also indicate fairly high temperatures, higher than 900°C (using Lindsley et al. 1981).

The Al content in clinopyroxene, expressed as the Ca-Tschermak's component, is, among other factors, dependent on the temperature. Herzberg (1978) experimentally studied the Al content of pyroxene in several lherzolitic assemblages. In the spinel lherzolite field (assemblage Opx-Cpx-Fo-Sp) the Al content increases with increasing temperature, while in the plagioclase and garnet lherzolite fields the Al content also is dependent on pressure. In the Rogaland marbles the highest Al contents are observed in spinel-bearing marbles of location A. By analogy with the spinel lherzolite system they must represent fairly high temperatures, but the absence of experimental data in the siliceous-aluminous dolomite system, with assemblages different from those in the lherzolitic system, excludes the determination of exact temperatures belonging to these high-Al diopsides.

The Mg-Fe-Mn distribution between forsterite and phlogopite and spinel is shown in Fig. 21. Generally the forsterite-phlogopite pairs from location A show a tendency to plot closer to the $K_D=1$ line than the pairs from locations B and C. However, bulk-chemical and crystal-chemical factors also play a large role in phlogopite. Generally the Al content is larger in spinel-bearing marbles, but also the Ba and Ti contents influence the Mg/Fe ratio in phlogopite.

The Mg-Fe-Mn distribution between forsterite and spinel (Fig. 21) (X_{Mg} spinel corrected for Fe^{3+}) shows K_D values in a closer range than for instance the distribution between forsterite and phlogopite in the same samples. Also the forsterite-spinel pairs of the contact metamorphic marbles of Rice (1977a) and those from the regional metamorphosed marbles from Spitzbergen and Greenland (Bucher-Nurminen 1981, 1982 respectively) show a similar distribution. Some of the

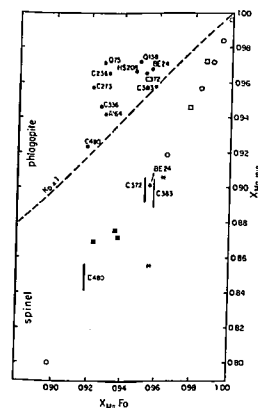


Fig. 21. X_{Mg} of forsterite versus X_{Mg} of phlogopite and spinel. Dots and lines: Rogaland samples, see Fig. 19, C383: loc. B, asterisks: Glassley (1975), open circles: Rice (1977a), open squares: Bucher-Nurminen (1981), solid squares: Bucher-Nurminen (1982).

Lofoten marbles (Glassley 1975) show forsterite-spinel pairs with lower K_D values. The Mg-Fe-Mn distribution in the Rogaland forsterite-spinel pairs suggest a certain degree of equilibration; the almost similar distribution of other pairs from various areas even suggest a general reequilibration of forsterite-spinel pairs in marbles. Such a reequilibration is also commonly observed in other rock types, for instance lherzolitic rocks (Fabrizi 1979, Roeder et al. 1979) and in other spinel-mineral pairs (spinel-cordierite, Kars et al. 1980). Spinel-olivine geothermometry will thus only reflect reequilibration temperatures. The use of these geothermometers (Fabrizi 1979, Roeder et al. 1979) gives very variable results. For marbles from location A: BE24: Fabrizio 670°C, Roeder 950°C; C480: Fabrizio 695-835°C, Roeder 1080-1295°C; C338: Fabrizio 645-875°C, Roeder 850-1090°C. The temperatures obtained from the Roeder thermometer often give unreasonable results. The large variation in temperatures within one sample mainly is caused by the close spacing of the iso-temperature lines in this high-Mg part of the spinel-forsterite K_D plot. Furthermore, the K_D values for these Cr-free spinels only show little

variation with temperature. So, small differences, even within analytical error, in X_{Mg} of spinel and forsterite result in large temperature differences. Also the small differences in Fe^{3+} in spinel lead to relative large temperature variations. Applying the geothermometer of Fabriès (1979) to the marbles of Rice (1977a) and Bucher-Nurminen (1981, 1982), yields temperatures which lie up to 100 to 250° higher than the metamorphic temperatures inferred for these areas. These results show that spinel-olivine geothermometry is unreliable when used for marbles.

GENERAL PETROGENESIS

The textural and chemical data presented in this and in preceding chapters indicate a very complex, polymetamorphic and metasomatic history of the Rogaland marbles. The apparent succession of processes in the normal, closed, siliceous dolomite system and metasomatic, open system processes makes the metamorphic history of these types of rocks difficult to unravel.

In the metapelitic rocks of the Rogaland area four metamorphic stages are recognized, M1 to M4 (Kars et al. 1980, Maier et al. 1981). These stages are correlated with four main geochronological events, around 1200 Ma, 1050 Ma, 950 Ma and 400 Ma (see Wielens et al. 1981 for a review). A very old M0 stage is indicated only geochronologically at an age of 1500 Ma. M1 (1200 Ma) is mainly an upper amphibolite facies, M2 (1050 Ma) an amphibolite facies in the east grading to granulite facies in the west, M3 a lower granulite facies to upper amphibolite facies and M4 a greenschist facies to very low-grade metamorphism. The cooling path after M3 is characterized by amphibole blocking temperature (550–490°C) ages of about 950 Ma and biotite blocking temperature (about 400°C) ages of about 870 Ma. The Caledonian M4 metamorphism is divided in a very low-grade M4a metamorphism and a greenschist M4b metamorphism (Verschure et al. 1980, Sauter et al. 1983).

In the marbles geochronological data are lacking, so that the general petrogenesis and the correlation with the regional metamorphic history must be based on textures, stability fields for minerals and mineral assemblages and, possibly, geothermometry. Indicators for metamorphic pressures are not present in the Rogaland marbles. A pressure of 5 kb is used here, being a reasonable estimate for the

pressure during the M2 metamorphism (Hermans et al. 1976). The pressure during the M1 stage might have been somewhat higher, about 7 kb (Rietmeijer 1979, Jansen and Maier 1980).

The succession of formation of the minerals, tentatively fitted in the regional metamorphic history, is shown in Fig. 22, and is discussed in the following paragraphs.

Both calcite and dolomite can be early as well as late mineral phases. The formation of calcite has taken place during all stages of decarbonation and successive exsolution. It can also have formed during retrograde reactions. Dolomite was the main carbonate phase in the carbonate rocks prior to metamorphism (Chapter 5), but it may also have formed in the prograde sequence as a result of the reaction $Tr+Cc=Di+Do$ (Fig. 3) and in the retrograde path as a result of exsolution. Assuming a complete homogenization of Mg-calcite at the peak metamorphic temperatures, exsolution starts in the cooling trajectory, during or after M3. The rhombohedral dolomite exsolution presumably is a late M3 or M4a product, while symplectitic exsolution appears to be related with M4b metamorphism (Chapter 3).

The occurrence of forsterite in the marbles is indicative for high metamorphic temperatures, approximately 700°C at 5 kb fluid pressure (Fig. 3). The disappearance of dolomite in location A as a result of the forsterite forming reaction $Di+Do=For+Cc$ (Fig. 3), clearly reflects the M2 event. In the marbles of locations B and C the equilibrium assemblage still seems to be present, thus reflecting the thermal gradient induced by the intrusion of the lower part of the loplitth

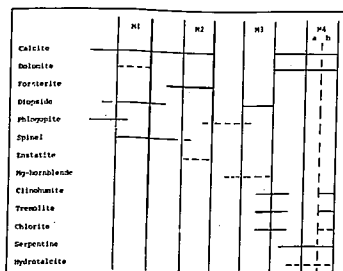


Fig. 22. Formation of minerals in the Rogaland marbles in metamorphic stages M1 to M4.

during the M2 stage. It is not known whether a part of forsterite already has formed during the M1 amphibolite facies. Calcite marbles in the amphibolite facies terrain near Kristiansand (about 100 km to the SE) do not show forsterite (Falkum 1966), but their different chemistry (no dolomite present) excludes a direct comparison. The assemblage tremolite-calcite-diopside in the Kristiansand marbles indicates that the forsterite producing reaction (13) has not taken place, but this assemblage has a stability higher than the lower stability of forsterite-calcite in the dolomitic Rogaland marbles, for a range of X_{CO_2} values (see Fig. 3). The forsterite rims along diopside rocks or clusters may be of the same age and origin as the discrete forsterite grains, growing at the expense of earlier formed diopside rocks, or they may be contemporaneous with this diopside rock, growing in activity gradients across the marble-diopside rock-quartzite contact.

Diopside was formed mainly in two different periods, firstly at M1, and secondly, post-forsterite, presumably in the M3 stage, formed by metasomatic reactions (Chapter 2).

Phlogopite is found as inclusions in forsterite, diopside and, rarely, in spinel. This indicates a relatively early formation, as is also indicated by the reactions in the T- X_{CO_2} diagram, where phlogopite can be formed at temperatures slightly below the upper stability of dolomite-quartz (Fig. 3). Phlogopite thus can be formed at least prior to the M1 stage. High-Ba phlogopite presumably has formed later than forsterite and spinel, in the M2 or M3 stage.

Spinel can occur as inclusions in forsterite, while sporadically phlogopite inclusions in spinel are observed. This indicates a growth of spinel after the first formation of phlogopite and before the last formation of forsterite. The T- X_{CO_2} diagram suggests a formation in M1 as possible.

The data for enstatite and magnesio-hornblende are scarce. Cpx-Opx geothermometry suggests a high-temperature M2 equilibration, whereas the possible pigeonitic origin of enstatite suggests an M2 age for the formation of the mineral. The magnesio-hornblende chemistry indicates a high-temperature formation, its textures possibly a post-forsterite, post-spinel M3 age.

The formation of the retrogressive minerals already may have begun at high temperatures. Clinohumite, chlorite and tremolite may have formed in a late M3 cooling stage. Serpentine formation may have taken place still later during cooling and also in Caledonian M4a and M4b retrogressive stages. The age of hydrotalcite is uncertain, at least it must be later than the Mg-chlorite alteration of spinel, possibly in

late M3 or M4. The overgrowth of clinohumite/chondrodite, tremolite and talc on serpentine, especially in locations B and C, suggest a M4b metamorphic age.

REFERENCES

- Aoki, K., Fujino, K. and Akaogi, M. 1976: Titanochondrodite and titanoclinohumite derived from the upper mantle in the Buell Park Kimberlite, Arizona, USA. *Contrib. Mineral. Petrol.* 56, 243-253.
- Bucher-Nurminen, K. 1976: Chlorit-Spinell Paragenesen aus Dolomitmarmoran des Bergell-Ostrand. *Schweiz. mineral. petrogr. Mitt.* 56, 95-100.
- Bucher-Nurminen, K. 1981: Petrology of chlorite-spinel marbles from NW Spitsbergen (Svalbard). *Lithos* 14, 203-213.
- Bucher-Nurminen, K. 1982: Mechanism of mineral reactions inferred from textures of impure dolomitic marbles from East Greenland. *J. Petrol.* 23, 325-343.
- Carswell, D.A., Curtis, C.D. and Kanaris-Sotiriou, R. 1974: Vein metasomatism in peridotite at Kalskaret near Tafjord, South Norway. *J. Petrol.* 15, 383-402.
- Deer, W.A., Howie, R.A. and Zussman, J. 1962: Rock-forming minerals. Vol. 3: Sheet silicates. Longmans, London, 270 pp.
- Eggert, R.G. and Kerrick, D.M. 1981: Metamorphic equilibria in the siliceous dolomite system: 5 kbar experimental data and geological implications. *Geochim. Cosmochim. Acta* 45, 1039-1049.
- Fabias, J. 1979: Spinel-olivine geothermometry in peridotites from ultramafic complexes. *Contrib. Mineral. Petrol.* 69, 329-336.
- Falkum, T. 1966: Geological investigations in the Precambrian of southern Norway. I. The complex of metasediments and migmatites at Tveit, Kristiansand. *Norsk Geol. Tidsskr.* 46, 85-110.
- Farmer, G.L. and Boettcher, A.L. 1981: Petrologic and crystal-chemical significance of some deep-seated phlogopites. *Am. Min.* 66, 1154-1163.
- Forbes, W.C. and Flower, M.F.J. 1974: Phase relations of titan-phlogopite, $K_2Mg_4TiAl_2Si_6O_{20}(OH)_4$: a refractory phase in the upper mantle? *Earth Plan. Sci. Lett.* 22, 60-66.
- Franz, G. and Ackermand, D. 1980: Phase relations and metamorphic history of a clinohumite-chlorite-serpentine marble from the Western Tauern Area (Austria). *Contrib. Mineral. Petrol.* 75, 97-110.
- Frondel, C. 1941: Constitution and polymorphism of the pyroaurite and sibirgite groups. *Am. Min.* 26, 295-315.
- Gasper, J.C. and Wyllie, P.J. 1982: Barium phlogopite from the Jacupiranga carbonatite, Brazil. *Am. Min.* 67, 997-1000.
- Glassley, U.E. 1975: High grade regional metamorphism of some carbonate bodies: significance for the orthopyroxene isograd. *Am. J. Sci.* 275, 1133-1163.
- Hartman, P. 1969: Can Ti^{4+} replace Si^{4+} in silicates? *Min. Mag.* 37, 366-369.

- Hermans, G.A.E.M., Hakstge, A.L., Jansen, J.B.H. and Poorter, R.P.E. 1976: Sapphirine occurrence near Vikesø in Rogaland, southwestern Norway. *Norsk Geol. Tidsskr.* 56, 397-412.
- Herzberg, C.T. 1978: Pyroxene geothermometry and geobarometry: experimental and thermodynamic evaluation of some subsolidus phase relations involving pyroxenes in the system $\text{CaO-MgO-Al}_2\text{O}_3\text{-SiO}_2$. *Geochim. Cosmochim. Acta* 42, 945-957.
- Jansen, J.B.H. and Majfer, C. 1980: Mineral relations in metapelites of SW Norway. *Int. Coll. High-grade metamorphic Precambrian and its intrusive masses*. Utrecht, May 1980. (Abstr.).
- Johannes, W. 1969: An experimental investigation of the system $\text{MgO-SiO}_2\text{-H}_2\text{O-CO}_2$. *Am. J. Sci.* 267, 1083-1104.
- Kars, H., Jansen, J.B.H., Tobi, A.C. and Poorter, R.P.E. 1980: The metapelitic rocks of the polymetamorphic Precambrian of Rogaland, SW Norway - Part II. Mineral relations between cordierite, hercynite and magnetite within the omphacite-in isograd. *Contrib. Mineral. Petrol.* 74, 235-244.
- Köse, H.R. and Metz, P. 1980: Experimental investigation of the metamorphism of siliceous dolomites - IV. Equilibrium data for the reaction: 1 diopside + 3 dolomite = 2 forsterite + 4 calcite + 2CO_2 . *Contrib. Mineral. Petrol.* 73, 151-159.
- Kretz, R. 1980: Occurrence, mineral chemistry and metamorphism of Precambrian carbonate rocks in a portion of the Grenville province. *J. Petrol.* 21, 573-620.
- Leake, B.E. 1978: Nomenclature of amphiboles. *Can. Miner.* 16, 501-520.
- Lindsley, D.H., Grover, J.E. and Davidson, 1981: The thermodynamics of the $\text{Mg}_2\text{Si}_2\text{O}_6\text{-CaMgSi}_2\text{O}_6$ join: a review and an improved model. In: Newton, R.C. et al. (eds.). *Advances in Physical Geochemistry*, Vol. 1, Springer-Verlag, New York, 149-175.
- Majfer, C., Jansen, J.B.H., Hebeda, E.H., Verschure, R.H. and Andriessen, P.A.M. 1981: Omphacite, an approximately 970 Ma old high-temperature index mineral of the granulite facies metamorphism in Rogaland, SW Norway. *Geol. Mijnb.* 60, 267-272.
- Manaker, W.L., Ewing, R.C. and Keil, K. 1979: Barian-titanian biotites in nephelinites from Oahu, Hawaii. *Am. Min.* 64, 156-159.
- Martignole, J. 1975: Le Précambrien dans le sud de la province tectonique de Grenville (Bouclier Canadien) - Etude des formations catazonales et des complexes anorthositiques. Thèse Toulouse, Université de Montreal, 405 pp.
- Misch, P. and Rice, J.M. 1975: Miscibility of tremolite and hornblende in progressive Skagit metamorphic suite, North Cascades, Washington. *J. Petrol.* 16, 1-21.
- Powell, M. and Powell, R. 1974: An olivine-clinopyroxene geothermometer. *Contrib. Mineral. Petrol.* 48, 249-263.
- Ribbe, P.H. 1979: Titanium, fluorine and hydroxyl in the humite minerals. *Am. Min.* 64, 1027-1035.
- Rice, J.M. 1977a: Contact metamorphism of impure dolomitic limestone in the Boulder Aureole, Montana. *Contrib. Mineral. Petrol.* 59, 237-259.
- Rice, J.M. 1977b: Progressive metamorphism of impure dolomitic limestone in the Marysville Aureole, Montana. *Am. J. Sci.* 277, 1-24.
- Rice, J.M. 1980a: Phase equilibria involving humite minerals in impure dolomitic limestones - Part I. Calculated stability of clinohumite. *Contrib. Mineral. Petrol.* 71, 219-235.
- Rice, J.M. 1980b: Phase equilibria involving humite minerals in impure dolomitic limestones - Part II. Calculated stability of chondrodite and norbergite. *Contrib. Mineral. Petrol.* 75, 205-223.
- Rietmeijer, F.J.M. 1979: Pyroxenes from iron-rich igneous rocks in Rogaland, SW Norway. *Geol. Ultralect.* 21, 341 pp.
- Robert, J.L. 1976: Titanium solubility in synthetic phlogopite solid solutions. *Chem. Geol.* 17, 213-227.
- Roeder, P.L., Campbell, I.H. and Jamieson, H.E. 1979: A re-evaluation of the olivine-spinel geothermometer. *Contrib. Mineral. Petrol.* 68, 325-334.
- Sack, R.O. 1982: Reaction skarns between quartz-bearing and olivine-bearing rocks. *Am. J. Sci.* 282, 970-1011.
- Sanford, R.F. 1980: Textures and mechanisms of metamorphic reactions in the Cockeysville Marble near Texas, Maryland. *Am. Min.* 65, 654-669.
- Sauter, P.C.C. 1978: Metamorfose van siliceuze dolomieten en gerelateerde gesteenten in granuliet-facies Precambrium van Rijksuniversiteit Utrecht. Internal report, Dept. of Petrology, 91 pp.
- Sauter, P.C.C. 1981: Mineral relations in siliceous dolomites and related rocks in the high-grade metamorphic Precambrian of Rogaland, SW Norway. *Norsk Geol. Tidsskr.* 61, 35-45.
- Sauter, P.C.C., Hermans, G.A.E.M., Jansen, J.B.H., Majfer, C., Spits, P. and Wegelin, A. 1983: Polyphase Caledonian metamorphism in the Precambrian basement of Rogaland/Vest-Agder, Southwest Norway. *Norges Geol. Unders.*, in press.
- Sinkin, T. and Smith, J.V. 1970: Minor-element distribution in olivine. *J. Geol.* 78, 304-325.
- Struve, H. 1959: Data on the mineralogy and petrology of the dolomite-bearing northern contact zone of the Quérigut granite, French Pyrenees. *Leids Geol. Med.* 22, 235-349.
- Swannberg, H.E.C. 1980: Fluid inclusions in high-grade metamorphic rocks from S.W. Norway. *Geol. Ultralect.* 25, 147 pp.
- Teske, H. 1977: Geochemisch en petrologisch onderzoek aan de marmeren in Rogaland. Internal report, Dept. of Petrology, Rijksuniversiteit Utrecht.
- Thomassin, J.-M. and Touray, J.-C. 1982: L'hydrotalcite, un hydroxycarbonate transitoire précocement formé lors de l'interaction verre basaltique - eau de mer. *Bull. Minéral.* 105, 312-319.
- Trommsdorff, V. 1966: Progressive Metamorphose - kieseliger Karbonatgesteine in den Zentralalpen zwischen Bernina und Simplicon. *Schweiz. mineral. petrogr. Mitt.* 46, 431-460.
- Trommsdorff, V. and Evans, B.W. 1980: Titanian Hydroxyl-Clinohumite: Formation and breakdown in antigorite rocks (Malenco, Italy). *Contrib. Mineral. Petrol.* 72, 229-242.
- Trommsdorff, V. and Schwander, H. 1969: Brucit marnore in den Bergelleralpen. *Schweiz. mineral. petrogr. Mitt.* 49, 333-340.
- Venhuis, G.J. 1982: Geologisch veldwerkverslag van de Faurefjell formatie ten noorden van Vikesø. Internal report, Dept. of Petrology, Rijksuniversiteit Utrecht, 47 pp.

- Verschure, R.H., Andriessen, P.A.M., Boelrijk, N.A.I.M., Hebeda, E.H., Maier, C., Priem, H.N.A. and Verdurmen, E.A.Th. 1980: On the thermal stability of Rb-Sr and K-Ar biotite systems: evidence from coexisting Sveconorwegian (ca 870 Ma) and Caledonian (ca 400 Ma) biotites in SW Norway. *Contrib. Mineral. Petrol.* 74, 245-252.
- Wells, P.R.A. 1977: Pyroxene thermometry in simple and complex systems. *Contrib. Mineral. Petrol.* 62, 129-139.
- Wendlandt, R.F. 1977: Barium-phlogopite from Haystack Butte, Highwood Mountains, Montana. *Carnegie Inst. Wash. Year Book* 76, 534-539.
- Widmark, E.T. 1980: The reaction Chlorite + Dolomite = Spinel + Forsterite + Calcite + Carbon Dioxide + Water. *Contrib. Mineral. Petrol.* 72, 175-179.
- Widmark, T. 1981: Hydrothermal experiments: the reaction chlorite + dolomite = forsterite + calcite + spinel + fluid and ideas about a new buffer technique. *Geol. Fören. Stockholm Förh.* 103, 128-130.
- Wielens, J.B.W., Andriessen, P.A.M., Boelrijk, N.A.I.M., Hebeda, E.H., Priem, H.N.A., Verdurmen, E.A.Th., and Verschure, R.H. 1981: Isotope geochronology of the high-grade metamorphic Precambrian of Southwestern Norway: New data and reinterpretations. *Norges Geol. Unders.* 359, 1-30.
- Winkler, H.G.F. 1979: *Petrogenesis of metamorphic rocks* 5th ed., Springer-Verlag, Berlin-Heidelberg-New York, 348 pp.
- Wood, B.J. 1976: An olivine-clinopyroxene geothermometer: A discussion. *Contrib. Mineral. Petrol.* 56, 297-303.
- Wood, B.J. and Banno, S. 1973: Garnet-orthopyroxene and orthopyroxene-clinopyroxene relationships in simple and complex systems. *Contrib. Mineral. Petrol.* 42, 109-124.

CHAPTER 5

WHOLE ROCK CHEMISTRY

INTRODUCTION

To get an impression of the wide variety in whole rock compositions within the Faurefjell formation, whole rock analyses were made of several rock types from locations A, B and C (Fig. 1 in Chapter 1). The rock types involved are: forsterite marbles, diopside marbles, diopside and diopside-phlogopite rocks, diopside-alkalifeldspar rocks, a quartz-diopside gneiss, quartz-alkalifeldspar rocks and an alkalifeldspar-phlogopite rock. The general petrography of these rock types, their occurrence and relationships, are described in Chapter 1 (Sauter 1981). Representative whole rock analyses, as well as a list of mineral contents of these samples, are given in the Appendix. Some whole rock analyses were made of associated granites and pegmatites. The pegmatite samples form a successive series (e.g. C506-C499B) in an outcrop in location B (See photograph at first pages of this thesis). This pegmatite seems to have originated by small-scale migmatization in surrounding quartz-diopside gneisses (C393). It has intruded the marbles, forming plagioclase-rich zones (C499B) and diopside (-phlogopite) rocks at the rims. Some granite samples were taken at location A, where, at the discordant contact with the marbles, a leucogranite (C242) changes via a syenitic composition to a pure microcline rock (C21). Small, retrograded plagioclase veins intrude the marble, forming rims of diopside rock. Unfortunately such contact phenomena between granites or pegmatites and the marbles are accompanied by retrograde metamorphism. Especially the outer, plagioclase-rich zones of the pegmatite, at the very contact with the diopside rock, are often heavily retrograded.

Most whole rock analyses were performed at the Service Laboratory of the Instituut voor Aardwetenschappen (rapid rock method), some others were performed at the Vening Meinesz Laboratory (XRF). The rapid rock method is based on the single-solution method of Shapiro (1967), using both colorimetry and atomic absorption. Trace elements (Rb and Sr) were analysed with atomic absorption. Representative analyses are listed in the Appendix.

The chemical variation between the analysed rocks is depicted in Fig. 1. Here the samples are plotted in a compositional triangle, as functions of SiO_2 , $\text{Al}_2\text{O}_3 + \text{H}_2\text{O} + \text{Na}_2\text{O} + \text{BaO}$ and $\text{CaO} + \text{MgO} + \text{FeO} + \text{MnO}$. The analysed rocks show a trend from the forsterite marbles close to the CaO-MgO corner to the quartz-alkalifeldspar rocks close to the SiO_2 apex.

The marbles show a large variation in composition, mainly in the SiO_2 content. In Forsterite-spinel marble C372 it is about 8 wt%, in diopside marble C235 about 30 wt% SiO_2 . As can be seen from Fig. 1, the increase of SiO_2 is accompanied by a moderate increase of Al and the alkalis. In the samples in question this is reflected by an increasing phlogopite content. The increasing Si-K-Al trend is extended in the

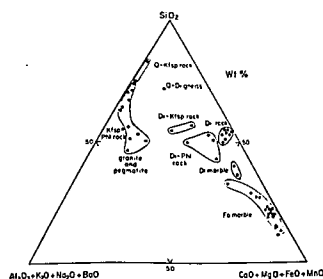


Fig. 1. Whole rock analyses of the Fawcett formation, plotted as function of wt% SiO_2 , Al_2O_3 , $\text{K}_2\text{O}+\text{Na}_2\text{O}+\text{BaO}$ and $\text{CaO}+\text{MgO}+\text{FeO}+\text{MnO}$. Asterisks: average composition of carbonate rocks and limestones, calculated by Vinogradov and Ronov and by Wedepohl (both in Wedepohl 1969). Fo = forsterite, Di = diopside, Do = dolomite, Phl = phlogopite, Kfs = alkalisfeldspar, Q = quartz.

diopside-phlogopite rocks, diopside-alkalifeldspar rocks, quartz-diopside gneiss into to quartz-alkalifeldspar rocks. Some diopside rocks however, lie only on an increasing Si trend. The pegmatites show a reversed trend from quartz-alkalifeldspar rich to more Ca- and Mg-rich compositions.

In Fig. 2 the mole fractions SiO_2 , CaO and $\text{MgO}+\text{FeO}+\text{MnO}$ of the marbles are plotted. It is shown that in the forsterite marbles the molar Ca/Mg ratio is about equal to one.

The tie lines in the compositional triangle of Fig. 2 indicate the reaction $\text{IDt} + 3\text{Do} = 2\text{Fo} + 4\text{Cc} + 2\text{CO}_2$ (14) in the system $\text{CaO-MgO-SiO}_2\text{-CO}_2\text{-H}_2\text{O}$ (Chapter 1). In fact the whole rock analyses should be corrected for the presence of phlogopite and spinel when plotting them in the CaO-MgO-SiO_2 system. However, such a correction only results in a slight shift towards the CaO corner. Two samples from location A, A164 and C481, plotting above the forsterite-calcite tie line, contain the association Fo-Di-Cc , in accordance to their position in the triangle. The absence of dolomite in all samples from this location indicates that reaction (14) really seems to have proceeded to the right. The samples from locations B and C however, generally show the association Fo-Di-Cc-Do . The study of zoning in diopside (Chapter 2) has shown the complexity of the occurrence of diopside. Both primary diopside and metasomatic diopside seem to occur. The presence of reasonable amounts of dolomite in rocks so close to or even above the forsterite-calcite tie line might indicate that Fo-Di-Cc-Do is the equilibrium assemblage

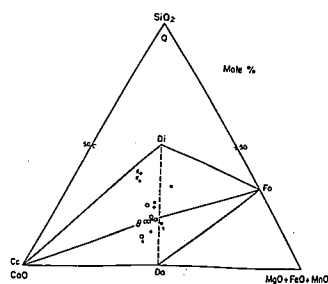


Fig. 2. Whole rock analyses of forsterite marbles (s = including spinel) and diopside marbles (d), from locations A (x), B (o) and C (+), plotted as mole fractions of SiO_2 , CaO and $\text{MgO}+\text{FeO}+\text{MnO}$. Tielines: see text. Other abbreviations: see Fig. 1.

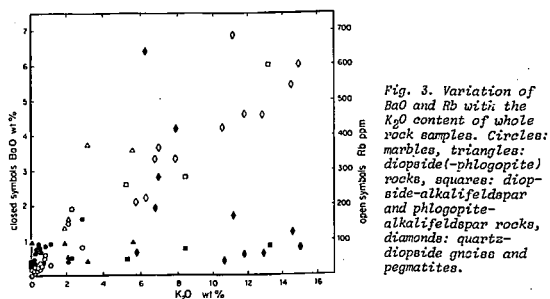


Fig. 3. Variation of BaO and Rb with the K_2O content of whole rock samples. Circles: marbles, triangles: diopside-(phlogopite) rocks, squares: diopside-alkalifeldspar and phlogopite-alkalifeldspar rocks, diamonds: quartz-diopside gneiss and pegmatites.

of reaction (14), or that it is a disequilibrium association, due to a shift from the Fo-Cc-Do field towards the SiO_2 apex, as a result of metasomatic formation of diopside.

A rather conspicuous feature of the Rogaland marbles is their Ba content. A highest value of 1.6 wt% BaO is analysed in Al64. In Fig. 3 is shown that in the marbles Ba shows a positive correlation with K, reflecting the presence of Ba in phlogopite. Another main Ba carrier is barite, which is an accessory phase in several marbles. In most other rock types the Ba content does not exceed that of the marbles. Only at the margin of the pegmatite Ba is strongly enriched, up to 6 wt% BaO (Fig. 3). In these rocks Ba increases with an increasing Ca and a decreasing K content. (Fig. 4).

Rb shows in all rock types a good positive correlation with K. In the marbles this element will be concentrated in phlogopite, in the other rock types mainly in alkalifeldspar. The Rb content in the marbles is the highest in diopside marbles, amounting to 200 ppm. In most forsterite marbles Rb does not exceed 50 ppm. In high-K rocks, such as diopside-phlogopite rocks, diopside-alkalifeldspar rocks and alkalifeldspar pegmatites, Rb is much higher, up to 680 ppm in a pegmatite.

The Sr content in the marbles shows a maximum content of about 200 ppm, while most values fall in the range of 60 to 140 ppm (Fig. 4). No clear relation between Ca and Sr is present in the marbles. In other

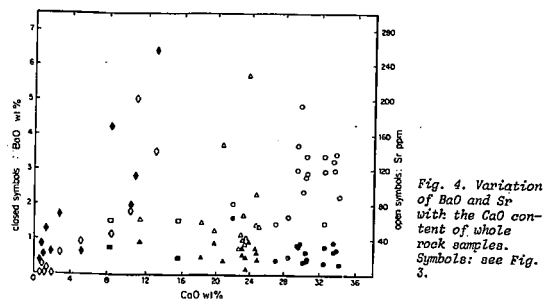


Fig. 4. Variation of BaO and Sr with the CaO content of whole rock samples. Symbols: see Fig. 3.

rock types the maximum amount of Sr is about the same as in the marbles. In the pegmatites Sr and Ca do show a positive correlation, apparently due to the incorporation of Sr in plagioclase. In the diopside rocks high as well as low Sr contents are analysed. No positive correlation with the phlogopite content, and thus with the Rb content, is present, so that the contribution of radiogenic Sr is not demonstrable. In these rocks Sr will be mainly concentrated in diopside.

The amount of Ti in the marbles generally is low, not higher than 0.08 wt% TiO_2 . Only in phlogopite rich marbles it is higher, up to 0.25 wt% in Al64, suggesting that in these rocks Ti is mainly concentrated in phlogopite. In other rocks of the formation comparatively high Ti contents are especially observed in quartz-diopside gneisses and in diopside-alkalifeldspar rocks (maximum 0.5 wt% in a diopside-alkalifeldspar rock). These rocks generally contain sphene.

The Mn content in the marbles is about 0.2 to 0.4 wt% MnO. The main Mn carriers in these rocks are carbonate and forsterite, so, as expected, in diopside rocks the Mn content is somewhat lower, while in the other rock types only low Mn contents are present.

DISCUSSION OF ORIGIN

The Rogaland marbles show a high Si content, compared with other Precambrian limestones and marbles. The Grenville marbles studied by Kretz (1980) generally have a modal carbonate content larger than about 90%. For comparison the modal amount of carbonate in the low-Si marble C372 is about 80%, all other marbles contain less carbonate. The marble bodies in the Lofoten (Glassley 1975) also contain a high amount of carbonates, 80 to 90%. Somewhat lower carbonate contents, closer to the composition of the Rogaland marbles, are found in marbles from the Caledonian fold belt in Greenland (Bucher-Nurminen 1982) and in Early-Precambrian marbles from the Brazilian Shield (Sighinolfi 1974). In the compositional triangle (Fig. 1) average chemical compositions of limestones and carbonate rocks, calculated by Vinogradov and Ronov and by Wedepohl (both in Wedepohl 1969), plot close to the low-Si Rogaland marbles. However, these average compositions show larger molar Ca/Mg ratios (3 and 16) than the Rogaland marbles, where this ratio is about equal to one. This value fits well in the common trend of a decreasing Ca/Mg ratio in carbonate rocks back through time (see e.g. Fairbridge 1967). If it is assumed that Ca nor Mg preferentially left the Rogaland marbles in considerable amounts, dolomite was the main carbonate mineral in their source rock.

The Sr/Ca ratio in dolomite also shows a decrease with increasing age (Veizer 1977). The ratio in the Rogaland marbles generally falls well within the range observed for Precambrian dolomites (1000Sr/Ca about 0.2 to 0.5). The Rb content of the marbles falls within the range of carbonate sediments (Wedepohl 1969).

It can be concluded that the Rogaland marbles show many sedimentary affinities. The Ca/Mg ratio, the Sr/Ca ratio, the carbon and oxygen isotopes (although partly these are strongly influenced by retrograde metamorphism, Chapter 3), all indicate the sedimentary, dolomitic origin of the marbles. This is confirmed by the field relations. The marbles are often associated with quartzites and within the migmatites they occur in certain levels which can be traced over long distances in the field.

The Ba content is the main deviation from a normal sedimentary composition, while also the Si content may be comparatively high. The Ba content in the Rogaland marbles is a factor 50 to 150 larger than the mean value of 105 ppm for non-recent carbonate rocks, calculated by Puchelt (1967). This high content, together with the occurrence of rocks with alkalic affinities, like the diopside-alkalifeldspar and

quartz-alkalifeldspar rocks, might suggest a carbonatitic origin of the marbles. However, the characteristics mentioned above, as well as the absence of any other specific chemical characteristics of carbonatites, such as high P₂O₅, high Ti and high Sr, excludes a carbonatitic origin.

Various other sources of Ba in the marbles might be considered. It could have been present in detrital clay material in the original sediments, or precipitated as barite during diagenetic processes. The high Ba contents, coupled with high Zn contents (analysed in spinel), might also suggest hydrothermal activity, possibly associated with exhalative volcanism. Are the alkalifeldspar-rich rocks the remnants of such volcanics? The chemistry of these rocks is very inconclusive. The quartz-alkalifeldspar rocks show very high Si, the diopside-alkalifeldspar rocks low Ti and P compared with igneous rocks in the same range of major elements. Na is very low relative to the K content. The texture of these rocks is metamorphic, while they often show high-variance mineral assemblages, indicative for metasomatism. A sedimentary, arkosic, origin for these rocks, later modified by metasomatism, can not be excluded.

As a whole the Ba content in the Rogaland migmatites is fairly high, about 1000 ppm and higher (Schreurs et al. pers. comm.). Therefore a metasomatic origin of Ba in the marbles, during migmatitic stages, also has to be taken into account. However, the behaviour of Ba in the pegmatite does not suggest introduction of Ba. At the plagioclase-rich rims of the pegmatite Ca and Ba are enriched relative to the core of the pegmatite. The enrichment of Ca will be due to a relative depletion of Si and K, forming diopside and phlogopite, as well as diffusion of Ca from the marble. Given the relatively low Ba content in the marble, the enrichment of Ba in the marginal pegmatite zone presumably will be due solely to the relative depletion of Si and K. Such an enrichment thus indicates that Ba does not easily migrate together with Si and K into the marbles.

REFERENCES

- Bucher-Nurminen, K. 1982: Mechanism of mineral reactions inferred from textures of impure dolomite marbles from East Greenland. *J. Petrol.* 23, 325-343.
 Fairbridge, R.W. 1967: Carbonate rocks and paleoclimatology in the biogeochemical history of the planet. In: Chilingar, Rissell and Fairbridge (eds.): Carbonate rocks. Development in sedimentology 9A. p. 399-432.
 Glassley, W.E. 1975: High grade regional metamorphism of some carbonate bodies: significance for the orthopyroxene isograd. *Am. J. Sci.*, vol. 275, p. 1133-1163.
 Kretz, R. 1980: Occurrence, mineral chemistry and metamorphism of Precambrian carbonate rocks in a portion of the Grenville province. *J. Petrol.* 21, 573-620.
 Puchelt, H. 1967: Zur Geochemie des Bariuns im exogenen Zyklus. *Sitzungsber. Heidelb. Akad. Wiss. Math-nat. Kl.*, 4. Abh., 85-287.
 Sauter, P.C.C. 1981: Mineral relations in siliceous dolomites and related rocks in the high-grade metamorphic Precambrian of Rogaland, SW Norway. *Norsk Geol. Tidsskr.* 61, 35-45.
 Shapiro, L. 1967: Rapid analysis of rocks and minerals by a single-solution method. *U.S. Geol. Surv. Prof. Paper* 575-B, B187-B191.
 Sighinolfi, G.P. 1974: Geochemistry of Early Precambrian carbonate rocks from the Brazilian shield: implications for Archean carbonate sedimentation. *Contrib. Mineral. Petrol.* 46, 189-200.
 Veizer, J. 1977: Diagenesis of pre-quaternary carbonates as indicated by trace studies. *J. Sed. Petrol.* 47, 565-581.
 Wedepohl, K.H. 1969: *Handbook of geochemistry*, vol. I and II. Springer-Verlag, Berlin-Heidelberg-New York.

APPENDIX

Table A. List of mineral contents of samples used for microprobe and whole rock analyses.

Table B. Representative electron microprobe analyses.

Each analysis is indicated by its sample number (e.g. A164) and by its microprobe-spot code (e.g. K152).
 b.d.: below detection limit.
 FeO: total Fe calculated as Fe²⁺.
 $X_{Mg} = X_{Mg}(a) = Mg / (Mg + Fe^{tot} + Mn)$ (all minerals except spinel).
 $X_{Mg} = X_{Mg}(b) = Mg / (Mg + Fe^{2+} + Mn)$ (spinel and diopside).
 $X_{Fe^{3+}} = Fe^{3+} / (Fe^{3+} + Fe^{2+})$.
 $X_F = F / (F + OH)$.
 tet/oct = tetrahedral/octahedral ratio.
 Totals corrected for F, if analysed.

Table C. Representative whole rock analyses.

In wt% oxides, Rb and Sr in ppm.
 b.d.: below detection limit.

Comprehensive list of mineral and whole rock analyses available on request.

Department of Petrology
 Instituut voor Aardwetenschappen
 Rijksuniversiteit Utrecht
 Postbus 80.021
 3508 TA Utrecht
 The Netherlands

Table A. List of mineral contents

SAMPLE	COORD.	LOCATION	Presence	Diopside	Phenocryst	Quartz	Albite/Anorthite	Plagioclase	Microcline	Orthoclase	Triclinic/Albite	Chlorite	Talc	Muscovite	Pyroxene	Spinel	Ilmenite	Monazite	Apatite	Strom	Pyrite	Opac
A164		Po marble	336-076	A	x	x	x	x	x	x	x	x	x	x	x	x	x	x	x	x	x	x
A168		Q-kfz rock	337-076	A	x	x	x	x	x	x	x	x	x	x	x	x	x	x	x	x	x	x
B224		Po marble	336-076	A	x	x	x	x	x	x	x	x	x	x	x	x	x	x	x	x	x	x
C21		microcline rock	192-316	C	x	x	x	x	x	x	x	x	x	x	x	x	x	x	x	x	x	x
C164		Di-kfz rock	192-316	C	x	x	x	x	x	x	x	x	x	x	x	x	x	x	x	x	x	x
C165		Di-Pil rock	192-316	C	x	x	x	x	x	x	x	x	x	x	x	x	x	x	x	x	x	x
C235		Di marble	192-316	C	x	x	x	x	x	x	x	x	x	x	x	x	x	x	x	x	x	x
C236		Po marble	192-316	C	x	x	x	x	x	x	x	x	x	x	x	x	x	x	x	x	x	x
C242		leuco granite	192-316	C	x	x	x	x	x	x	x	x	x	x	x	x	x	x	x	x	x	x
C247		Po marble	192-316	C	(x)	x	x	x	x	x	x	x	x	x	x	x	x	x	x	x	x	x
C273		Po marble	192-316	C	x	x	x	x	x	x	x	x	x	x	x	x	x	x	x	x	x	x
C336		Po marble	337-076	A	x	x	x	x	x	x	x	x	x	x	x	x	x	x	x	x	x	x
C347		Di-Po-Pil rock	337-069	A	x	x	x	x	x	x	x	x	x	x	x	x	x	x	x	x	x	x
C372		Po marble	268-260	B	x	x	x	x	x	x	x	x	x	x	x	x	x	x	x	x	x	x
C383		Po marble	267-261	B	x	x	x	x	x	x	x	x	x	x	x	x	x	x	x	x	x	x
C393		Q-Di gneiss	255-273	B	x	x	x	x	x	x	x	x	x	x	x	x	x	x	x	x	x	x
C397		Di rock-Pil zone	255-273	B	x	x	x	x	x	x	x	x	x	x	x	x	x	x	x	x	x	x
C407		Kfz-Pil rock	336-076	A	x	x	x	x	x	x	x	x	x	x	x	x	x	x	x	x	x	x
C478a		Di rock	336-076	A	x	x	x	x	x	x	x	x	x	x	x	x	x	x	x	x	x	x
C480		Po marble	336-076	A	x	x	x	x	x	x	x	x	x	x	x	x	x	x	x	x	x	x
C481		Po marble	336-076	A	x	x	x	x	x	x	x	x	x	x	x	x	x	x	x	x	x	x
C498a		Di rock	255-273	B	x	x	x	x	x	x	x	x	x	x	x	x	x	x	x	x	x	x
C499b		Diagl pegmatite	255-273	B	x	x	x	x	x	x	x	x	x	x	x	x	x	x	x	x	x	x
C506		Kfz granite	255-273	B	x	x	x	x	x	x	x	x	x	x	x	x	x	x	x	x	x	x
C509a		Po marble	255-273	B	x	x	x	x	x	x	x	x	x	x	x	x	x	x	x	x	x	x
H2008		Po marble	267-259	B	x	x	x	x	x	x	x	x	x	x	x	x	x	x	x	x	x	x
H4431		Q-kfz rock	336-076	A	(x)	x	x	x	x	x	x	x	x	x	x	x	x	x	x	x	x	x
Q75		Po marble	270-252	B	x	x	x	x	x	x	x	x	x	x	x	x	x	x	x	x	x	x
Q138		Po marble	269-261	B	x	x	x	x	x	x	x	x	x	x	x	x	x	x	x	x	x	x
Q159		Di marble	261-272	B	(x)	x	x	x	x	x	x	x	x	x	x	x	x	x	x	x	x	x
X75		Po marble	274-261	B	(x)	x	x	x	x	x	x	x	x	x	x	x	x	x	x	x	x	x

Mineral presence: x: major; o: minor; a: accessory; r: retrogressive; (): totally or for the greater part decomposed;
 o: only residual dolomite present; an: other amphibole than tremolite; al: microcline; or: orthoclase; s: sanidine;
 For: forsterite; q: quartz; kfz: alkali feldspar; di: diopside; pil: plagioclase; mt: magnetite; plag: plagioclase.

Table B. Microprobe analyses

DIOPHIDE													FUCHSITE												
Sample	A164	B224	C165			C235			C336	C347			C372	C480			H2008								
No.	K152	K081	K043	K101	K102	K113	K153	K061	K082	K122	K132	K044	K100												
SiO ₂	53.23	52.70	54.75	50.61	53.27	54.41	52.11	54.07	55.21	54.27	50.24	45.65	53.17	55.37											
TiO ₂	b.d.	0.18	b.d.	0.40	0.18	0.10	0.14	0.04	b.d.	0.04	1.39	0.65	0.42	0.05											
Al ₂ O ₃	2.05	3.89	0.77	5.46	2.49	0.70	3.85	0.41	0.07	1.40	1.29	2.66	2.42	0.21											
FeO	1.61	0.96	0.45	3.20	2.65	1.36	2.02	1.18	1.36	1.19	2.04	2.55	2.55	0.01											
MnO	0.21	0.19	0.19	0.23	0.22	0.28	0.18	0.21	0.50	0.17	0.17	1.80	1.60	0.45											
MgO	16.41	16.64	16.14	14.82	16.50	17.13	16.15	17.79	19.06	17.38	15.82	13.63	16.60	17.75											
CaO	25.31	25.49	25.44	25.33	25.48	25.57	25.70	25.37	25.53	25.03	24.98	23.53	25.02	25.49											
Na ₂ O	0.09	b.d.	b.d.	0.06	0.06	0.03	0.06	0.04	0.05	b.d.		0.21	0.15	0.48											
Total	99.11	100.05	99.54	100.31	100.85	99.96	99.72	99.91	99.78	99.48	99.46	99.18	99.93	99.89											
Ions per f.o.																									
Si	1.932	1.909	1.989	1.855	1.931	1.977	1.904	1.990	1.998	1.974	1.846	1.701	1.935	2.008											
Al ^{IV}	0.048	0.091	0.011	0.145	0.070	0.023	0.096	0.010	0.022	0.056	0.154	0.299	0.045												
Al ^{VI}	0.041	0.075	0.005	0.091	0.037	0.007	0.070	0.008	0.001	0.034	0.055	0.063	0.044	0.009											
Ti	b.d.	0.005	b.d.	0.011	0.005	0.003	0.004	0.001	b.d.	0.039	0.102	0.101	0.041	0.001											
Fe ²⁺	0.025	0.023	0.014	0.065	0.053	0.029	0.040	0.031	b.d.	0.039	0.062	0.043	0.044	0.009											
Fe ³⁺	0.014	0.006	0.006	0.036	0.037	0.012	0.022	0.034	0.041	0.025	0.042	0.032	0.045	0.020											
Mn	0.006	0.006	0.006	0.007	0.007	0.005	0.006	0.006	0.015	0.005	0.005	0.006	0.007	0.010											
Mg	0.908	0.899	0.982	0.810	0.891	0.949	0.879	0.943	1.028	0.912	0.866	0.757	0.901	0.966											
Ca	0.993	0.989	0.990	0.995	0.990	0.996	0.992	0.986	0.912	0.976	0.984	1.000	0.976	0.987											
Na	0.007	b.d.	b.d.	0.004	0.004	0.002	0.004	0.004	0.003	b.d.	0.015	0.011	0.014												
Σ	10.943	10.963	10.974	10.882	10.911	10.951	10.921	10.958	10.948	10.950	10.927	10.899	10.936	10.975											
(al)	0.957	0.969	0.980	0.918	0.937	0.962	0.950	0.962	0.949	0.952	0.945														

DIOPHIDE - continued													FUCHSITE												
Sample	Q75	Q138	C155 ¹			C235 ¹			C336	C347			C372	C383			C400								
No.	K011	K010	K011	K011	K011	K011	K011	K011	K011	K011	K011	K011	K011	K011	K011	K011									
SiO ₂	51.97	54.98	52.31	51.11	51.02	51.29	51.29	51.29	51.29	51.29	51.29	51.29	51.29	51.29	51.29	51.29									
TiO ₂	0.24	0.46	0.16	0.05	0.16	0.22	0.22	0.22	0.22	0.22	0.22	0.22	0.22	0.22	0.22	0.22									
Al ₂ O ₃	1.19	0.21	0.35	0.84	0.84	0.84	0.84	0.84	0.84	0.84	0.84	0.84	0.84	0.84	0.84	0.84									
FeO	1.15	0.64	2.06	1.03	1.03	1.03	1.03	1.03	1.03	1.03	1.03	1.03	1.03	1.03	1.03	1.03									
MnO	0.17	0.18	0.22	0.25	0.25	0.25	0.25	0.25	0.25	0.25	0.25	0.25	0.25	0.25	0.25	0.25									
MgO	17.58	17.78	17.90	17.95	17.95	17.95	17.95	17.95	17.95	17.95	17.95	17.95	17.95	17.95	17.95	17.95									
CaO	25.26	25.20	24.65	25.00	25.00	25.00	25.00	25.00	25.00	25.00	25.00	25.00	25.00	25.00	25.00	25.00									
Na ₂ O	0.03	b.d.	0.04	b.d.	b.d.	b.d.	b.d.	b.d.	b.d.	b.d.	b.d.	b.d.	b.d.	b.d.	b.d.	b.d.									
Total	99.88	99.22	99.49	98.74	98.74	98.74	98.74	98.74	98.74	98.74	98.74	98.74	98.74	98.74	98.74	98.74									
Ions per f.o.																									
Si	1.959	2.001	1.915	1.957	1.957	1.957	1.957	1.957	1.957	1.957	1.957	1.957	1.957	1.957	1.957	1.957									
Al ^{IV}	0.041	0.041	0.041	0.041	0.041	0.041	0.041	0.041	0.041	0.041	0.041	0.041	0.041	0.041	0.041	0.041									
Al ^{VI}	0.018	0.009	0.047	0.047	0.047	0.047	0.047	0.047	0.047	0.047	0.047	0.047	0.047	0.047	0.047	0.047									
Ti	0.009	0.001	0.004	0.001	0.001	0.001	0.001	0.001	0.001	0.001	0.001	0.001	0.001	0.001	0.001	0.001									
Fe ²⁺	0.028	0.020	0.063	0.027	0.027	0.027	0.027	0.027	0.027	0.027	0.027	0.027	0.027	0.027	0.027	0.027									
Fe ³⁺	0.003	0.006	0.004	0.007	0.007	0.007	0.007	0.007	0.007	0.007	0.007	0.007	0.007	0.007	0.007	0.007									
Mn	0.008	0.006	0.007	0.008	0.008	0.008	0.008	0.008	0.008	0.008	0.008	0.008	0.008	0.008	0.008	0.008									
Mg	0.951	0.974	0.901	0.912	0.912	0.912	0.912	0.912	0.912	0.912	0.912	0.912	0.912	0.912	0.912	0.912									
Ca	0.943	0.963	0.967	0.967	0.967	0.967	0.967	0.967	0.967	0.967	0.967	0.967	0.967	0.967	0.967	0.967									
Na	0.002	b.d.	0.003	b.d.	b.d.	b.d.	b.d.	b.d.	b.d.	b.d.	b.d.	b.d.	b.d.	b.d.	b.d.	b.d.									
Σ	10.960	10.974	10.915	10.954	10.954	10.954	10.954	10.954	10.954	10.954	10.954	10.954	10.954	10.954	10.954	10.954									
(al)	0.966	0.928	0.960	0.966	0.966	0.966	0.966	0.966	0.966	0.966	0.966	0.966	0.966	0.966	0.966	0.966									

1) wet-chemical

Table B. Microprobe analyses, continued

FERTILISER - continued						SPEND					
Sample	#208	Q75	Q130	175		Sample	#204	C372	C387	C397	C402
No.	#081	P011	P111	P052		No.	#021	#023	#081	#021	#025
SiO ₂	42.29	41.49	41.20	42.07		Al ₂ O ₃	71.37	67.21	65.63	67.44	64.13
P ₂ O ₅	4.64	6.36	4.55	3.39		P ₂ O ₅	4.37	6.73	9.04	9.51	9.98
K ₂ O	0.34	0.51	0.47	0.49		K ₂ O	0.30	0.22	0.22	0.69	0.27
MgO	32.62	31.85	32.49	32.31		MgO	1.82	1.12	0.15	3.12	2.43
Total	99.89	100.23	99.71	99.26		Total	73.99	74.65	74.20	70.20	72.19
Ions per 4						Ions per 4					
Si	1.013	0.999	0.991	1.009		Al	2.015	1.949	1.909	1.980	1.939
P	0.093	0.128	0.092	0.068		P ₂ O ₅	0.051	0.091	0.090	0.020	0.061
K	0.011	0.011	0.010	0.010		K ₂ O	0.068	0.068	0.096	0.178	0.120
Mg	1.077	1.062	1.018	1.005		Mg	0.006	0.007	0.005	0.015	0.006
M ₂ O	0.947	0.931	0.950	0.961		Mg	0.032	0.002	0.003	0.095	0.040
						Ca	0.857	0.904	0.897	0.750	0.820
						Mg	0.001	0.006	0.000	0.796	0.859
						M ₂ O	0.369	0.480	0.102	0.819	0.819
						P ₂ O ₅					
FERTILISER - continued											
FERTILISER						SPEND					
Sample	#154	#274	C165	C375	C402	Sample	#206	C312	C383	C480	11
No.	#155	#011	#081	#011	#011	No.	#031	#012	#032	#011	#046
SiO ₂	38.21	37.21	38.23	40.54	40.54	SiO ₂	37.79	36.43	36.39	26.34	26.52
P ₂ O ₅	0.50	0.60	0.58	0.52	0.44	P ₂ O ₅	0.78	0.87	0.82	2.63	13.16
Al ₂ O ₃	16.87	18.06	16.22	14.55	1.31	Al ₂ O ₃	17.20	17.07	16.27	17.07	10.87
P ₂ O ₅	2.46	1.36	3.90	2.50	2.50	P ₂ O ₅	1.50	1.56	1.95	3.37	6.07
K ₂ O	0.05	0.04	0.04	0.07	0.04	K ₂ O	b.d.	b.d.	b.d.	b.d.	0.11
MgO	34.56	34.66	34.07	35.81	26.36	MgO	23.78	24.53	25.29	22.77	11.98
MgO	1.68	1.68	0.08	0.16	0.16	MgO	3.07	0.17	2.41	1.40	2.42
MgO	0.06	0.12	0.21	0.13	0.13	MgO	0.015	0.11	0.58	0.38	0.23
MgO	9.90	9.48	10.11	10.62	10.20	MgO	9.57	10.25	12.34	2.91	8.43
F	0.5	0.5	1.3	1.3	1.3	F	0.5	0.5	0.5	0.5	0.5
Total	94.79	94.29	93.97	96.00	94.80	Total	93.71	94.18	94.61	94.56	100.96
Ions per 4						Ions per 4					
Si	5.495	5.322	5.572	5.778	5.706	Si	5.208	5.524	5.371	5.349	3.947
P	0.059	0.110	0.251	0.417	0.247	P	0.286	0.286	0.298	0.299	3.652
Al	2.054	0.072	0.064	0.056	0.047	Al	0.086	0.086	0.086	0.286	1.363
K	0.005	0.013	0.013	0.013	0.013	K	0.005	0.005	0.005	0.005	0.005
P ₂ O ₅	0.06	0.06	0.06	0.06	0.06	P ₂ O ₅	0.06	0.06	0.06	0.06	0.06
K ₂ O	0.005	0.005	0.005	0.005	0.005	K ₂ O	0.005	0.005	0.005	0.005	0.005
MgO	0.005	0.005	0.005	0.005	0.005	MgO	0.005	0.005	0.005	0.005	0.005
MgO	0.005	0.005	0.005	0.005	0.005	MgO	0.005	0.005	0.005	0.005	0.005
MgO	0.005	0.005	0.005	0.005	0.005	MgO	0.005	0.005	0.005	0.005	0.005
MgO	0.005	0.005	0.005	0.005	0.005	MgO	0.005	0.005	0.005	0.005	0.005
MgO	0.005	0.005	0.005	0.005	0.005	MgO	0.005	0.005	0.005	0.005	0.005
MgO	0.005	0.005	0.005	0.005	0.005	MgO	0.005	0.005	0.005	0.005	0.005
MgO	0.005	0.005	0.005	0.005	0.005	MgO	0.005	0.005	0.005	0.005	0.005
MgO	0.005	0.005	0.005	0.005	0.005	MgO	0.005	0.005	0.005	0.005	0.005
MgO	0.005	0.005	0.005	0.005	0.005	MgO	0.005	0.005	0.005	0.005	0.005
MgO	0.005	0.005	0.005	0.005	0.005	MgO	0.005	0.005	0.005	0.005	0.005
MgO	0.005	0.005	0.005	0.005	0.005	MgO	0.005	0.005	0.005	0.005	0.005
MgO	0.005	0.005	0.005	0.005	0.005	MgO	0.005	0.005	0.005	0.005	0.005
MgO	0.005	0.005	0.005	0.005	0.005	MgO	0.005	0.005	0.005	0.005	0.005
MgO	0.005	0.005	0.005	0.005	0.005	MgO	0.005	0.005	0.005	0.005	0.005
MgO	0.005	0.005	0.005	0.005	0.005	MgO	0.005	0.005	0.005	0.005	0.005
MgO	0.005	0.005	0.005	0.005	0.005	MgO	0.005	0.005	0.005	0.005	0.005
MgO	0.005	0.005	0.005	0.005	0.005	MgO	0.005	0.005	0.005	0.005	0.005
MgO	0.005	0.005	0.005	0.005	0.005	MgO	0.005	0.005	0.005	0.005	0.005
MgO	0.005	0.005	0.005	0.005	0.005	MgO	0.005	0.005	0.005	0.005	0.005
MgO	0.005	0.005	0.005	0.005	0.005	MgO	0.005	0.005	0.005	0.005	0.005
MgO	0.005	0.005	0.005	0.005	0.005	MgO	0.005	0.005	0.005	0.005	0.005
MgO	0.005	0.005	0.005	0.005	0.005	MgO	0.005	0.005	0.005	0.005	0.005
MgO	0.005	0.005	0.005	0.005	0.005	MgO	0.005	0.005	0.005	0.005	0.005
MgO	0.005	0.005	0.005	0.005	0.005	MgO	0.005	0.005	0.005	0.005	0.005
MgO	0.005	0.005	0.005	0.005	0.005	MgO	0.005	0.005	0.005	0.005	0.005
MgO	0.005	0.005	0.005	0.005	0.005	MgO	0.005	0.005	0.005	0.005	0.005
MgO	0.005	0.005	0.005	0.005	0.005	MgO	0.005	0.005	0.005	0.005	0.005
MgO	0.005	0.005	0.005	0.005	0.005	MgO	0.005	0.005	0.005	0.005	0.005
MgO	0.005	0.005	0.005	0.005	0.005	MgO	0.005	0.005	0.005	0.005	0.005
MgO	0.005	0.005	0.005	0.005	0.005	MgO	0.005	0.005	0.005	0.005	0.005
MgO	0.005	0.005	0.005	0.005	0.005	MgO	0.005	0.005	0.005	0.005	0.005
MgO	0.005	0.005	0.005	0.005	0.005	MgO	0.005	0.005	0.005	0.005	0.005
MgO	0.005	0.005	0.005	0.005	0.005	MgO	0.005	0.005	0.005	0.005	0.005
MgO	0.005	0.005	0.005	0.005	0.005	MgO	0.005	0.005	0.005	0.005	0.005
MgO	0.005	0.005	0.005	0.005	0.005	MgO	0.005	0.005	0.005	0.005	0.005
MgO	0.005	0.005	0.005	0.005	0.005	MgO	0.005	0.005	0.005	0.005	0.005
MgO	0.005	0.005	0.005	0.005	0.005	MgO	0.005	0.005	0.005	0.005	0.005
MgO	0.005	0.005	0.005	0.005	0.005	MgO	0.005	0.005	0.005	0.005	0.005
MgO	0.005	0.005	0.005	0.005	0.005	MgO	0.005	0.005	0.005	0.005	0.005
MgO	0.005	0.005	0.005	0.005	0.005	MgO	0.005	0.005	0.005	0.005	0.005
MgO	0.005	0.005	0.005	0.005	0.005	MgO	0.005	0.005	0.005	0.005	0.005
MgO	0.005	0.005	0.005	0.005	0.005	MgO	0.005	0.005	0.005	0.005	0.005
MgO	0.005	0.005	0.005	0.005	0.005	MgO	0.005	0.005	0.005	0.005	0.005
MgO	0.005	0.005	0.005	0.005	0.005	MgO	0.005	0.005	0.005	0.005	0.005
MgO	0.005	0.005	0.005	0.005	0.005	MgO	0.005	0.005	0.005	0.005	0.005
MgO	0.005	0.005	0.005	0.005	0.005	MgO	0.005	0.005	0.005</		

140

Table B. Microprobe analyses, continued

ISOTACTIC		SYNDIO-TACTIC		TETRA-TACTIC		BLENDS-GROUP	
Sample C147	C183	C187		Sample C336	C372		
No. (C93) ¹	T051	T033		No. C141	C044	C025	C075 C75 C081 C080
SiO ₂ 56.40	46.71	57.56		SiO ₂ 30.27	37.49	42.00	36.72 37.98 38.30
TiO ₂ 3.6	11.30	0.19		TiO ₂ 0.83	2.24	1.49	0.46 0.50 0.16
FeO 4.09	3.94	2.81		FeO 4.87	2.24	2.26	4.73 2.27 1.27
MgO 1.00	0.05	0.27		MgO 1.71	1.41	0.43	0.72 0.32 1.27
P ₂ O ₅ 35.39	19.06	12.76		Al ₂ O ₃ 49.70	50.90	50.67	53.77 54.32 55.59
CaO 0.67	13.64	0.18		P	2.2	AI	0.72 P 3.2
Na ₂ O 0.03	0.32	0.30		Total	96.15	96.23	96.49 99.15 95.78 93.58
Fe ₂ O ₃				Iron per 17 g			9 g
Total 99.63	95.71	96.28		Si	4.153	3.977	4.195 4.042 4.023 2.038
Iron per 6 g	23 g	22 g		Ti	0.060	0.259	0.158 0.464 0.007
Fe 2.006	6.717	7.974		Fe	0.442	0.199	0.198 0.417 0.201 0.061
Al 0.002	1.698	0.39		Mn	0.157	0.123	0.119 0.038 0.028 0.062
Pi h.c.	0.125	0.036		Mg	0.259	0.024	0.752 0.438 0.638 0.784
Fe 0.118	0.474	0.332		Al	0.090	P 1.10	
Mn 0.058	0.006	0.006		Fe	0.910	0.962	0.961 0.945 0.974 0.975
Mg 1.812	4.006	4.705		Ca/Mn	0.481	0.452	0.513 0.564 0.455 0.415
Ca 0.025	2.103	1.093					0.456
Na	0.028	0.049					
Al 0.002	0.089	0.052					
P	0.057						
Fe 0.925	0.935	0.929					

ISOTACTIC		SYNDIO-TACTIC		BLENDS-GROUP	
Sample C181		Sample C372		Sample C372	
No. (C093) ¹	C063 ²	C041 ²	C04 ²	No. C018	
SiO ₂ 29.07	20.42	28.85		SiO ₂ 16.3	
TiO ₂ 0.12	h.d.	0.87		FeO 0.1	
Al ₂ O ₃ 18.11	20.33			P ₂ O ₅ 36.0	
FeO 2.21	1.01	1.88		Total 52.5	
MgO 33.41	34.31	32.89		Iron per 6 g	
Total 85.00	83.85	83.94		Si	4.209
Iron per 28 g				Fe	0.02
Si 5.587	5.821	5.682		Mg	5.84
Al 4.570	4.727	4.650			
Ti 0.017	h.d.	h.d.			
Fe 0.158	0.164	0.305			
P 9.572	9.884	9.517			
Mg 0.964	0.984	0.969			

ISOTACTIC		SYNDIO-TACTIC		BLENDS-GROUP	
Sample C372		Sample C372		Sample C372	
No. C013	C04 ²	No. C018		No. C018	
SiO ₂ 33.60	29.87	SiO ₂ 33.60		SiO ₂ 16.3	
Al ₂ O ₃ 2.74	0.12	FeO 0.1		P ₂ O ₅ 36.0	
MgO h.d.	0.05	Total 52.5		Iron per 6 g	
FeO 1.77	2.70	Si	4.209	Fe	0.02
MgO 39.65	42.09	Fe	0.02	Mg	5.84
Total 81.26	82.89				
Iron per 7 g					
Si 1.083	1.964				
Al 0.196	0.007				
Fe 0.016	0.002				
P 0.073	0.111				
Mg 2.883	2.948				
Fe 0.936	0.963				

- 1) decomposition of phlogopite
- 2) fine-grained at contact forsterite-spinel
- 3) coarse-grained decomposition of spinel

- 1) ex diopside?
- 2) ex forsterite

Table C. Whole rock analyses

Ph marble					Di marble		Di rock		Di-phl rock		Di-efep rock	
Location A					C		A		B		C	
Sample	A164	C480	C372	C509A	C236	C235	C478A	C478B	C165	C164		
SiO ₂	26.52	13.97	8.12	13.10	15.16	29.9	52.24	53.04	40.7	56.68		
TiO ₂	0.25	0.06	b.d.	0.02	0.01	0.17	0.06	0.07	0.32	0.27		
Al ₂ O ₃	5.56	3.35	1.61	1.77	0.93	4.05	3.81	1.89	7.5	7.92		
Fe ₂ O ₃	0.99	0.36	0.41	0.70	0.85	0.65	1.44	0.51	1.33	0.38		
FeO	1.30	2.32	0.74	1.32	1.15	1.17	1.07	1.65	1.69	1.80		
MnO	0.78	0.40	0.31	0.31	0.36	0.23	0.22	0.21	0.25	0.18		
MgO	18.44	20.08	17.68	15.75	18.84	16.6	15.90	15.64	17.9	10.81		
CaO	22.00	30.53	34.10	33.48	32.49	28.5	23.80	22.78	20.9	15.53		
NaCl	1.64	0.40	0.28	0.99	0.32	0.48	0.95	0.70	0.42	0.45		
Na ₂ O	0.01	0.82	0.05	b.d.	0.02	0.08	0.09	0.11	0.08	0.43		
K ₂ O	2.95	b.d.	b.d.	0.37	0.76	2.35	0.04	0.55	3.2	5.34		
P ₂ O ₅	0.01	b.d.	b.d.	0.09	0.02	0.09	b.d.	0.07	0.15	0.19		
H ₂ O	3.82	1.77	2.72	3.70	0.32		1.25	1.09				
CO ₂	16.30	26.30	32.30	29.80	29.69	17.85	0.87	0.60	5.64	0.83		
Total	100.21	99.96	98.32	100.20	100.42	102.12	101.74	99.31	99.97	100.36		
SD	82	b.d.	b.d.	22	17	192	20	42	372	256		
SE	80	112	90	130	119	66	228	30	150	62		

Q-Di omelas		Q-efep rock		Kfs-phl rock		Granite and pegmatite			
Location B		A		A		A			
Sample	C393	MA331	C407	C21	C242	C499B	C506		
SiO ₂	69.50	75.3	52.41	61.8	72.9	47.38	68.93		
TiO ₂	0.32	0.12	0.73	0.05	0.06	0.07	0.10		
Al ₂ O ₃	8.91	12.2	22.90	20.3	14.3	17.55	14.12		
Fe ₂ O ₃	0.4*	0.94	0.91	0.14	0.12	0.08	0.09		
FeO	1.43	0.23	1.23	0.11	0.27	0.16	0.15		
MnO	0.11	0.01	0.03	0.01	0.01	0.11	0.04		
MgO	4.04	0.02	4.29	0.23	0.15	3.03	0.51		
CaO	5.18	0.18	b.d.	1.56	0.31	12.95	0.99		
NaCl	0.68		0.83			6.43	0.58		
Na ₂ O	0.88	0.11	0.13	1.57	2.71	0.10	0.40		
K ₂ O	5.84	11.0	13.35	12.8	7.85	6.26	11.81		
P ₂ O ₅	0.24	0.07	0.11	0.13	0.08	0.13	0.03		
H ₂ O	1.65		3.21			1.33	1.07		
CO ₂	0.66	0.31	1.13	0.76	0.32	3.70	0.22		
Total	100.11	100.49	101.26	99.91	100.50	99.27	99.26		
SD	212		596			220	460*		
SE	38		b.d.			140	b.d.		

Curriculum Vitae

Toegevoegd op verzoek van het College van Decanen van de Rijksuniversiteit te Utrecht.

De schrijver van dit proefschrift behaalde in 1971 het diploma Gymnasium B aan het St. Janslyceum te 's-Hertogenbosch. In datzelfde jaar werd begonnen met de studie geologie aan de Rijksuniversiteit te Utrecht. In mei 1976 werd het kandidaatsexamen G 3 afgelegd, in januari 1979 volgde het doctoraal examen, met hoofdvak Petrologie en bijvakken Strukturele Geologie en Economische Geologie. In de jaren 1975 tot en met 1978 werden student-assistentschappen vervuld bij de afdeling Petrologie van het Instituut voor Aardwetenschappen van de Rijksuniversiteit te Utrecht. Van februari 1979 tot en met mei 1982 was de schrijver werkzaam bij dezelfde afdeling, als wetenschappelijk assistent in dienst zijnde bij de Nederlandse Organisatie voor Zuiver-Wetenschappelijk Onderzoek (Z.W.O.).